

The investigation of the thermal effect of contact lens wear

Sachiko Nishimura
Master of Philosophy

School of Optometry & Vision Sciences
Cardiff University
December 2014

DECLARATION

This work has not previously been accepted in substance for any degree and is not concurrently submitted in candidature for any degree.

Signed *Sachiko Nishimura*..... (candidate) Date ...5th... June... 2015..

STATEMENT 1

This thesis is being submitted in partial fulfillment of the requirements for the degree of MPhil.

Signed *Sachiko Nishimura*..... (candidate) Date ..5th... June 2015.....

STATEMENT 2

This thesis is the result of my own independent work/investigation, except where otherwise stated. Other sources are acknowledged by explicit references.

Signed *Sachiko Nishimura*..... (candidate) Date ..5th June 2015.....

STATEMENT 3

I hereby give consent for my thesis, if accepted, to be available for photocopying and for inter-library loan, and for the title and summary to be made available to outside organisations.

Signed *Sachiko Nishimura*..... (candidate) Date ..5th June 2015.....

Summary

Since their introduction over 70 years ago, corneal contact lenses have continued to be improved in design and are safely used all over the world. Nevertheless, there is still some risk of infection, especially in soft contact lens (SCL) wearers. In comparison, rigid gas permeable lenses are less likely to cause a serious eye disease than SCL, including both traditional and silicone hydrogel lenses (SiHCL). Two possible reasons for this may be the difference in the tear exchange rate beneath the lens while on the eye, and the influence of lens material on the ocular surface temperature (OST) during the lens wear. This thesis investigates these two factors.

Firstly, an in vitro model of the ocular surface was developed to investigate the effect of lens thermal conductivity amongst lens types, and the effect of the existence of the tear film on any subsequent temperature change. The experiment confirmed the successful use of an infrared camera to measure OST change, and also found that the tear film and the water content of the lens were factors in the OST over a lens surface.

Secondly, the effect of the tear film on the OST was examined in human eyes. This study confirmed the in vitro study results and the importance of replenishing the lens water content and limiting tear evaporation.

Finally, the dynamic changes in OST during lens wear were recorded with different lens types. The OST was measured at the central and peripheral lens, and the conjunctiva. This is the first study to compare the effect of RGP and SCL wear on OST in the same subjects. Once again, similar results emphasising the importance of tear exchange and water content were found, but no effect from tear exchange beneath the lens was observed.

In summary, this thesis presents important findings about the influence of both the quality of the tear film and the type of contact lens on the OST. Also it demonstrated the usefulness of ocular thermography to investigate ocular surface changes during lens wear non-invasively.

Acknowledgment

I would like to say a huge thank you to Professor Paul Murphy and Professor Christine Purslow for their continuous encouragement during my study. I could not have achieved what I have without your patience and endless support. I also thank you to Professor Rachel North for her support with completing my thesis. I appreciate the help from students at the Cardiff School of Optometry and Vision Sciences and also from my colleagues at Menicon who acted as my subjects. Also thank you to the support staff in the School for their practical help and advice. And also thank you to Professor Andrew Quantock and his wife Kayoko, and his colleagues for their encouragement and friendship.

I would like to give a special thank you to Menicon for sponsoring and giving me such a great opportunity. Also thank you to my colleagues; especially Sugimoto-san, Yamaguchi-san, Sakata-san, Miyake-san, Dr Oota and Dr Inagaki for their support. And I would like to extend my appreciation to Nakajima-san in Heaven for making a phone call at a weekend in concern for my safety.

I thank you to my parents for their encouragement and their support to my family in Japan while I was in the UK. And finally, a huge thank you to my husband Kisei and my son Kanata for their love. I am looking forward to sharing more pleasures of life with you.

Table of contents

Summary	1
Acknowledgment.....	2
Table of contents	3
List of tables	8
List of figures	10
Chapter 1. Literature review.....	12
1.1.The Contact lens	12
1.1.1.A brief history of contact lenses	12
1.1.2.Dispensing trends and popularity of contact lens wear	15
1.2.The tear film and contact lens wear.....	18
1.2.1.The tear film	18
1.2.2.The effect of lens wear on tear evaporation.....	19
1.2.3.The effect of lens wear on tear film thickness.....	20
1.2.4.The effect of lens wear on tear film structure.....	21
1.2.5.The effect of lens wear on tear stability.....	22
1.3.Contact lens wear and tear exchange.....	24
1.3.1.Oxygen supply to the cornea with contact lenses	26
1.3.2.Complications of Contact Lens Wear.....	29
1.4.Principles and history of infrared thermograph.....	36
1.5.Development of infrared imaging and its application in medicine.....	41
1.6.Measurement of ocular surface temperature	47

1.6.1.Early technique of ocular thermography	47
1.6.2.Modern ocular thermography	49
1.7.Factors that affect ocular surface temperature.....	52
1.7.1.Location of measurement	53
1.7.2.Experimental conditions	53
1.7.3.Subjective factors	53
1.7.4.Ophthalmic factors	54
1.8.Effect of contact lens wear	55
1.9.Summary	57
1.10.Aims of this thesis	58
Chapter 2. Experimental design	59
2.1.Laboratory set-up.....	59
2.1.1.Choice of camera.....	59
2.1.2.Experimental location.....	61
2.1.2.1. Camera set-u p in UK.....	61
2.1.2.2. Camera set-up in Japan	64
2.2.Conditions and techniques.....	65
2.2.1.Effect of image defocus.....	65
2.2.2.Adaptation	65
2.2.3.Repeatability of temperature measurement	66
2.2.4.Time of the day.....	67
2.2.5.Eye rubbing	68

2.2.6.Room temperature	68
2.3.Data collection and analysis	69
2.3.1.Instruction to subject on blinking	69
2.3.2.Analysing the data	69
2.3.3.Analytical localisation	73
2.4.Experimental protocol	76
Chapter 3. In vitro study (model eye study).....	77
3.1.Aims and objectives	77
3.2.Preliminary study.....	82
3.2.1.Aims	82
3.2.2.Methods	83
3.2.3.Results	86
3.3.Contact lens study.....	89
3.3.1.Aims	89
3.3.2.Methods	89
3.3.3.Results	93
3.3.4.Discussion.....	102
3.4.Contact lens and eye drop study	104
3.4.1.Aims	104
3.4.2.Methods	104
3.4.3.Result	107
3.4.4.Discussion.....	112

3.5.Conclusions	114
Chapter 4. Investigating the relationship between tear film stability and ocular surface temperature.....	115
4.1.Introduction	115
4.2.Methods	118
4.2.1.Subjects.....	118
4.2.2.Tear film stability assessment.....	119
4.2.3.Ocular surface temperature measurement	120
4.2.4.Other assessments.....	120
4.3.Results	122
4.3.1.Initial OST	122
4.3.2.Post-blink change in OST.....	123
4.4.Discussion	130
4.5.Conclusions	133
Chapter 5. An investigation of ocular surface temperature change with contact lens wear.....	134
5.1.Introduction	134
5.2.Methods	139
5.2.1.Subjects.....	139
5.2.2.Contact lens types.....	140
5.2.3.Study design and procedure.....	141
5.2.4.Other assessment	145
5.3.Results	146
5.3.1.Change in OST from the baseline.....	146

5.3.1.1.	Central OST	146
5.3.1.2.	Comparison of OSTP and OSTC	149
5.3.2.	Post-blink changes in OST with contact lens wear	155
5.3.2.1.	Post-blink change in the central OST.....	155
5.3.2.2.	Post-blink changes in OSTP and OSTC.....	157
5.4.	Discussion	163
5.5.	Conclusion.....	168
Chapter 6.	Summary and future work	169
References	173

List of tables

Table 1.1: Important dates and events in the history of contact lens invention (cited by (Heiting, 2010)).....	14
Table 1.2: Global contact lens type fitting characteristics between 2007 and 2013.....	16
Table 1.4: Pre- and post-lens tear film thickness during contact lens wear	22
Table 1.5: Surface treatment of silicone hydrogel contact lenses.	23
Table 1.6: Ocular pathology related to contact lenses and their care systems (adapted from an original table by Bailey (1999)).	30
Table 1.7: Ocular surface temperature without contact lens wear.	50
Table 1.8: Ocular surface temperature with lens wear.	51
Table 2.1: Specifications of thermal camera.....	60
Table 3.1: Physical constants of cornea and contact lenses taken from the literature (cited by Purslow (2005)).	79
Table 3.2: The temperature change on the model eye.....	88
Table 3.3: Specifications of SCL.	90
Table 3.4: Specifications of RGPCL.	91
Table 3.5: Specifications of SiHCL.	91
Table 3.6: Mean values for Δt_1 and Δt_2	95
Table 3.7: Mean values for Δp_1 and Δp_2 of SiHCL.	97
Table 3.8: The temperature difference from the initial.	99
Table 3.9: Contact lenses applied on the model eye.	105
Table 3.10: Decrease in temperature by time for contact lens groups.....	109
Table 3.11: Post-hoc test at 2 minutes.	110
Table 3.12: Post-hoc test at 4 minutes.	110
Table 3.13: Post-hoc test at 5 minutes.	110
Table 3.14: Post-hoc test at 6 minutes.	111
Table 3.15: Post-hoc test at 7 minutes.	111
Table 3.16: Post-hoc test at 8 minutes.	111
Table 3.17: Post-hoc test at 9 minutes.	112
Table 4.1: Number, gender and ages of subjects	118
Table 4.2: Post-blink change in OST (mean \pm 1S.D.).....	124
Table 4.3: NIBUT category.	125
Table 4.4: Post-blink change in OST on the spot (mean \pm 1S.D.).....	126
Table 4.5: OST change in the area (mean \pm 1S.D.).	128

Table 5.1: Typical values of thermal conductivity	138
Table 5.2: Details of subjects used in this study	139
Table 5.3: Specifications of lenses	140
Table 5.4: Median change in the central OST, from the pre-lens baseline, during and after lens wear, with statistical analysis.	148
Table 5.5: Comparison of the change in OSTP and OSTC from the baseline (median), with statistical analysis.	150
Table 5.6: Comparison of the change in OSTP and OSTC from the baseline (median, AIR Optix), with statistical analysis.	152
Table 5.7: Comparison of the change in OSTP and OSTC from the baseline (median, Clariti), with statistical analysis.	153
Table 5.8: Comparison of the change in OSTP and OSTC from the baseline (median, 1-day Acuvue), with statistical analysis.	154
Table 5.9: Post-blink change in the central OST (median), with statistical analysis.	156
Table 5.10: Comparison of post-blink change in OSTP and OSTC (median, Menicon Z- α), with statistical analysis. ..	158
Table 5.11: Comparison of post-blink change in OSTP and OSTC (median, Air Optix), with statistical analysis.	160
Table 5.12: Comparison of post-blink change in OSTP and OSTC (median, Clariti), with statistical analysis.	161
Table 5.13: Comparison of post-blink change in OSTP and OSTC (median, 1-day Acuvue), with statistical analysis..	162

List of figures

Figure 1.1: Global contact lens type fitting characteristics between 2008 and 2012 (from Morgan et al., 2012)	15
Figure 1.2: Percentage of different contact lens types prescribed in the USA (data from Nichols, 2009-2014).	17
Figure 1.3: Oxygen supply to cornea when lens is worn.	27
Figure 1.4: Illustration of the eight-layer oxygen diffusion model for a cornea covered by a contact lens.	28
Figure 1.5: Electromagnetic spectrum wavelength.....	37
Figure 1.6: Planck’s formula.	39
Figure 1.7: Black body spectral radiant emittance according to Planck’s law, plotted for absolute temperatures (Taken from FLIR SYSTEMS, 2007).....	40
Figure 1.8: Atmospheric attenuation.....	44
Figure 1.9: Example of an ocular thermogram.....	45
Figure 1.10: Thermal image of a patient with breast cancer, showing increased temperature in the left breast.....	46
Figure 1.11: Thermal image of acanthamoeba keratitis in the right eye (taken from http://www.bausch.com/en_US/ecp/resources/image_library/miscellaneous.aspx).	46
Figure 2.1: The model eye in the protective box in preparation for a measurement, with the thermal camera positioned vertically above, in the UK experimental set-up.	62
Figure 2.2: Patient seated in front of camera in preparation for a measurement, in the UK experimental set-up.....	63
Figure 2.3: Patient seated in front of the camera in preparation for a measurement, in the Japan experimental set-up. ...	64
Figure 2.4: Thermal image of OST with analysis tools and their temperature profile.	70
Figure 2.5: Typical temporal change in OST with blinking.	71
Figure 2.6: The thermal image of the model eye with analysis tools, showing the location of the 6 LEDs (red dots), and the selected spots for temperature analysis (X1-5), and the average area (striped area surrounded by blue circle)..	73
Figure 2.7: A thermal image of the eye with analysis tools.....	74
Figure 2.8: The thermal image of the eye under RGP lens wear with analysis tools.	75
Figure 2.9: The thermal image of the eye under SCL wear with analysis tools.	75
Figure 3.1: The model eye set on an electrical circuit board.	83
Figure 3.3: Thermal image of the model eye showing the location of the 6 LEDs (red dots), and the selected locations for temperature analysis (x1-5) and an area (striped area surrounded by blue circle).....	86
Figure 3.5: Surface temperature change produced with RGP.	93
Figure 3.6: Surface temperature change produced with SCL.....	93
Figure 3.7: Surface temperature change produced with SiHCL.	94
Figure 3.9: Time to reach (Δp_1) and (Δp_2), Left: RGPCL, Right: SCL and SiHCL.	96

Figure 3.10: Normalised temperature change of RGPCLs	100
Figure 3.11: Normalised temperature change of SCLs	101
Figure 3.12: Normalised temperature change of SiHCLs.....	101
Figure 3.13: Surface temperature changes with artificial tears.	107
Figure 4.1: The DR-1 (Kowa, Nagoya, Japan).....	116
Figure 4.2: Correlation between the initial central OST at the central cornea and NIBUT.	122
Figure 4.3: Correlation between the initial central OST over the test area and NIBUT.	123
Figure 4.4: Post-blink change in OST (mean±1S.D.).	123
Figure 4.5: OST change on the spot (mean±1S.D.).	125
Figure 4.6: OST change in the area (mean±1S.D.)......	127
Figure 5.1: Position of the OST recording points across the anterior eye as used by Purslow et al.....	136
Figure 5.2: The thermal image of the eye with RGP lens wear marked up with the software analysis tools.	142
Figure 5.3: The thermal image of the eye with SCL wear marked up with the software analysis tools.	143
Figure 5.4: Diagram illustrating time points for temperature measurement and analysis.....	144
Figure 5.5: Median change at 0.2 secs in the central OST, from the pre-lens baseline, during and after lens wear.	148
Figure 5.6: Comparison of the change in OSTP and OSTC from the baseline (median, Menicon Z- α).	150
Figure 5.7: Comparison of the change in OSTP and OSTC from the baseline (median, AIR Optix).	152
Figure 5.8: Comparison of the change in OSTP and OSTC from the baseline (median, Clariti).	153
Figure 5.9: Comparison of the change in OSTP and OSTC from the baseline (median, 1-day Acuvue).	154
Figure 5.10: Post-blink change in the central OST (median).....	156
Figure 5.11: Comparison of post-blink change in OSTP and OSTC (median, Menicon Z- α).	158
Figure 5.12: Comparison of post-blink change in OSTP and OSTC (median, Air Optix).	160
Figure 5.13: Comparison of post-blink change in OSTP and OSTC (median, Clariti).	161
Figure 5.14: Comparison of post-blink change in OSTP and OSTC (median, 1-day Acuvue).	162

Chapter 1. Literature review

1.1. The contact lens

1.1.1. A brief history of contact lenses

Modern contact lenses have been developed and expanded for over a half century, but the original concept of the contact lens was sketched by Leonardo da Vinci (1452–1519) in 1508, in which he proposed the theory that the optics of the corneal surface could be neutralised by water (Phillips and Speedwell, 2007). Approximately 300 years after da Vinci, Müller made the first contact lenses from glasses, which eventually led to the development and use of plastic materials when Tuohy introduced the first rigid corneal contact lens in the mid-1940s (Heiting, 2010, Stone and Phillips, 1986).

However, it was a decade later that contact lenses took their greatest progress towards becoming a popular consumer product, with the development of a hydrogel polymer called hydroxyl-ethyl-methacrylate (HEMA) by Wichterle and Lim (Bennett and Weissman, 2005). This material was used to produce the first soft contact lenses that were introduced to the market in 1971. The 1970s and 1980s saw developments in toric soft lenses, rigid gas permeable lenses for daily wear and extended wear and soft lenses for extended wear, leading to the introduction of the first disposable contact lenses in 1987. This lens wear modality expanded to include frequent replacement and daily disposable lenses.

The next big change in contact lenses came with the first silicone hydrogel contact lenses, which were commercially launched in 1998. Second and third generation lenses were subsequently introduced, and they became so popular that eye care practitioners and customers changed their type of contact lenses from traditional hydrogels to silicone hydrogels, as shown later in Figure 1.1. The history of these contact lens developments is summarised in Table 1.1.

Table 1.1: Important dates and events in the history of contact lens invention (cited by (Heiting, 2010)).

Year	Event
1508	Leonardo da Vinci described and sketched the first ideas for contact lenses.
1636	Rene Descartes suggested the idea of using a water filled tube to correct the vision.
1827	Sir John Herschel proposed making a mold of the wearer's eyes so contact lenses can be made to conform perfectly to the front of the eye.
1887	F.E. Muller produced the first glass contact lens.
1888	A.E. Fick and Edouard Kalt reported using glass contact lenses to correct vision.
1936	William Feinbloom produced the first contact lens containing both glass and plastic.
1948	Kevin Tuohy introduced the first rigid contact lenses.
1950	George Butterfield designed a plastic contact lens with multiple inside curves for better fitting characteristics and increased comfort.
1956	Otto Wichterle began making contact lenses with a soft, water-absorbing plastic.
1971	Bausch and Lomb introduced the first commercially available soft contact lens into the USA.
1978	The first toric soft contact lens was introduced in the USA for the correction of astigmatism.
1979	The first rigid gas permeable (RGP) hard contact lens was introduced.
1981	Extended wear soft contact lenses were introduced.
1983	The first tinted RGP lens became available for commercial distribution.
1986	An extended wear RGP lens became available for commercial distribution.
1987	Disposable soft contact lenses, a soft contact lens to change eye colour and a new formulation of fluorosilicone acrylate material for RGP lenses became available for commercial distribution.
1991	Frequent replacement soft contact lenses were introduced.
1992	Tinted disposable soft contact lenses were introduced.
1995	One-day disposable soft contact lenses were introduced by VISTAKON.
1996	First disposable lenses using ultra-violet absorber were available in the USA by VISTAKON.
1998	First silicone hydrogel soft lens (Balafilcon A) was introduced by ciba vision in the USA by CIBA VISION.
1999	Disposable bifocal soft contact lenses was introduced by VISTAKON.
2005	Second generation of silicone hydrogel soft lenses (Senofilcon A, Galyfilcon A) were introduced by VISTAKON.
2007	Third generation of silicone hydrogel soft lenses (Comfilcon A, Enfilcon A) were introduced by Cooper Vision.

1.1.2. Dispensing trends and popularity of contact lens wear

The number of contact lens wearers is estimated at 125 million people in the world, of whom 38 million people are in the USA, 15 million in Japan, and 3.5 million in the UK (SEED, 2011, Barr, 2005, CooperVision, 2014). Morgan et al. have published a series of papers that has reported on the dispensing trends for different types of contact lenses in the world since 2002. Figure 1.1 and Table 1.2 present a summary of these trends over the past 7 years (Morgan et al., 2013, Morgan et al., 2012, Morgan et al., 2011, Morgan et al., 2010, Morgan et al., 2009, Morgan et al., 2008, Morgan et al., 2007). In the latest report, they analysed more than 20,000 contact lens fits in 36 international contact lens markets. The most common lens type worn is a daily wear soft lens, which totalled 82% in 2012. Since the survey was first published in 2002, there has been a remarkable increase in silicone hydrogel use from close to 0% in 2002 to almost 35% in 2012.

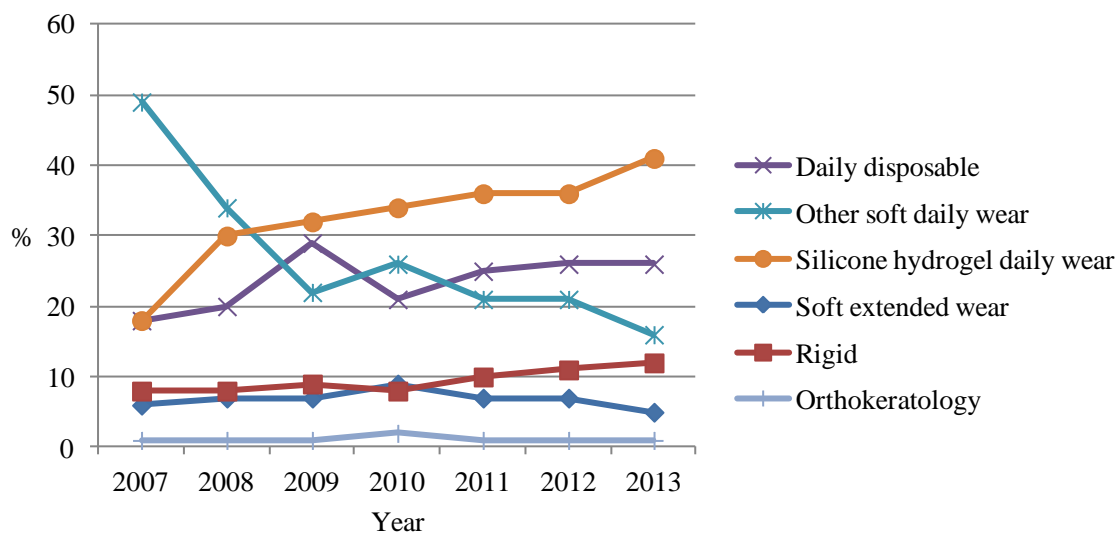


Figure 1.1: Global contact lens type fitting characteristics between 2008 and 2012 (from Morgan et al., 2012)

Table 1.2: Global contact lens type fitting characteristics between 2007 and 2013.

Category (lens) / Year	2007	2008	2009	2010	2011	2012	2013
Daily disposable (a) (%)	18	20	29	21	25	26	26
Other soft daily wear (b) (%)	49	34	22	26	21	21	16
Silicone hydrogel daily wear (c) (%)	18	30	32	34	36	36	41
Soft daily wear (a + b + c) (%)	85	84	83	81	82	83	83
Soft extended wear (%)	6	7	7	9	7	7	5
Rigid (%)	8	8	9	8	10	11	12
Orthokeratology (%)	1	1	1	2	1	1	1
Total (%)	100	100	100	100	100	100	100

Nichols has also produced annual reports that summarise the current state of the contact lens field in the United States of America, which has a large population of contact lens wearers (Nichols, 2014, Nichols, 2013, Nichols, 2012, Nichols, 2011, Nichols, 2010, Nichols, 2009). In the latest report (2014), 352 individual responses were obtained, revealing that more than half of the lens fits and refits were with a silicone hydrogel, whereas 26% were with traditional hydrogel lenses (Figure 1.2). The high dispensing rates of silicone hydrogel and hydrogel lenses are consistent with the Morgan et al surveys (Morgan et al., 2007, Morgan et al., 2008, Morgan et al., 2010, Morgan et al., 2011, Morgan et al., 2009, Morgan et al., 2012, Morgan et al., 2013). It seems likely that the use of silicone hydrogels will accelerate further in the near future.

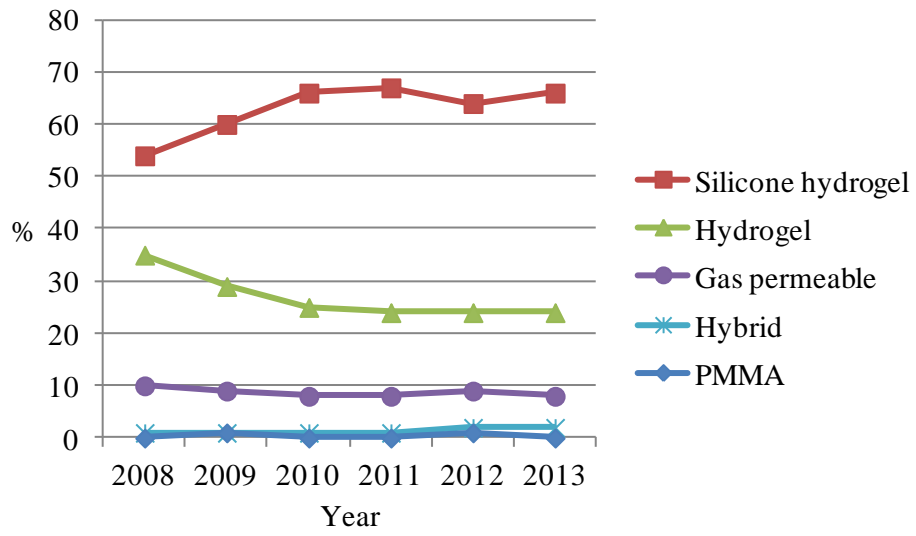


Figure 1.2: Percentage of different contact lens types prescribed in the USA (data from Nichols, 2009-2014).

1.2. The tear film and contact lens wear

1.2.1. The tear film

The pre-ocular tear film is considered as being formed into 3 layers: a superficial lipid layer, a middle aqueous layer, and an underlying mucous layer (Holly, 1981a, Rolando and Zierhut, 2001). Each layer has an important role. The principal function of the lipid layer is to prevent the tear film from evaporating. The aqueous layer is quantitatively the most important. It carries essential nutrients and oxygen to the cornea, and provides anti-inflammatory proteins. The mucous layer interacts with the microvilli of the corneal epithelium to anchor the tear film to the ocular surface, and the lipid layer assists in stabilising the tear film on the eye and limiting evaporation (Korb et al., 2002, Bron et al., 2004, Rolando and Zierhut, 2001).

A healthy tear film is essential for correct visual function of the eye. The pre-ocular tear film has several functions for the eye: it acts as a barrier to protect the eye from infection, it provides a smooth optical surface and nutrition to the ocular surface epithelia (Rolando and Zierhut, 2001). The tear film is renewed periodically to maintain a continuous covering following a blink. The average blink rate under concentration has been reported as 5 blinks/min (Tsubota and Nakamori, 1995). However, even a small change in tear film stability and/or volume can cause a significant alteration of the quality of the retinal vision. For example, it was reported that if the eye surface is not covered with the tear film, disruption of vision, discomfort and diseases of the eye at worst may result (Cedarstaff and Tomlinson, 1983). Montes-Mico (2007) also found that change in optical aberrations created by tear film breakup contributes to a reduction in retinal image quality.

When a contact lens is worn, tear exchange beneath the lens is an important factor. Oxygen to the cornea is primarily delivered to the cornea through the pre-lens tear film, contact lens and post-lens tear film. Although the oxygen permeability of the contact lens material has improved, the direct delivery of oxygen from the tear film is still essential for gas permeable lenses, and fresh tears should be circulated under the lens following each blink. Moreover, the tear exchange will contribute to washing away epithelial debris, toxic elements and foreign bodies under lenses (Rolando and Zierhut, 2001). In contrast, for soft contact lenses, there is very little tear exchange under the lens. It has been estimated that there is a tear exchange rate of 1-2%. This is very little compared to the one of hard contact lenses (Polse, 1979, McNamara et al., 1999). Polse reported the figure for a hard lens which is 10 to 20% per blink as the fractional tear replenishment rate (Polse, 1979). Also Paugh et al.(2001) stated that insufficient tear exchange under a soft lens has been cited as a key factor in the pathogenesis of contact lens-related infection. They cited the evidence presented by Mertz and Holden in 1981 who found that the post-lens debris obtained from a patient with an inflammatory reaction from an extended wear lens was composed of mucous, epithelial cells and neutrophils.

1.2.2. The effect of lens wear on tear evaporation

Since contact lens wear interferes with the organised structure of the tear film, and in particular with the formation of the superficial lipid layer, the rate of tear evaporation is also affected when contact lenses are worn (Korb et al., 2002). Guillon and Maissa (2008) reported that the presence of a contact lens resulted in a significantly reduced tear film stability and a thinner lipid layer.

Cedarstaff and Tomlinson (1983) measured the tear evaporation rate using resistance hygrometry in subjects wearing soft contact lenses. They found that: (1) contact lens wear disrupts the tear film and causes a significant increase in tear evaporation, (2) the increase in evaporation is not consistently related to the initial water content of soft contact lenses, and (3) the water lost by dehydration makes a minor contribution to the total increase in evaporation. A relationship was not found between the water content and the increase in tear evaporation.

The change in evaporation rate leads to a change in the rate of temperature change on the ocular surface. Purslow and Wolffsohn (2007) reported an inverse relationship between tear film stability and the ocular surface temperature (OST) in non-contact lens wearers. They suggested that temperature measurement may be useful for indirectly quantifying tear film dynamics.

1.2.3. The effect of lens wear on tear film thickness

Many researchers have examined the thickness of the tear film. It was initially believed that the total thickness of the tear film was less than $10\mu\text{m}$ (Holly, 1981a), and recent work by Wang (2003), using advancements in his original optical coherence tomography (OCT) technique, found the pre-corneal tear film thickness to be $3.3 \pm 1.5\mu\text{m}$ (Table 1.3). This result was similar to the $3\mu\text{m}$ value given by King-Smith et al (2000).

Table 1.3: Tear film thickness on the cornea (without lens wear)

Year	Author	Method	Subjects	Tear film thickness
1981	Holly	Unknown (Cited by Holly)	Unknown (Cited by Holly)	Less than 10 μ m
1992	Prydal et al.	Laser interferometry and confocal microscopy	6 subjects	34–45 μ m More than 4 times larger than earlier values
2000	King-Smith et al.	Interferometry	6 eyes	3 μ m
2003	Wang et al.	Ocular coherence tomography (OCT)	40 non-contact lens wearers	3.3 \pm 1.5 μ m (range: 0.8–8.2 μ m)

1.2.4. The effect of lens wear on tear film structure

Contact lens wear interferes with this organised structure, splitting the tear film into two layers, one layer in front of the lens and the other layer behind the lens: the pre-lens tear film (pre-LTF) and the post-lens tear film (post-LTF), respectively. Although researchers have measured the pre-LTF and post-LTF thickness, and the data obtained varies because different methods were used, there is a clear difference in results between soft and rigid lens types, with the post-LTF measured as being much thicker with rigid lens wear compared to soft lens wear (Table 1.4). A small difference was observed between the pre-LTF and Post-LTF when a soft lens was worn.

Table 1.4: Pre- and post-lens tear film thickness during contact lens wear

Year	Author	Method	Subject	Contact lens type	pre-LTF (mean±1S.D.)	Post-LTF (mean±1S.D.)
1986	Guillon*	Optical system and high- and low- magnification photography	Unknown	Unknown	5.5µm	n/a
1998	Fogt et al.*	Wavelength dependent fringes	Unknown	Unknown	2.7µm (0.5–5.0µm)	n/a
2003	Nichols and King-Smith	Measurement of reflectance spectra (direct estimate)	12 hydrogel lens wearers	Hydrogel (Acuvue II)	2.31µm (max 5.46µm)	2.34µm
2003	Wang et al.	Optical coherence tomography	80 eyes of 40 non-contact lens wearers	Silicone hydrogel (Night and Day)	3.9 ± 2.6µm	4.5 ± 2.3µm
				Hydrogel (Acuvue)	3.6 ± 2.1µm	4.7 ± 3.1µm
2003	Wang et al.	Optical coherence tomography	80 eyes of 40 non-contact lens wearers	Hard lens (PMMA)	9.8 ± 7.3µm	83.1 ± 24.1µm

*Cited by Nichols and King-Smith (2003)

1.2.5. The effect of lens wear on tear stability

In addition to the difference in tear film thickness, the stability of the tear film differs. Especially, the pre-LTF is considered unstable when a lens is worn (Holly, 1981). New generation silicone hydrogel lenses are designed to give a more stable tear film on the lens surface as they employ several strategies to improve the hydrophilicity of the lens surface such as plasma coating, plasma oxidation and internal wetting agent. Surface treatment of silicone hydrogel contact lenses in the market are summarised in Table 1.5. As many lenses use surface treatment, it could be expected that the wettability of the lens and the stability of the pre-lens tear film are increased.

Table 1.5: Surface treatment of silicone hydrogel contact lenses.

Commercial name (USAN*)	Manufacturer	Surface treatment
Clariti (Falcon II 3)	Sauflon	Non-disclosed
BIOFINITY (comfilcon A)	CooperVision	None
AVAIRA (enfilcon A)	CooperVision	None
Definitive (efrofilcon A)	Contamac	None
Acuvue OASYS (senofilcon A)	Johnson & Johnson	None; internal wetting agent (PVP**)
Acuvue Advance (galyfilcon A)	Johnson & Johnson	None; internal wetting agent (PVP**)
1 Day Acuvue TruEye (narafilcon A)	Johnson & Johnson	None; internal wetting agent (PVP**)
Air Optix Night & Day Aqua (lotrafilcon A)	Alcon	plasma coating
Air Optix Aqua (lotrafilcon B)	Alcon	plasma coating
Menicon PremiO (asmofilcon A)	Menicon	Plasma oxidation
PureVision (balafilcon A)	Bausch & Lomb	Plasma oxidation process
DAILIES TOTAL1 (delefilcon A)	Alcon	Soft surface gel with >80% water content

Adapted from an original table by Jones et al. (2013)

*USAN; United States Adopted Name, **PVP; polyvinyl pyrrolidone

To evaluate the surface wettability of contact lens *in vitro*, contact angle is measured by some researchers (Jones et al., 2013, Lin and Svitova, 2010, Read et al., 2009, Cheng et al., 2004). Contact angle is the angle formed by the intersection of the liquid-solid interface and the liquid-vapour interface. It is geometrically acquired by applying a tangent line from the contact point along the liquid-vapour interface in the droplet profile (Bracco and Holst, 2013). However, the contact angle is measured differently by each researcher; Chen et al. used the captive-bubble method, Read et al. used both sessile drop and captive bubble methods, and Lin and Svitova used a modified captive-bubble tensiometer-goniometer. However, as obtained contact angles are significantly affected by the methodology and experimental conditions, it is very difficult to make a comparison between soft lenses. Moreover, the strength of any relationship between *in vitro* measurement and

the clinical wetting evaluation on the eye *in vivo* has not been reported. Jones et al. (2013) stated that conclusive evidence that laboratory measurement of contact angle can predict the wetting performance of a contact lens on eye is lacking. The conclusion was that the tear film with lens wear has a complex and dynamic nature, and current techniques are not able to accurately reflect these characteristics.

In vivo wettability can be assessed by several different methods, such as the pre-lens non-invasive tear break-up time (NIBUT), tear thinning time, the rate of evaporation from the lens surface, and techniques based around specular reflection (Jones et al., 2013). For example, Thai et al. (2004) investigated the effect of contact lens materials on tear physiology. They measured several tear film parameters for five different hydrogel lenses; four traditional hydrogels and one silicone hydrogel (balafilcon A). They found no significant differences between traditional and silicone hydrogels in tear structure, wetting ability and tear thinning time. Similarly, Wang et al. investigated changes in the post-LTF thickness when silicone hydrogels were worn (Table 1.4), but did not find any statistical differences between hydrogel and silicone hydrogel contact lenses.

1.3. Contact lens wear and tear exchange

The most obvious difference between soft and rigid lenses is the larger size of pre-LTF in rigid lenses, which leads to a much higher tear exchange rate for rigid lenses than soft lenses (Kok et al., 1992; McNamara et al., 1999; Lin et al., 2002). This is due to the rigid lens material and to the design of these lenses. The rigid material means that the lens cannot align perfectly with the corneal surface, and effectively bridges over the

central lens. This creates a space behind the contact lens, which fills with tears. Each time the patient blinks, mechanical pressure is applied to the contact lens, which expresses the tears from under the lens, and which draws tears back under the lens when the lid retreats after the blink. This action creates a 'tear pump' that was important for old PMMA (Poly-methyl-methacrylate) rigid lenses, and which is impermeable to oxygen. The tear pump ensured oxygen was supplied to the cornea under the lens. Fink et al. (1992) investigated whether the difference in the base curve radius of rigid contact lenses affects the tear pump efficacy. A contact lens fitted in alignment with the corneal curvature was associated with the greatest central cornea oxygen debt under a static condition (without blinking), indicating limited tear exchange under the lens. However, no difference was observed amongst different fittings under a dynamic condition (with blinking).

As shown in section 1.2.1, adequate tear circulation around the lens washes away foreign bodies and infectious intrusions, such as bacteria and viruses (Rolando and Zierhut, 2001, Pflugfelder et al., 2004). However, the amount of tear exchange beneath the soft contact lens is considered to be very low because a well-fitted hydrogel lens covers the entire cornea and moves little following each blink. Therefore, significant tear exchange would not be expected. Estimating the rate of tear circulation over a lens is difficult, and does not appear to have been reported in the literature, but it may be possible to quantify the effect of tear movement indirectly using thermometry: the temperature of the contact lens and its rate of change may describe some aspects of the effect of different lens materials on the contact lens during wear. Thermography

might assist in understanding tear exchange by observing the change in temperature of the contact lens or ocular surface – a poor tear exchange will mean less heat exchange occurring between the lens and the tear film, and the lens may gradually heat up by retention of heat transferred from the eye. This might also be affected by the thermal characteristics of the lens material.

1.3.1. Oxygen supply to the cornea with contact lenses

Oxygen permeability and tear circulation are necessary for maintaining eye health. For the avascular cornea, oxygen is mainly supplied from oxygen within the atmosphere dissolving in the tears and being transferred through the surface epithelium (Figure 1.3). The peripheral cornea will also receive some oxygen through the limbal blood supply, but this has limited penetration. Similarly, the posterior cornea will receive some oxygen dissolved within the aqueous humour (Kwan et al., 1972). Placing a contact lens over the cornea interferes with this natural supply, and the inability of the cornea to obtain adequate oxygen may be a factor in ocular surface complications of contact lens wear, such as superior acute punctate keratitis, corneal erosion, or corneal oedema in the short term, and a decrease in the number of endothelial cells and onset of neovascularisation in the long term (Efron, 2001). Such complications may still occur even though the oxygen transmission of contact lens materials has markedly improved with each passing year, and research is performed continually to examine other factors that may contribute to these complications.

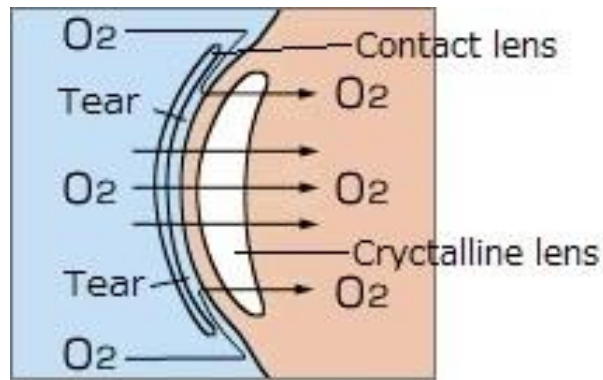


Figure 1.3: Oxygen supply to cornea when lens is worn.

In the past few decades, contact lens manufacturers have improved oxygen permeability (Dk) of lens materials, which is a product of diffusion (D) and solubility (k). Researchers have investigated the level of oxygen supply needed to avoid unwanted complications to ocular health. In the early 1980s, Holden and Mertz reported the minimum acceptable Dk/t (Dk per thickness of the lens) required to prevent lens induced corneal swelling as 24 and 87×10^{-9} ($\text{cm/sec})(\text{mlO}_2/\text{ml.mmHg}$) for open and close eye wear, respectively (Holden and Mertz, 1984).

In a similar manner, Brennan (2001) more recently calculated the contact lens oxygen flux under an open and closed eye with and without lens wear using a mathematical model. The equivalent oxygen percentage (EOP) was used to estimate the oxygen concentration beneath a contact lens. The oxygen flux information obtained from his study and the data from Holden and Mertz were incorporated and showed that the closed eye condition is more likely to induce corneal swelling and need a higher Dk/t of the lens material compared to an

open eye with the same contact lens and oxygen flux. Brennan also developed an oxygen diffusion model of the cornea by separating it into layers, as shown in Figure 1.4 (Brennan, 2005). Using this model, the oxygen consumption at different rates could be examined.

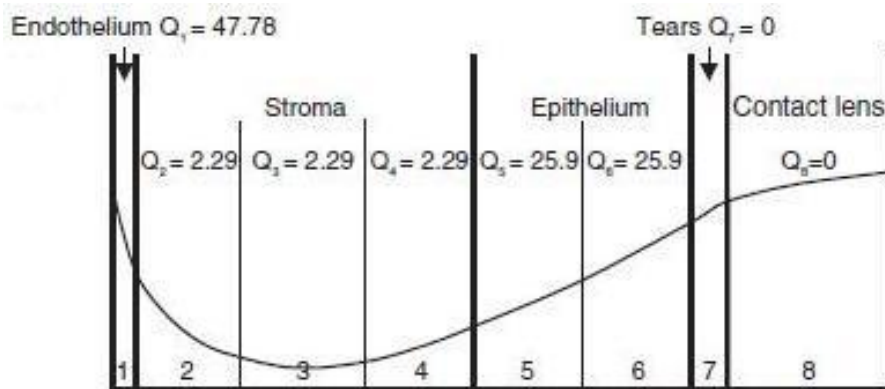


Figure 1.4: Illustration of the eight-layer oxygen diffusion model for a cornea covered by a contact lens. The curve represents an approximate pO_2 profile across the cornea. The layers are numbered sequentially from endothelium with Q_n as the consumption of the n th layer. pO_2 is always > 0 , so intra-corneal layer $Q \neq 0$ for any n . (Taken from Brennan, 2005)

Silicone hydrogel materials have a higher Dk compared to traditional soft lens materials because oxygen is more soluble in silicone rubber than in water. Thus, the problems associated with previous materials, such as corneal swelling and oedema due to insufficient Dk have been solved (Sweeney, 2004). However, Purslow et al have also shown that silicone hydrogel materials show a higher thermal capacity for retaining heat (Purslow et al., 2005). They found significantly greater OST in patients wearing silicone hydrogel contact lenses compared to traditional hydrogels; 37.5 ± 1.5 °C versus 35.3 ± 1.1 °C, respectively.

1.3.2. Complications of Contact Lens Wear

1.3.2.1. Contact lens related disease

As contact lens wear has become increasingly popular, the number of wearers exposed to potential risks and complications has also increased. There are various factors which influence the types of complications with contact lens wear. Bailey (1999) proposed an outline of contact lens diseases and their management, and the conditions often seen in contact lens wearers are summarised in Table 1.6. The majority of conditions occur on the cornea, but other complications such as pinguecula, CL-associated papillary conjunctivitis (CLPC) and giant papillary conjunctivitis (GPC) can be seen on the bulbar and tarsal conjunctiva (Itoi et al., 2005).

Table 1.6: Ocular pathology related to contact lenses and their care systems (adapted from an original table by Bailey (1999)).

Condition	Aetiology	Lens type	Symptoms	Signs
Abrasion	Trauma, Foreign body Clumsy handling, Damaged lens	Most seen in rigid, then soft	Pain, Lacrimation, Watering Photophobia	Red eye Linear corneal fluorescein uptake
Superior epithelial arcuate lesions (SEAL)	Mechanical	Soft	Chronic discomfort	Superior paralimbal epitheliopathy
Epithelial oedema	Hypoxic/toxic	All	Visual blur on lens removal	Dull corneal reflex
Corneal vessels (Neovascularisation)	Hypoxia	Most seen in soft, then PMMA and rigid	Visual blur if vessels cross axis	Corneal vessels
Stromal oedema	Metabolic	Usually EW of soft	± Visual blur	± corneal haze, Pachymetry Slit-lamp microscopy
Endothelial blebs	Metabolic	All	None	Slit-lamp microscopy
Toxicity	Chemicals	Usually soft	Severe pain on inserting lens	Ciliary flash Punctate corneal fluorescein uptake
Lens related red eye	Lens spoilation	More seen in soft then rigid	Chronic discomfort Redness	± punctate corneal fluorescein uptake
Infection	Contamination of lens or lens care materials Altered corneal response	More seen in soft then rigid	Pain, Red eye Purulent discharge, Visual blur	Red eye, Purulent discharge Corneal ulcer, Corneal oedema
Dellen, 3-9 o'clock stain	Local drying	Rigid	± redness, ± discomfort	Interpalpebral redness
Dry eye	Metabolic	All	Red eye, Eyelids stick together Blurred vision	feelings of dryness, grittiness or soreness
Corneal endothelial disorder	Hypoxia	All	None	Number of cells decline. Morphology changes.
Epithelial microcysts	Hypoxia	All	None	cystic vesicles on the epithelial surface of the cornea

According to the UK College of Optometrists guidelines for clinical management, CLPC and GPC are more often seen in soft lens wearers compared with rigid lenses (College of Optometrists, 2013). Both conditions are associated with the progressive development of protein deposits on the anterior lens surface during lens wear promoting an inflammatory reaction in the tarsal conjunctiva.

After insertion of the lens, it begins to be coated immediately, and around 90% of the surface area is likely to be covered with deposits after eight hours of wear (Bailey, 1999). The deposits are derived from substances in the tear film. These deposits serve as an immunogenic stimulus for the development of the disease. As care systems and lens materials have been improved, the deposit on the lens surface is reduced. However, if the lens is not properly cleaned, or the wearing time is longer, deposits on the lens surface can still cause a change in the upper lid tarsal conjunctiva. Similar changes can also be induced by thick or poorly designed or manufactured lens edges, as well as by meibomian gland dysfunction and atopy (College of Optometrists, 2013).

Bailey suggested that the modality of the lens wear, the oxygen requirement of the cornea, and deposits on the contact lens surface are the main factors in contact lens complications (Bailey, 1999). In addressing these factors, contact lens manufacturers have adopted two main approaches: a move towards disposable or planned replacement of lenses, and new materials, particularly silicone hydrogel. Silicone hydrogel lenses are available in most countries, and their introduction has almost completely solved corneal oedema problems due to a low Dk

material, particularly in extended wear modality. However, several non-inflammatory complications still exist (Dumbleton, 2003): post lens debris is more likely to be found in patients who wore their lenses for 30 days than 7 days; superior epithelial arcuate lesions (SEALs) can develop as a result of the stiffness of the material and their inflexibility to conform to the limbus; and corneal erosions can occur due to mechanical stress.

Forister et al. also reported the prevalence of contact lens related complications and its relationship with lens type and wearing modality (Forister et al., 2009). According to them, gas permeable lens (GP) wearers were statistically less likely to have a complication compared to soft contact lens (SCL) wearers. Lid papillae and giant papillary conjunctivitis were the most prevalent complications for both GP and SCL wearers. Silicone hydrogel lenses had a slightly lower rate of complications than non-silicone hydrogel lenses, although this was not statistically different. Moreover, extended wear of any kind of CLs had a higher complication rate compared with daily wear, although, again, this was not statistically significant.

1.3.2.2. Relationship between lens wear and infection

Despite developments in contact lenses, the risk of infections, such as microbial keratitis, remains a problem. Although contact lenses are safely used all over the world, contact lens use carries the risk of eye infection. This is regarded as a significant problem, because the worst cases may result in serious vision loss.

According to Stapleton et al. (2008), vision loss occurs in 0.6 per 10,000 wearers. Particularly, microbial keratitis is the most common infection associated with contact lens wear. In addition, recent outbreaks of keratitis in contact lens wearers have included fusarium keratitis, a fungal form of the infection, and acanthamoeba keratitis (American Academy of Ophthalmology, 2012). Although infection is rarely observed in a normal healthy eye, various factors have been considered to increase the risk of microbial keratitis with contact lens wear. When a healthy eye is infected, certain cytotoxic bacteria may damage the epithelium on an uninjured corneal surface if bacterial contact is prolonged.

People who wear soft contact lenses are more likely to experience eye infections than those who wear rigid gas permeable (RGP) lenses (Stapleton et al., 2008). Further, extended/continuous wear increases the risk of infection compared to daily wear, with extended soft contact lens users having a 36.8-fold higher risk compared to that of RGP contact lenses users (Stapleton et al., 1993). The risk of infections appears to increase as overnight use increases: compared to up to 6 nights of use, the risk is 3.26-fold greater for continuous use of 7 to 12 nights. In the same way, the frequency of contact lens-related ulcerative keratitis and its relationship to the type of contact lens have been investigated. Mah-Sadorra et al. (2005) reported that the soft daily wear frequent replacement lens was the most common lens type associated with corneal ulcers. These authors postulated that contact lens-related corneal ulcers will continue to be a serious problem, despite advances in contact lens technology.

Schein et al. (2005) investigated the effects of the extended wear of silicone hydrogels on the risk of microbial keratitis with and without loss of visual acuity. In a 12-month study, 10 of

5561 patients presented with microbial keratitis, resulting in an overall annual microbial keratitis rate of 18 per 10,000 [95% confidence interval (CI): 8.5–33.1]. Two cases were observed as microbial keratitis with loss of visual acuity, and an additional 8 cases without loss of visual acuity. The rate of microbial keratitis was lower among individuals who wore contact lenses overnight for more than 3 weeks compared to those with less than 3 weeks: 11.6 per 10,000 (CI: 3.7–27.3) and 39.7 per 10,000 (CI: 12.7–92.8), respectively.

As many researchers have reported, extended wear is considered a significant risk for infection because of the limited tear exchange during sleep. As discussed in Section 1.2.1, tear exchange has an important role to prevent these CL related complications, since, if the tear film exchange is not enough, trapped waste products of metabolism will not be washed away. This may increase the risk of the infectious disease.

1.3.2.3. The effect of contact lens material

Contact lens material may also be a factor affecting complications. As can be seen in Table 1.6 some diseases such as corneal neovascularisation, corneal endothelial disorders and epithelial microcysts are induced by an insufficient oxygen supply. As described in Section 1.3.1, the oxygen requirement to the cornea is very important and it depends on the oxygen permeability of the lens material.

Efron and Morgan (2009) also suggested a relationship between increased lens material modulus and contact lens-associated keratitis. The study, named the Manchester Keratitis Study,

demonstrated that the severity of keratitis was significantly reduced in those subjects wearing silicone hydrogel lenses versus those using traditional hydrogel lenses for overnight wear. This was expected because the cornea is able to obtain the increased oxygen supply through a silicone hydrogel lens. However, it conflicts with the results of Stapleton et al. (2008). In their findings, the incident rate of microbial keratitis in overnight wear of silicone hydrogel lenses was higher than that of hydrogel lenses. This difference may be due to lens modulus (Efron and Morgan, 2009). They suggested a relationship between increased modulus and contact lens associated keratitis, due to the increased pressure and possible sub-clinical trauma to the cornea caused by the eyelid/silicone hydrogel lens combination. Since silicone hydrogel lenses available at that time of the Stapleton et al. study were of a higher modulus, this might have influenced her findings.

In addition to the modulus, other factors such as surface treatment or wettability of the material may affect the subjective discomfort and dry eye symptoms. Although the silicone hydrogel material reduces the risk of insufficient oxygen supply, it is not enough to abolish other problems.

1.3.2.4. Other factors

There are also patient-related factors, such as environment, hygiene, and compliance, which play an important role. Also, the smoking habits, hygienic conditions associated with lens cases and internet purchase of contact lenses may be related. According to Rabinovitch, a severe contact lens-related ulcer is more likely to occur in warmer conditions (Rabinovitch et al., 1987),

and Stapleton reported that severe microbial keratitis related to contact lenses is more likely to be observed in warm, humid regions (Stapleton et al., 2007).

In summary, it appears that the infection risk cannot be assessed simply in terms of lens type or oxygen permeability. In addition, tear exchange and tear temperature may be more important than previously thought. Moreover, the effect of contact lenses on ocular surface temperature may be related to the incidence of infection. Therefore, research to investigate the ocular surface temperature, its distribution and also its dynamic change is very important.

1.4. Principles and history of infrared thermograph

Infrared imaging is now widely used in many situations including medical and industrial areas as a way of measuring temperature of an object's surface. In ophthalmic research, as Purslow listed (Purslow, 2005), this ability plays an important role in both research and clinical situations, such as ocular physiology and pathology, ocular blood flow, tear assessment with and without contact lenses. Modern thermometry relies on infrared imaging technology, which is entirely non-invasive and risk-free since it monitors the heat energy emitted by the human body.

The origin of this principle is based on the finding of infrared radiation by the British astronomer Sir William Herschel (1738-1822). He discovered the invisible rays beyond the visible spectrum in 1800. He noticed that infrared radiation behaves similarly to visible light, and could be reflected and refracted (Hildebrandt et al., 2010, Ring and Ammer, 2012). After this finding, he referred to this new portion of the electromagnetic spectrum as the

‘thermometrical spectrum’. The radiation itself he sometimes referred to ‘dark heat,’ or simply ‘invisible rays’. The term ‘infrared’ began to appear around 75 years later, but it is not clear who came up with the name.

Infrared radiation is just one part of the electromagnetic spectrum (Figure 1.5), which can be divided into a number of wavelength regions. Infrared radiation ranges about 700nm (0.7 μ m) to about 0.1mm (100 μ m) and it consists of near, middle, far, and the extreme infrared. Thermometry mainly detects middle infrared radiation (Breithaupt, 2003).

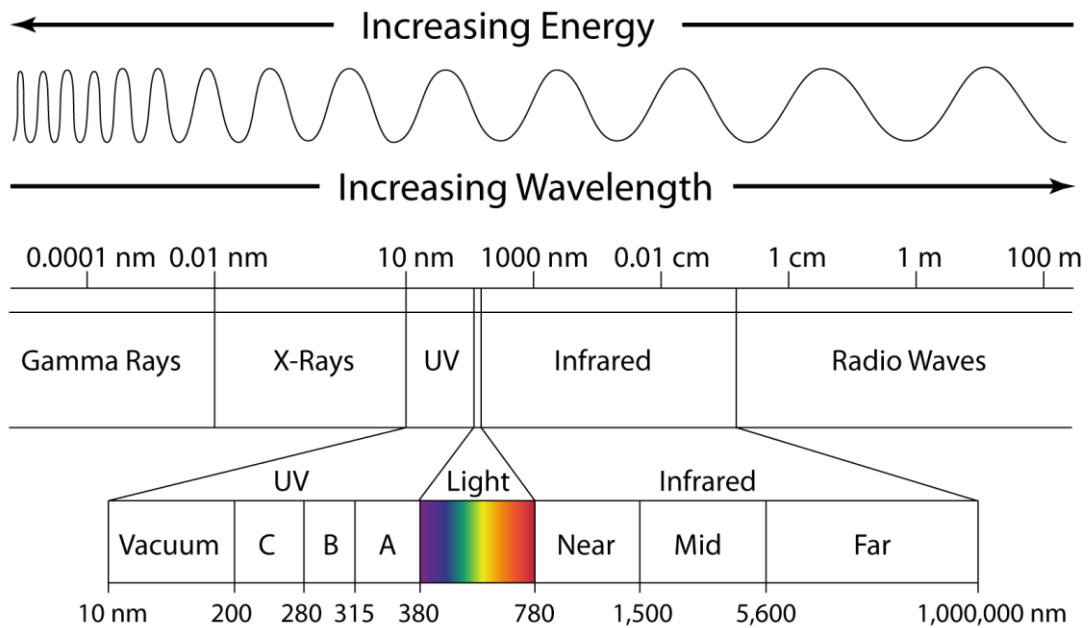


Figure 1.5: Electromagnetic spectrum wavelength

(Taken from <http://www.windowimage.sg/images/electromagnetic-spectrum.png>)

After Herschel noticed the existence of infrared radiation, he tried to look for a point at which the heating effect reaches a maximum. He proceeded to test the heating effect of the various colours of the spectrum formed on the top of a table by passing sunlight through a glass prism. He placed thermometers inside and outside (as a control) the sun's rays. The thermometers showed that the temperature detected steadily increased when moving from the violet end to the red end of the visible spectrum, and that the maximum point was beyond the visible red end.

1.4.1. Blackbody

When a body is warmer than its surroundings, it radiates more energy than it absorbs. A perfect black body is defined as an object that absorbs all radiation incident on it: visible, infrared, ultraviolet, or otherwise. Also the body is able to emit energy at exactly the same rate at which it absorbs energy. This is explained by Kirchhoff's law (Lerner, 1996). It states that a body capable of absorbing all radiation at any wavelength is equally capable in the emission of radiation (Hildebrandt et al., 2010, Ring and Ammer, 2012).

In addition, there are another three laws that describe the radiation emitted from a black body. Firstly, Planck's law describes the spectral distribution of the radiation from a black body by means of a formula. The energy density of radiation per unit frequency interval for black-body radiation is described by the Planck formula as below (Figure 1.6).

$E(\lambda, T) = \frac{2\pi hc^2}{\lambda^5 (e^{hc/\lambda kT} - 1)}$ <p>where [E] = W/m²/m</p>	λ ... Wavelength c ... Speed of light k ... Boltzmann's constant h ... Planck's constant $e = 2.718$... Base of Natural Logarithms	$[T] = \text{Kelvin}$ $[\lambda] = \text{meters}$ $h = 6.626 \times 10^{-34} \text{ Js}$ $c = 2.998 \times 10^8 \text{ m/s}$ $k = 1.381 \times 10^{-23} \text{ J/K}$
--	---	--

Figure 1.6: Planck's formula. (Taken from Federation of American Scientists, http://fas.org/irp/imint/docs/rst/Sect9/Sect9_1.html)

Using this formula he produced a family of curves (Figure 1.7), which shows the maximum radiant emission for different temperatures: the higher the temperature, the shorter the wavelength at which maximum occurs.

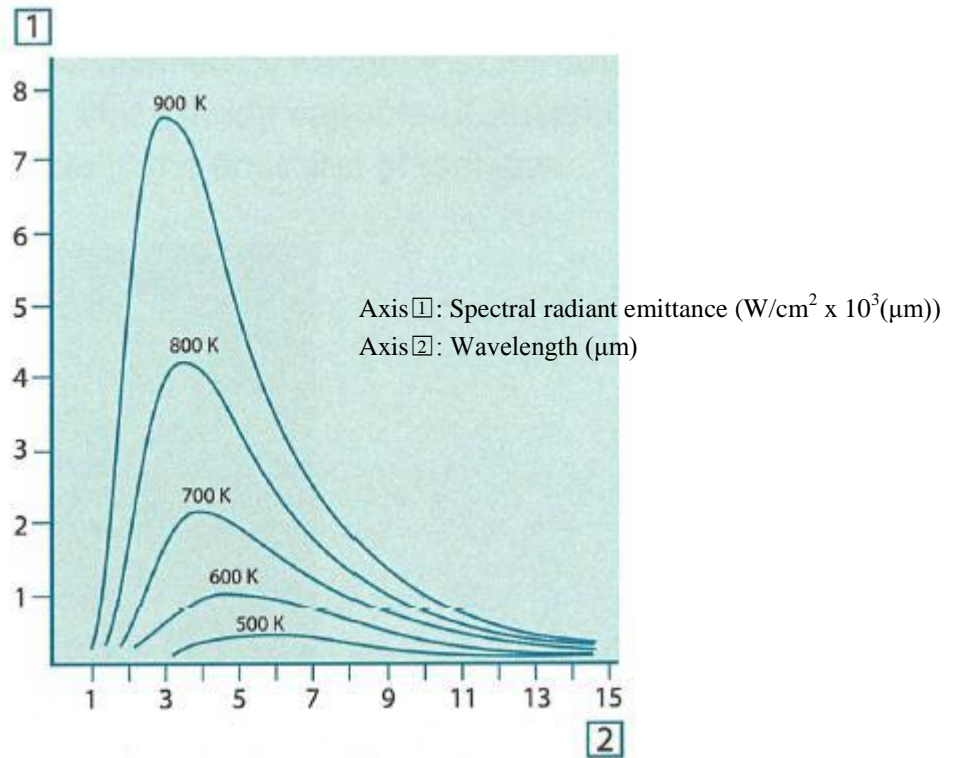


Figure 1.7: Black body spectral radiant emittance according to Planck’s law, plotted for absolute temperatures (Taken from FLIR SYSTEMS, 2007).

Secondly, Wien’s displacement law expresses mathematically the common observation that colours vary from red to orange or yellow as the temperature of a thermal radiator increases. And thirdly, Stefan-Boltzmann’s law can calculate the total radiant emittance of a black body.

1.4.2. Measurement of the ocular surface

To measure the ocular surface temperature (OST), the infrared radiation emitted from the combined tear film, cornea and associated tissues is detected. Both the tear film and cornea have high water contents, and so can be considered as a single continuous phase, and because water acts as an effective absorber of infrared radiation (Lerman, 1980), these structures can be regarded as black bodies that absorb all electromagnetic radiation and emit energy at the same rate (Lerner, 1996). According to Mapstone (1968a), the deeper ocular structures contribute very little to the radiation from the anterior eye, so the measured temperature of the eye can be treated as the temperature of the anterior eye. That is to say, the measured temperature is that of tears, and the radiation of the cornea itself can be measured only when the tears are absent.

As the tear film is a dynamic structure, its thickness is an important factor in measuring the temperature. According to Hamano et al. (1969b), a tear film thickness of 20 μm or more will exhibit 100% absorption and emission of infrared radiation, whereas a tear film thickness of 10 μm will absorb 80% and that of 4 μm will absorb only 55%. The thickness of the tear film is under debate, but is generally assumed to be around 3 μm (King-Smith et al., 2000, Wang et al., 2003).

1.5. Development of infrared imaging and its application in medicine

The technology of thermal imaging in medicine shifted to the practical stage in the 20th century. According to Diakides, the United States was the pioneer in the development of the clinical use of infrared imaging, which began in the late 1960s for neurology, surgery, oncology, dentistry, and dermatology (Diakides, 1998). Diakides stated that the origin of thermal imaging

technology was military, including target acquisition, reconnaissance, and surveillance. This technique has also been applied for plant maintenance, in automotive, chemical, civil engineering, and construction industries, weather forecasting, and astronomical observation.

The first instrument to detect skin temperature was invented by Hardy in 1934 (Purslow and Wolffsohn, 2005). However, there were some disadvantages of thermal imaging, such as low temperature resolution, limited magnification, and long scanning times at this point.

From the 1960s to the 1980s, a new detector with a strip of cadmium-mercury-telluride designed to achieve noise reduction within the element was developed by Dr C.T. Elliot (Ring, 1998). It became possible to obtain ultra-high resolution by using this detector. Moreover, the ability to detect temperature across a wide area reached the stage of practical application. A thermal sensitivity of up to 0.05 Kelvin and a spatial resolution of 25–50 μm were developed. This breakthrough also reduced the cost of camera and led to the widespread use of the technique (Diakides, 2000).

In the 1990s, infrared measurement reached a further level of high performance. The new devices included a special lens system that allowed a specific portion of the infrared spectrum to pass through to a photosensitive detector, and the infrared energy was subsequently converted into a measurable voltage, current, or resistance (Purslow and Wolffsohn, 2005). The displayed image on a monitor is termed a “thermograph” at this stage.

The construction of modern infrared thermal camera is similar to a digital video camera. The main components comprise a lens that focuses infrared radiation onto a detector, and electronics and software to process and display the signals and images.

The majority of infrared cameras have a focal plane array (FPA) as a detector instead of a charge coupled device (CCD), which digital cameras use. The FPA has micrometer size pixels made of various materials sensitive to infrared radiation. FPA detectors can be classified into two categories: thermal detectors and quantum detectors. A common type of thermal detector is an uncooled microbolometer made of a tiny vanadium oxide (VO_x) or amorphous silicon (a-Si). The advantages of microbolometers are a lower cost and a broader spectral response than quantum detectors (FLIR SYSTEMS, 2010).

The performance of the detector is a function of sensitivity, resolution and range. Sensitivity, which is the ability to resolve two objects of nearly equal apparent temperature, is described by the level of noise. The Noise Equivalent Temperature Difference (NETD) is the same parameter as thermal sensitivity. A better (small) NETD value means that the camera is able to provide a better performance range: the thermal camera can detect minute temperature differences between the background and an object.

Microbolometer operates according to non-quantum principles. This means that they respond to radiant energy in a way that causes a change of state in the bulk material, such as resistance or capacitance. Generally, a microbolometer does not require a cooling system, which allows

compact camera designs and low cost. Calibration software in these cameras is oriented toward thermographic imaging and temperature measurement.

For the measurement of thermographs, atmospheric windows must be used because transmissivity of the atmosphere is very high. As can be seen in Figure 1.8, there are two windows: 3-5 μm , the mid-wave windows and 8-14 μm , the long-wave windows.

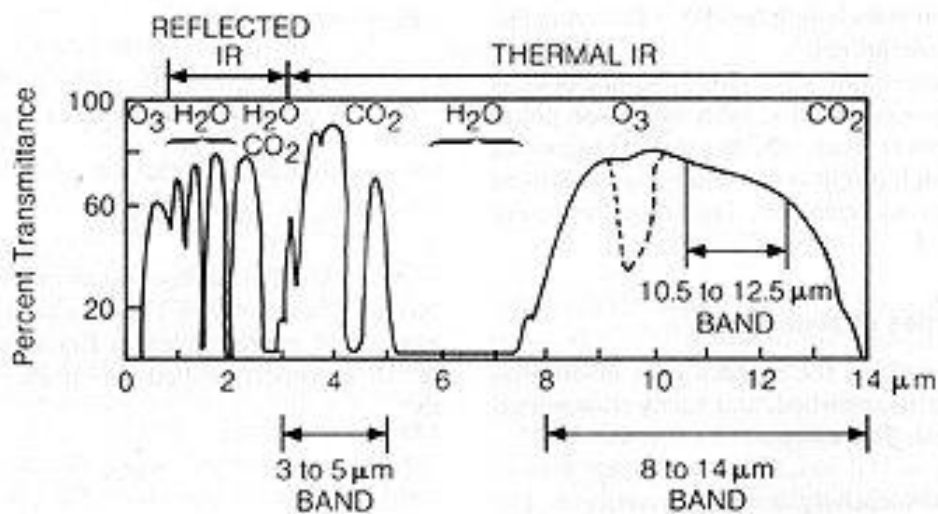


Figure 1.8: Atmospheric attenuation. (Taken from Sabins (1987))

In atmospheric windows, the camera receives three different sources which are a) the emission from the object, b) reflected emission from ambient sources and c) emission from the atmosphere. To obtain the correct target object temperature, the thermal camera software requires inputs for the emissivity of the object, atmospheric attenuation and temperature, and temperature of the ambient surroundings (FLIR SYSTEMS, 2010).

Obtained data is displayed as a colour thermal picture (thermogram) on a monitor (Figure 1.9). Yellowish area has a higher temperature, bluish area has lower. The temperature distribution is isotherm. A thermogram presents areas of equal temperature by similar colour. Corneal isotherms presents elliptically-shaped with long axis horizontal (Purslow, 2005).

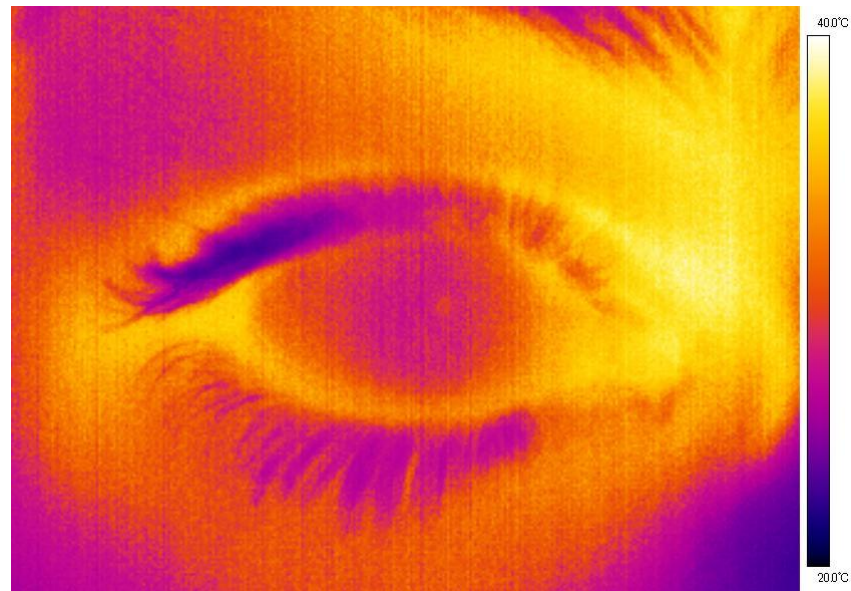


Figure 1.9: Example of an ocular thermogram.

Currently, infrared thermography is employed as a diagnostic technique for the detection and treatment of vascular disorders, breast cancer, arthritis, and rheumatism (Ring and Ammer, 2012). When a tissue is injured, inflammation results in various reactions: heat, swelling, redness, pain, and loss of function. Therefore, the infrared camera can detect the area with abnormalities because the area produces heat. An example of this effect is shown in Figure 1.10, where a patient with breast cancer has an increased temperature in the left breast compared to the right breast, indicating the location of the abnormality. A similar effect is seen with ocular conditions in Figure 1.11, for a patient with acanthamoeba keratitis in the right eye.

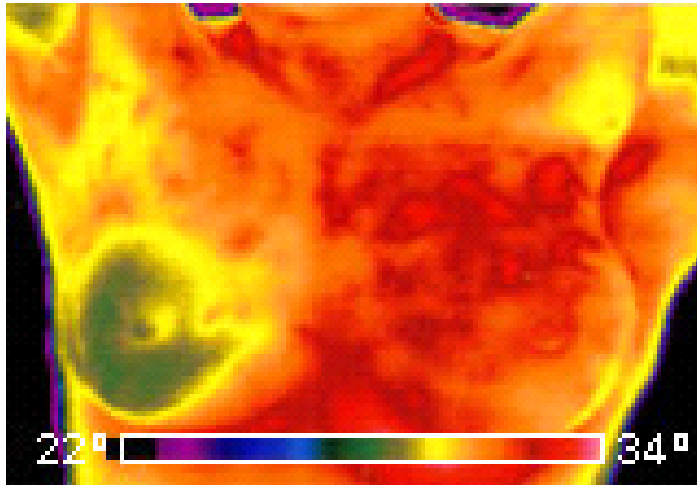


Figure 1.10: Thermal image of a patient with breast cancer, showing increased temperature in the left breast (taken from <http://www.flir.com/thermography/eurasia/en/content/?id=11444>).

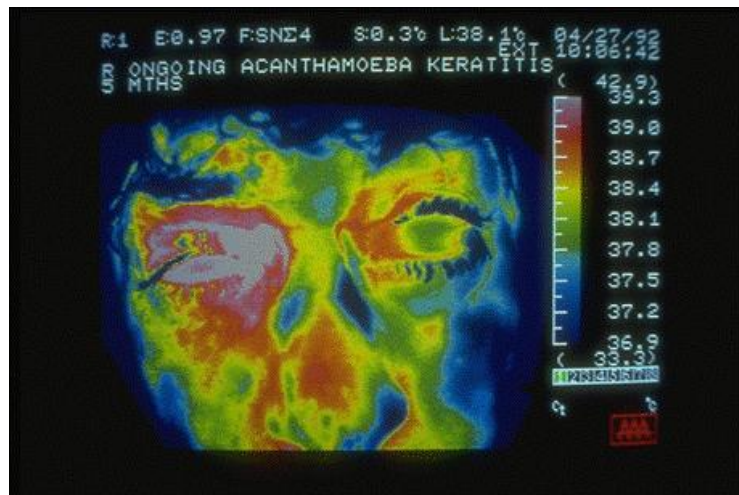


Figure 1.11: Thermal image of acanthamoeba keratitis in the right eye (taken from http://www.bausch.com/en_US/ecp/resources/image_library/miscellaneous.aspx).

1.6. Measurement of ocular surface temperature

1.6.1. Early technique of ocular thermography

1.6.1.1. Contact Method (Thermistor)

The thermistor was used as a typical contact method until the late 1980s. The thermistor consists of a lucite tube in which a ceramic probe is sealed in a glass envelope. It detects changes in resistance within the coiled wire probe, and converts this to a temperature (Hill and Leighton, 1965a). However, this technique has several disadvantages principally because contact methods disrupt the tear film structure and interfere with the sensation of the ocular surface and may induce reflex tears. Several studies have used topical anaesthetics to reduce the subjective discomfort, but this can also affect tear film stability and temperature. For example, Wilson et al. (1975) found that benzalkonium chloride, which is often used as a preservative substance in anaesthetics, shortened the time required for the presence of dry spots on the corneal surface. This indicates that tear film stability has been affected, and along with it, tear evaporation. Moreover, the temperature of the anaesthetic when instilled may influence the temperature of the object.

Alternatively, the thermistor was attached to a scleral lens to investigate the temperature of tear film beneath the lens (Hill and Leighton, 1965c, Hill and Leighton, 1965a, Hill and Leighton, 1965b), or was sandwiched between two soft contact lenses (Martin and Fatt, 1986). The most crucial disadvantage of the contact methods is that they can only measure at 1 spot at any given time and cannot measure the temperature gradient across the eye.

Even so, the thermistor can still provide useful information. For instance, Dixon and Blackwood (1991) investigated the thermal variation of the human eye and its adnexa and compared this with the oral measurements by means of direct methods, such as a digital fever thermometer, a tele-thermometer, and a diameter micro thermistor probe. Their results showed that the temperature in the mouth was the highest, with the surface of the cornea, the cornea under a contact lens, and the surface of the contact lens showing, respectively, decreasing temperatures. Furthermore, they did not find a significant difference in the magnitude of the decrease in the corneal temperature under rigid or soft contact lenses.

1.6.1.2. Non-Contact Method (Bolometer)

The first non-contact method using radiometry was developed by Zeiss in 1930, and the technique was improved and made practical by Mapstone (Mapstone, 1968b). Unlike X-rays, magnetic resonance imaging (MRI), or ultrasound, this non-invasive method is not associated with risks, and it can precisely measure the ocular surface temperature. In response to the disadvantages of the contact methods, a series of new instruments were invented to improve the accuracy of measurement, and the first such instrument was the bolometer.

The bolometer is a non-contact method that detects infrared radiation in the range 1-25 μ m. The principal of the bolometer is to convert the radiation readings to the true temperature. Although the bolometer is able to measure the temperature distribution across the eye, the area is limited to a 10 mm diameter because the bolometer must be positioned very close (about 5 mm) to the cornea. In previous research, OST was measured using the bolometer over a 4mm diameter area and within a range of 33-36 °C (Fatt and Chaston, 1980).

1.6.2. Modern ocular thermography

The latest infrared thermal cameras improved over the disadvantages of the bolometer, such as low sensitivity, the limit of measurement to a small sample area, and a very short distance to the target. Also, real-time measurement is possible at a high frame rate. Frame rate means how many thermal images per second the camera records. The infrared cameras used in this thesis can record up to 60 images per second (60Hz), which is fast enough to capture the dynamic change of OST as a video (FLIR SYSTEMS, 2009).

In the late 1990s, the use of the modern infrared camera became popular and some researchers started to report OST (Table 1.7). However, there have been only a few reports in the literature that have measured OST with lens wear, and only a few researchers have reported the observation of the anterior eye with contact lens wear (Table 1.8 including results with thermistor and bolometer).

Table 1.7: Ocular surface temperature without contact lens wear.

Year	Authors	Infrared camera (Manufacturer)	Subject	Location	Time after blink	Temperature (°C)
1995	Morgan et al.	Thermo Tracer 6T62 (NEC San-ei Instruments)	36 dry eye patients 27 control group	Central cornea	4 to 5 s	31.94 ± 0.54
1999	Girardin et al.	THI-500 (Tasco Japan)	266 Caucasians	Central cornea	2 s	33.7 ± 0.6
2000	Craig et al.	Thermo Tracer 6T62 (NEC San-ei Instruments)	9 with dry eye, 13 healthy control subjects	Central cornea	0 s	33.82 ± 0.36
2005	Purslow et al.	Thermo Tracer TH7102MX (NEC San-ei Instruments)	8 subjects (control group)	Central cornea	0.15 s	35.0 ± 1.1
2007	Purslow and Wolffsohn	Thermo Tracer TH7102MX (NEC San-ei Instruments)	Right eyes of 25 subjects	Average of 9 points	0.15 s	36.14 ± 1.11
					2 s	35.4 ± 1.3
2009	Sodi et al.	Agema THW880 (Agema Infrared Systems, Sweden)	a) 51 with diabetic retinopathy b) 53 healthy controls	Central cornea	Unknown	a) 34.80 ± 0.54 b) 35.42 ± 0.56
2009	Tan et al.	Thermo Tracer TH9100MV (NEC San-ei, Japan)	60 Chinese subjects	Geometric centre of cornea	Unknown	34.49 ± 0.47
2009	Acharya et al.	Vario Therm Camera	67 normal subjects c) below 30 yr of age d) 30–49 yr of age e) 50 yr of age and above	Average corneal temperature	Unknown	c) 34.038 ± 0.59 d) 33.35 ± 0.53 e) 32.64 ± 0.22
2010	Kassel et al.	Fluke Ti25 (Fluke, USA)	11 healthy subjects	Corneal temperature	Unknown	36

Table 1.8: Ocular surface temperature with lens wear.

Year	Authors	Infrared camera (manufacturer)	Subject	Contact lens type	Location	Time after blink	Temperature (°C) and findings
1969	Hamano et al.	Infrared medical radio-thermometer (MT-3, Barnes & Co., USA)	2 habitual wearers	Hard lens	Centre of cornea	Unclear	The difference between the naked eye and that with a lens was within 0.5 °C.
1980	Fatt and Chaston	Bolometer (Dermo-Therm of Raytek, Inc.)	6 subjects	Hard lens, Soft contact lenses	Circle on cornea with a 4 mm diameter	Unclear	31.5–33 with hard lens 34–35 with soft lens
1994	Soh	Unknown	98 normal subjects	RGP/soft extended wear	Central cornea	Unclear	The surface temperature in soft lens wearing was lower than that in controls (RGPs).
2005	Purslow et al.	Thermo Tracer TH7102MX (NEC San-ei Instruments)	48 in total, 8 in each group including control	Lotrafilcon A DW/CW* Balafilcon A DW/CW Etafilcon A DW	Central, nasal, superior, inferior, temporal	8 sec after blink	Average of all lenses 37.1 ± 1.7

*DW: daily wear, CW: continuous wear

OST without lens wear can be considered as being the temperature of the tear film in the eye. As noted earlier, when a lens is worn, the tear film is divided into two phases, the pre and post-lens tear film. Lin et al. (2003) suggested that both pre and post-lens tear film influence OST. However, as the pre-lens tear film is more likely to change and disrupt in the short term (Korb, 1994), it will have a more significant effect on the OST, compared to the contact lens itself or the post-lens tear film. Therefore, the quality of tear film of subjects will be an important factor.

There is a range of normal ocular surface temperature, given in Table 1.7, without contact lens wear of 32-36°C. This range is most likely due to the different cameras and analytical methods (software tool or selected points/area to calculate) used, and the different time points after blink at which temperature is measured, as well as subject variables. Details of subjective factors and other possible factors are discussed in the next section.

1.7. Factors that affect ocular surface temperature

Kassel et al. (2010) reported that the corneal temperature is related to both body temperature and environmental conditions – temperature, humidity, air movement. In their study, a linear relationship between corneal and body temperature was found in the rat. Although an initial relationship was found in a human study, the corneal temperature reached a plateau at 36.5–37.0°C. A linear relationship was also found between the environmental and corneal temperatures, but the slope was less steep compared to that observed between the cornea and core body temperature.

1.7.1. Location of measurement

A thermograph of the ocular surface describes a series of ellipsoidal isotherms with their long axis in the horizontal. Efron et al. (1989) observed that the coolest area of the OST was slightly inferior to the geometric centre of the cornea. In contrast, the limbal area is warmer than the corneal centre by 0.45°C in normal eyes, presumably due to the closer location of a blood supply. The central cornea has greater exposure to the surroundings and is further from the blood supply, which is thought to explain why the temperature of this area decreases at a faster rate compared to other areas after blinking.

1.7.2. Experimental conditions

Purslow (2005) performed a detailed investigation of experimental conditions that might affect ocular surface temperature measurement, such as environmental factors and subject adaptation, and provided a summary of the experimental conditions that should be considered in any study:

- Subjects should be assessed at similar times of day (± 1 hr).
- Room temperature and humidity should be controlled within $\pm 1^\circ\text{C}$ and $\pm 1\%$, respectively, and should be recorded.
- Subjects should be given at least 10 mins to adapt to room conditions, and should have been in the building for at least 20 mins prior to this.

In this thesis, the experimental conditions satisfied these criteria.

1.7.3. Subjective factors

Several studies have revealed relationships between eye temperature and gender, race, or age (Schwartz et al., 1968). In the early 1980s, Alio and Padron (1982) evaluated the influence of age and gender on eye temperature with infrared thermometry, reporting a significant reduction

in eye temperature with age, but no correlation with gender. In 1993, Morgan also found no relationship between ocular temperature and age when using an advanced infrared camera; further, this study found no relationship between eye temperature and gender (male vs. female) or race (Caucasian vs. Chinese). In another study, Morgan et al. (1999) investigated the rate of temperature reduction and found a change of -0.010°C per year. Although the data from Alio and Padron's study and Morgan's study cannot be compared directly because the thermometry method differed between these studies, age appears to be an effective factor for OST.

Fujishima et al. (1996), who investigated corneal thermal temperature change following blinking in patients with dry eye, using an infrared radiation thermometer, found that the OST decreased rapidly when the eye was kept open. Further, these authors stated that the corneal temperature in subjects with dry eye is stable and shows a small change after each blink due to reduced evaporation. In their experiments, the mean corneal temperatures in subjects with dry eye and in normal subjects were 34.0°C and 34.2°C , respectively.

1.7.4. Ophthalmic factors

Purslow and Wolffsohn (2007) found no relationship between the OST and corneal curvature or anterior chamber depth. Although Morgan found a significant decrease in the OST with increasing corneal thickness (Morgan, 1994), Purslow and Wolffsohn only found a weak negative correlation, but this observation may have been due to a smaller sample size.

Mapstone (Mapstone, 1968c) found a small temperature difference between the right and left eye corneal temperatures, which was normally no greater than 0.4 and 0.6°C . He also noted that

there were 2 thermal patterns of the corneal temperature generally observed in normal subjects: either that one side is hotter or colder than the other, or that no difference exists.

1.8. Effect of contact lens wear

Contact lens wear induces the change in the tear film especially in the short term (Glasson et al., 2006). According to Glasson, there was a statistically significant decrease in the non-invasive break up time (NIBUT) after six hours of lens wear. Also, the type of lenses worn may affect the stability of the pre-lens tear film. The water content, surface treatment and wettability would be associated with the dehydration rate of the pre-lens tear film.

Kojima et al. (2011) compared the effect of environmental change on the tear function with silicone hydrogel and traditional hydrogel. They compared results obtained from two different environmental conditions: a warm and humid (23-25°C and 30-40%) condition and a controlled environment chamber (18°C and 18%). Tear function with hydrogel wear was significantly affected by the environmental change. For instance, the mean blink rate increased with significant decrease in the mean symptom VAS scores.

It is also known that the thickness of the tear film on SCL becomes thinner, NIBUT becomes shorter and dryness increases as the environmental temperature and relative humidity decreases (Maruyama et al., 2004).

Purslow (2005) also reported the effect of these factors on OST in her thesis. She conducted a series of studies to investigate the effect of the wearing modality, type of lenses and the wearing period on the OST.

The results can be summarised as follows:

- Lens wear increases OST compared to naked eyes.
- There was no statistically difference between daily wear and continuous wear.
- The OST was lower with traditional hydrogel than silicone hydrogels.
- Silicon hydrogel with higher water content is likely to decrease OST in short term.

In addition to these findings, it would be interesting to compare the effect of RGP lens wear on OST, since an RGP lens will have different thermal characteristics to soft lenses. The pre-lens tear film on an RGP lens is less stable than that of SCL. Also, as the pre-lens tear film is influenced by tear mixing between the pre-lens tear film and the post-lens tear film during a lens wear, which may be also influence OST. However, RGP has not been investigated in past studies using modern thermography.

1.9. Summary

In this chapter, the history of contact lenses, the adverse events related to a contact lens wear, the thermography development and its application to medical fields including eye research were introduced. It has been known in the literature that the measured OST on the eye represents that of the tear film, and several ocular surface properties. The latest thermal cameras have overcome the potential difficulties of previous methods (thermistor and bolometer) such as the imaging range, the speed of the image processing, portability and the cost of affordability. The ability of measuring OST in real time using the latest thermal camera provides useful information to aid in understanding the physiology of the eye, with and without contact lenses. However, there is limited research regarding the influence of a contact lens wear especially about RGP wear and, it would be worthwhile to use infrared thermography to examine the difference in thermal dynamics on the ocular surface between RGP and SCL wear. The different thermal dynamics between RGP and SCL materials, and the tear exchange that occurs, may also have an influence on the retained temperature of the ocular surface during contact lens wear, which may itself have an influence on conditions for ocular infections. Any differences might contribute to the noted lower infection risk for RGP lens wear over SCL wear.

1.10. Aims of this thesis

This thesis attempts to observe the thermal dynamics of OST after a blink, and during contact lens wear. The aims are summarised as:

- To evaluate the stability of the tear film and the OST (without lens wear).
- To examine the effects of a short-term contact lens wear on the dynamics of tear film exchange and OST.
- To examine the effects of different types of hydrogel and rigid contact lenses on OST, both *in vitro* and *in vivo*.
- To examine the difference in the rate of the OST change between the rigid lens and soft lens.

Chapter 2. Experimental design

2.1. Laboratory set-up

2.1.1. Choice of camera

As reported in Chapter 1, thermography is a useful tool in medical practice and research, by providing detailed information on local temperature changes within the body. As a result of limitations in technology, previous studies were able to only produce a static image or low frame rate, but now it is possible to record images in real time with concurrent improvements in image processing and frame speed.

Two thermal cameras were selected for this thesis: ThermoVision A40M (FLIR SYSTEMS, UK), and A325 (FLIR SYSTEMS, Japan). The specifications of both cameras are summarized in Table 2.1. In addition to the basic configuration, a close-up lens was attached to each camera to allow measurements of the test object or eye at short working distances.

Table 2.1: Specifications of thermal camera.

Thermal camera	A40M (used in UK)	A315 (used in Japan)
Imaging and optical data		
Spatial resolution	1.3 mrad*	1.36 mrad
Thermal sensitivity (NETD**)	0.08 °C at 30°C	0.05°C at 30°C
Maximum frame rate	60 Hz	60 Hz
Focus	Automatic	Automatic or Manual (built in monitor)
Detector data		
Detection range	7.5-13µm	7.5-13µm
Detector	Uncooled microbolometer	Uncooled microbolometer
IR resolution	320 x 240 pixels	320 x 240 pixels
Measurement		
Accuracy	±2°C or ±2%	±2°C or ±2%
Ethernet		
Connection to PC	Fire Wire	Gigabit Ethernet
Attached close up lens	x4 Spatial resolution: 100µm	x4 Spatial resolution: 100µm

*mrad: milli-radian

**NETD: noise-equivalent temperature difference

The optical system of the camera focuses and transmits the radiation from the subjects. As glass does not transmit infrared radiation well, both cameras use a Germanium lens because its' high refractive index is able to refract the infrared wavelengths, and high reflective loss is prevented by an anti-reflective coating on the lens surface.

The detector used in both cameras is an uncooled type, Vanadium Oxide (VOx). It acts as a microbolometer, which changes its electrical resistivity as its temperature changes.

The detector has a small mass ensuring that, as the material varies in its reaction to temperature across the array, a precise calibration of the processing electronics is important in order to generate a clear picture. Since the thermal camera has a shutter that closes off the optics, the calibration data can be measured. This happens at every couple of minutes while the camera is operating.

2.1.2. Experimental location

In this thesis, clinical studies were conducted at two locations: Cardiff University School of Optometry and Vision Sciences in the UK, and a clinical laboratory in a contact lens manufacturer, Menicon in Japan. There were different experimental set-ups in each location.

2.1.2.1. Camera set-up in UK

The laboratory in the UK was within a small room, without windows, located on the ground floor of the building. The laboratory was air-conditioned to provide stable measurement conditions, and the laboratory door was kept shut during measurements to limit the effect of any environmental change. The humidity and temperature of the laboratory was measured by a hygro-thermometer (Maplin Electronics, UK; indoor temperature range: 0 to +50°C, humidity range: 20 to 99% relative humidity (RH)). These readings were recorded and inputted into the thermal camera control software.

The thermal camera was set up in two positions, depending on the test object/subject. When using the model eye (in chapter 3), the camera was mounted on a tripod (Manfrotto, UK) and positioned vertically above the model eye, which was itself located on a circuit board and laid on a table (Figure 2.1). The test distance was fixed at 8cm.

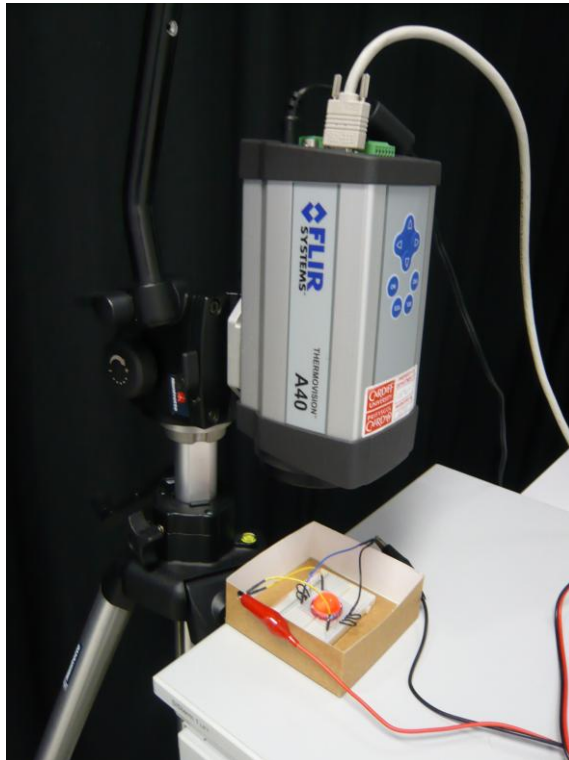


Figure 2.1: The model eye in the protective box in preparation for a measurement, with the thermal camera positioned vertically above, in the UK experimental set-up.

When using human subjects (in chapters 4 and 5), the camera was mounted on a slit-lamp biomicroscope, which permitted control of the image focus manually using the joystick (Figure 2.2). The slit lamp was placed on a standard ophthalmic table with a chin-rest and head-rest to position and support the subject's head.



Figure 2.2: Patient seated in front of camera in preparation for a measurement, in the UK experimental set-up.

The camera was connected to a desktop computer and controlled by the software: ThermaCAMTM Researcher Professional Edition, version 2.9 (FLIR Systems, UK). A further independent display was also connected to the camera, to assist in instrument alignment - once a recording was initiated, it was impossible to observe the camera image on the computer screen, as the processing demand on the computer CPU prevents the continuous display of the object's thermal image in real time. By providing a second image output, the examiner was able to check whether the subject maintained the correct eye and head position, and also if the eye blinked normally during the measurement. To further enhance consistency in eye position, a transparent film was placed over the independent display to indicate the geometric centre of the cornea. The subject's eye was then aligned using this film throughout the same study for each subject, time and day.

2.1.2.2. Camera set-up in Japan

The laboratory in Japan was in part of a room, partitioned off with a curtain. Although the room was air-conditioned, this was set to a low level to avoid strong changes in room environment.

The temperature and humidity was recorded as being the same as the laboratory in the UK.

The camera was mounted on the base of a dismantled ophthalmic instrument, with a chin-rest and head-rest (Figure 2.3). The camera was then controlled using a joystick to move the platform back and forth. Also the height was adjustable up and down by using a lab jack.



Figure 2.3: Patient seated in front of the camera in preparation for a measurement, in the Japan experimental set-up.

The difference between the UK and Japan set-up was that the camera A315 used in Japan was not able to split the image signal so an independent monitor was not connected. However, the *in vivo* experiment in Japan was completed in one day, and so the guide to mark the locations for ocular surface temperature (OST) was not necessary.

2.2. Conditions and techniques

Purslow (2005) reported on the desirable conditions for thermography measurements.

2.2.1. Effect of image defocus

During measurements, subjects may produce movements towards or away from the camera. This will cause defocus in the thermal image, and an artifactual temperature change. To investigate the correlation between the distance and the object, Purslow (2005) constructed a model eye consisting of a resin, convex dome with LED lights inside which acted as a heat source. She reported that there was a significant negative correlation between the measured central radiated temperature of the model eye and the distance to the thermal camera. To avoid this movement, subjects were encouraged to rest their head against a head-rest and chin-rest.

2.2.2. Adaptation

As eye temperature is related to body temperature (Schwartz et al., 1968, Mapstone, 1968c, Freeman and Fatt, 1973, Morgan et al., 1993), it is important to consider the adaptation of the body to changing environmental conditions before measurements are taken. In previous research, a range of 15-45 minutes was chosen as a suitable time for a subject to adapt to the testing room environment before an experiment, based on studies that examined the adaptation time effect in human and rabbit eyes (Alio and Padron, 1982, Rysa and Sarvaranta, 1974). In one study with 12 subjects, OST was noted to change for up to 15 minutes after entering the laboratory. In a similar study, Purslow (2005) found a statistical difference for only the first 6 minutes, and subsequently chose a 10 minute adaptation period, with the additional requirement that subjects should be in the building for at least 20 minutes prior to this.

In this thesis, invited subjects were allowed to adapt from outside environmental conditions to the internal building conditions (in both the UK and Japan) before they came to the laboratory, and therefore a 10 minute adaptation within the test laboratory was considered to be enough.

2.2.3. Repeatability of temperature measurement

Repeatability within and between visits was investigated by Purslow (2005). To examine within visit repeatability, the same operator measured OST continuously for 8 seconds, on 10 separate test runs with 4 subjects. The separation between each recording was approximately 10 seconds. The variation in central OST (absolute value and cumulative average), the square of the deviations from the mean values, and the change in the magnitude of post-blink cooling upon repeated measures were calculated. Purslow concluded that the variation in OST of repeated measurements at a single session is initially large, but repeatability becomes acceptable if the first three successive measures are averaged. However, similar to the effect on the tear film of repeated measurements for tear stability, once the tear film becomes unstable by repeated blinking, there is a risk that the OST will also become excessively variable. To control for this effect, the measurement of the OST was recorded once per eye, per measurement time point throughout this thesis.

In a separate study, Purslow (2005) also examined repeatability between visits with 14 subjects. The OST of each subject was measured weekly over five weeks, at the same time of the day. Inter-session variability in central OST and the magnitude of post-blink cooling was analysed. Most subjects displayed considerable variability in central OST and there was a significant difference between recordings especially between weeks 1 and 2. However, the magnitude of

the post-blink cooling showed less variation and there was no statistical difference. Purslow concluded that observation of OST for an individual on separate occasions is less reproducible, and suggested that a new 'baseline' measurement should be taken at each visit for reference if repeated measures of the same subjects for different conditions are required.

2.2.4. Time of the day

It is reported that there is evidence in the literature of diurnal variations in various physiological parameters, such as human body temperature, tear film stability, corneal thickness, blood flow to the eye and intraocular pressure (cited by Purslow, 2005). For instance, human body temperature is lowest on waking and reaches a maximum in the late afternoon.

Purslow (2005) recorded the OST of 18 subjects at three different times of day: 10am, 1pm and 4pm. The results showed that OST increased throughout the day in more than 60% of subjects. There was also a significant difference in OST between different times of day, especially comparing the morning and afternoon recordings. The average increase in OST from 10am to 4pm was $+1.4 \pm 0.9^{\circ}\text{C}$.

From these results, it was concluded that the time of day is an important factor in the measurement OST. To avoid the effect of OST increase throughout the day in this study, measurements were taken at similar times, or within a single morning or afternoon session.

2.2.5. Eye rubbing

The effect of eye rubbing has been investigated as a stimulus to OST. Purslow (2005) examined the effect of eye rubbing in a small number of subjects (n=3). Although there was an increase in OST after rubbing three times with the knuckles of their right index finger, it did not show statistical significance. Eye rubbing may affect the tear film and the eyelid, in a similar manner as contact lens wear, insertion and removal. Therefore, it should be avoided during the adaptation time and measurements.

2.2.6. Room temperature

Heat transfer will occur between the eye surface and its environment, and consequently the room temperature is related to OST measurements. In the literature, this environmental effect in OST has been reported.

- In 4 human subjects, measured 17 times over an 8 week period, a mean fall in OST of 0.145°C per 1°C decrease in environmental temperature over the range of 18-27°C was found (Mapstone, 1968a).
- A linear decrease with ambient temperature drop was observed in rabbit eyes (Freeman and Fatt, 1973).
- OST decreases in cool conditions (Hata et al., 1994).

2.3. Data collection and analysis

2.3.1. Instruction to subject on blinking

In addition to the experimental conditions and techniques described above, control of blinking also has an important effect on OST *in vivo*. Hill and Leighton (1965) investigated the effect of forced and natural eye closures on OST. They reported that relaxed closure produces stable temperatures while, on the other hand, forced closure causes an increase in OST. Also, excessive blinking may produce reflex tears, resulting in an unstable tear film, leading to changes in evaporation rate, and thus OST. Therefore, when recording the OST *in vivo*, subjects were asked to blink normally.

2.3.2. Analysing the data

The proprietary analytical program, ThermaCAM™ Researcher Professional Edition, version 2.9 (FLIR Systems, UK), allows the positioning of analysis tools at specified locations on the thermal camera display to enable the continuous recording of anterior eye temperature at that location during a measurement period. The software can replay the recorded continuous images and pick up the temperature from the selected area and/or points after measurements.

Figure 2.4 shows a captured image with analysis tools applied. In this figure, the analysis tools were a blue cross (SP01) and a circle (AR01). They specify a point and area at which the software calculates the temperature, either as a single spot temperature or as a maximum, minimum or average temperature, respectively. Different shapes of tools, such as box and line, can be used. It is also possible to create formulas to obtain the mathematical analyses of the tool sampling. For example, the average of several points on an image can be calculated.

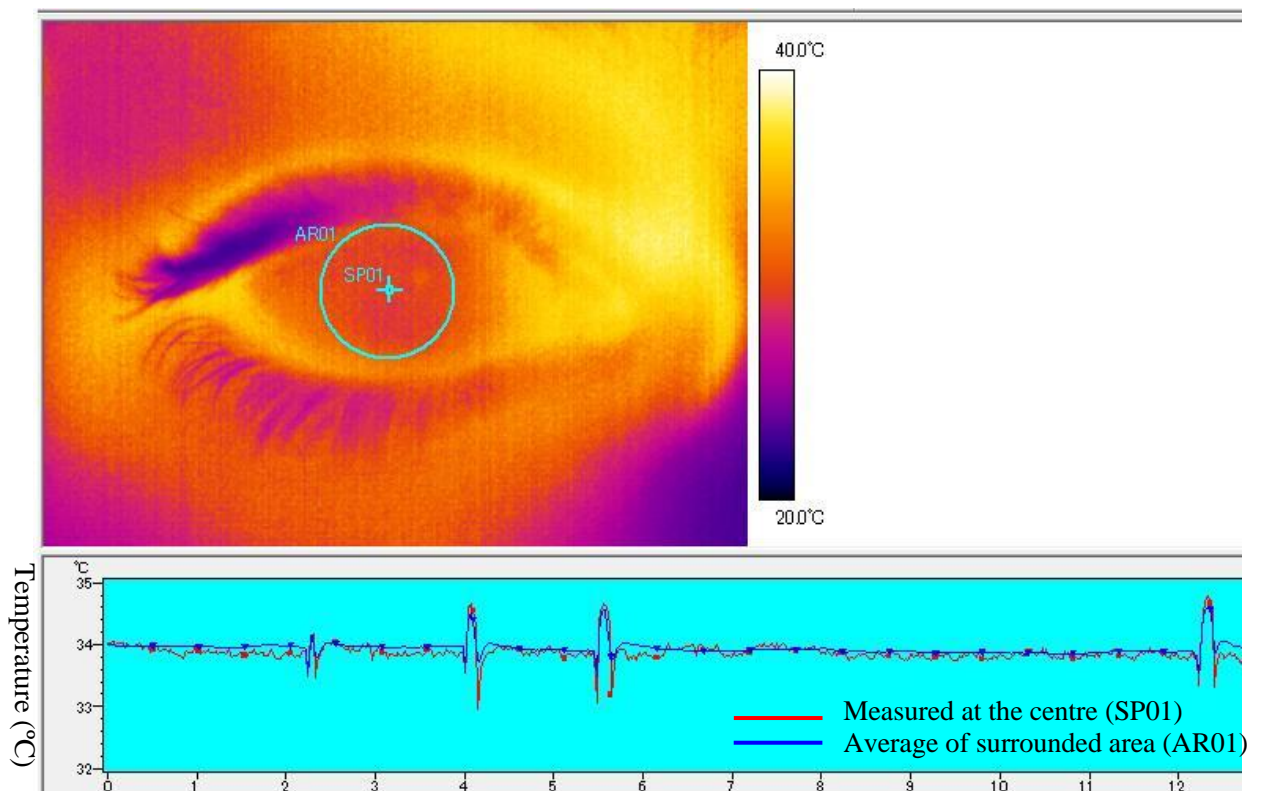


Figure 2.4: Thermal image of OST with analysis tools and their temperature profile.

If the OST is continuously recorded, for example to assess the dynamic change in the tear film, it is possible to analyse the variation in temperature over time and present it graphically. The software plots a graph to represent the temperature from the analysis tool, as illustrated in Figure 2.4. In this example, the sharp peaks and troughs in the graph plot represent blinks, and are caused by the movement of the eyelid, which has a different temperature profile to the cornea. In these studies, the OST was continuously recorded over a measured period of time, and analysis of calculated temperatures could be obtained by output of the results as a text file for conversion into a Microsoft Excel spreadsheet for later analysis.

When recording the OST as a short video for 10 seconds in the highest frame rate (60Hz), approximately 600 temperature measurements are produced in a spreadsheet form. To manage this data, spreadsheet templates were used to smooth the data (average of temperature within $\pm 0.3s$), and a line plot drawn to represent the change in OST over time, including pre- and post-blink (Figure 2.5).

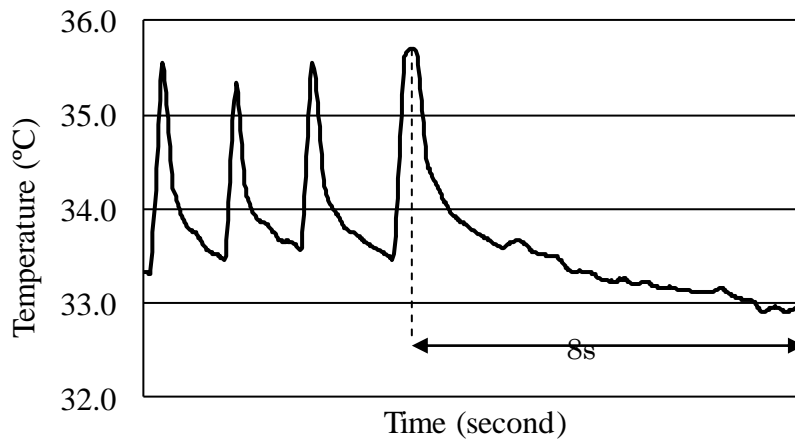


Figure 2.5: Typical temporal change in OST with blinking.

When the relatively hotter eyelid covered the cornea as a blink, the thermal camera detected this as a peak in the plot. For data analysis, one peak was manually selected and its time and temperature were recorded. The closing and opening of the upper eyelid was used to set the starting point for the 8 seconds measurement. Purslow (2005) adopted a practice of choosing a time point of 0.2secs after the peak value as the point of eye opening. This decision was made by considering the speed of the eyelid motion, and the time for the superior cornea to be exposed after blink. Therefore, the term 'initial OST' refers to the temperature calculated at 0.2secs just after a blink. Once the initial point was set, the data was manipulated within the Excel template to reveal the total change in OST over the period after a blink. The duration of

data collection was selected of 8 seconds. This was felt to be an appropriate time to assess the tear film without causing reflex tearing, as the average blink rate under concentration has been reported as 5 blinks/min (Tsubota and Nakamori, 1995).

2.3.3. Analytical localisation

To analyse the data, the transparent film template was used to mark the position of the specific sets of analytical tools used on subjects in each experiment to ensure consistency in analysis of test locations. Each template was designed to avoid measuring the skin or eyelash temperature.

In this thesis, the shape and number of tools were chosen according to the purpose of each study:

- In Chapter 3 (model eye study), **five spots** were positioned over the model eye in a cross pattern since the purpose of this preliminary study was to see whether the surface of the model eye heated up equally (Figure 2.6). With the finding that there was no significantly difference between the spots, only **one spot tool** was placed at the centre of the model eye when testing with the contact lens in place.

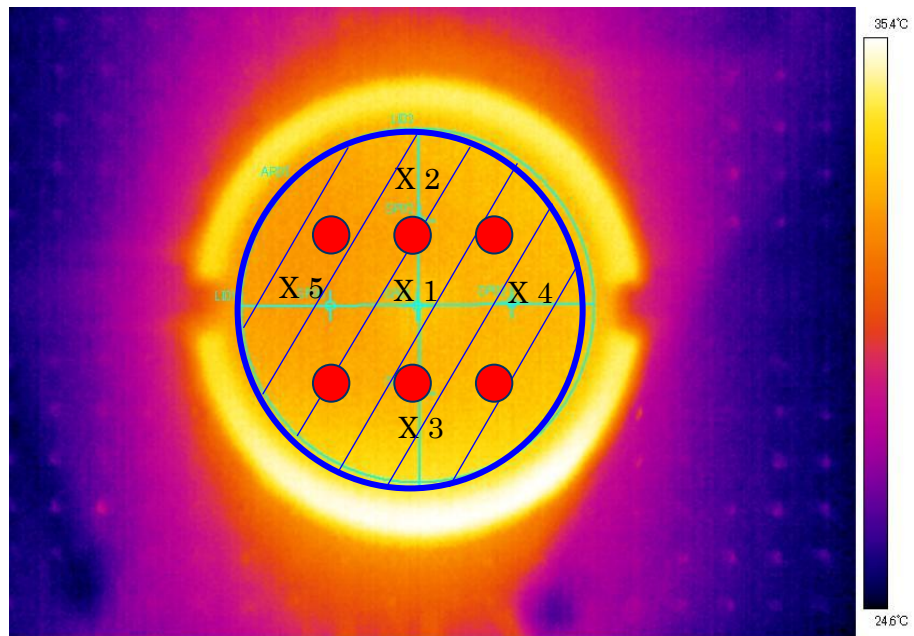


Figure 2.6: The thermal image of the model eye with analysis tools, showing the location of the 6 LEDs (red dots), and the selected spots for temperature analysis (X1-5), and the average area (striped area surrounded by blue circle).

- In Chapter 4 (tear film stability study), **one spot and one circle** tool were placed on the centre of the cornea (Figure 2.7). One spot was chosen because the centre of the cornea is most exposed to the environment and it was felt that this would show the greatest change. The circle was set to show the average change across the corneal area. Although the typical HVID is 11-12mm (Davis and Becherer, 2005), the diameter of the circle was set at 8mm because the subject often moves slightly during the test, and the smaller diameter ensured that only the cornea and not the conjunctiva was sampled. The measurement was taken once after at least ten minutes adaptation time.

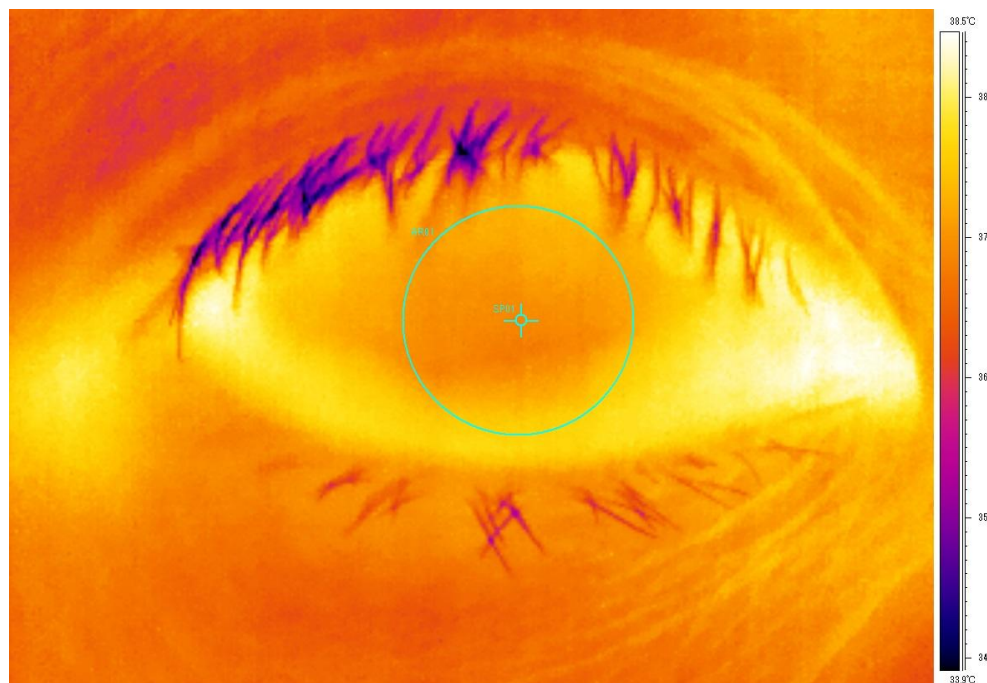


Figure 2.7: A thermal image of the eye with analysis tools

- In Chapter 5 (4 CL study), **six spots** were placed: three on the conjunctiva and three on the peripheral cornea to assess the effect of lens wear and tear exchange on the OST; and additional **one spot** was placed on the centre of the cornea. The spots on the conjunctiva were positioned beyond the contact lens edge and measured the OST (hereafter OSTC),

while the spots on the lens periphery measured the OST (hereafter OSTP). Figure 2.8 and Figure 2.9 show examples of the thermal image when wearing a RGPCL and SCL, respectively. The circle tool was placed as its diameter, at 10mm, was almost same as the diameter of the RGPCL (9.6mm) used in this study, consequently, the spots for OSTP were placed inside the circle when an RGPCL was worn, but were placed outside with a SCL.

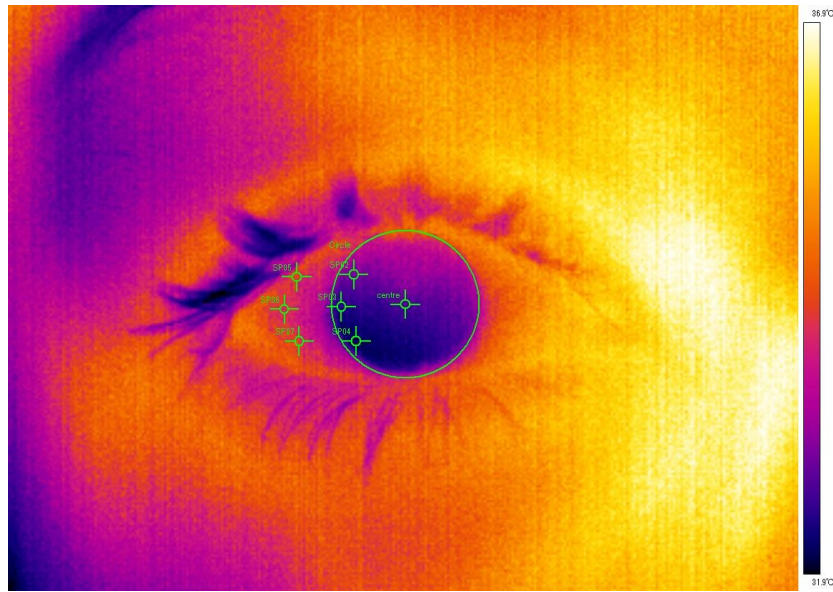


Figure 2.8: The thermal image of the eye under RGP lens wear with analysis tools.

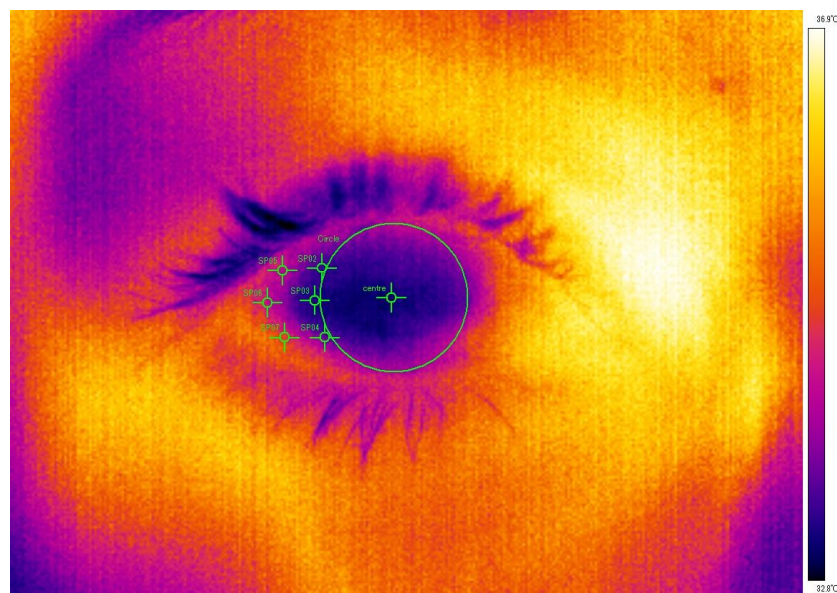


Figure 2.9: The thermal image of the eye under SCL wear with analysis tools.

2.4. Experimental protocol

The literature review of previous research led to a specific protocol for all human OST measurements:

- I. Subjects attended at similar times of day
- II. Room temperature and humidity were controlled as much as reasonably possible, were monitored and recorded.
- III. Subjects were allowed to adapt to room conditions for at least 10 minutes, and they had to have been in the building for at least the previous 20 minutes.
- IV. If repeated measures of the same subjects under different conditions were required, then a new 'baseline' was recorded at each visit.
- V. Subjects were asked to blink naturally and, when instructed, to conduct one last normal blink, and then keep their eye open for eight seconds.
- VI. Data collection and analysis was via ThermoCAM Researcher and Microsoft Excel.

Chapter 3. In vitro study (model eye study)

3.1. Aims and objectives

As reported in previous chapters, it is known that OST principally describes the temperature of the tear film on the cornea, since there is a limited depth within the tissue from which infra-red radiation can reach the surface and be detected. Energy conducted or radiated from deeper tissues is essentially absorbed by tissue more anteriorly placed, and while some energy is re-emitted, this is included in the anterior tissue radiation component.

When looking at thermal radiation from the eye, it is also important to consider how close the cornea is to being a perfect black body, since this affects the calculations of observed temperature relative to measured infrared radiation. Mapstone (1968b) reasoned that the true temperature of the cornea should be considered to be the same as the body core and therefore, if the Stefan-Boltzmann equation is applied, the cornea would have an emissivity of 0.97. As the cornea will be generally cooler than body temperature, the emissivity will actually lie between 0.97 and 1, and an emissivity value of 0.98 is generally accepted for both the skin and ocular surface. This means that 98% of the radiation escapes from the ocular surface (Mapstone, 1968b).

When a contact lens is then placed onto the eye, its presence interferes with this stable state, and now the contact lens becomes part of the energy absorbing component of the eye, as well as a potential source for infra-red radiation. The thermal capacity of the contact lens to absorb this ocular radiation, or any other source of heat, and to emit any radiation that can be detected through the tear film therefore becomes important when determining the observed OST on a contact lens wearing eye. It is also important when considering whether there are any negative or positive consequences for ocular health from having a potential heat source on the ocular surface.

In effect, the contact lens may act as an insulator for the cornea, preventing a normal rate of heat loss from the ocular surface, if the contact lens has a high thermal capacity and low thermal conductivity. In other words, the insulation rate increases inversely to the thermal conductivity of the material. The thermal properties of the eye and traditional contact lenses have been calculated by previous researchers (Table 3.1).

Table 3.1: Physical constants of cornea and contact lenses taken from the literature (cited by Purslow (2005)).

Medium	Density (g/cm ³)	Thermal conductivity (cal/[cm.sec. °C])	Source
Bovine cornea	1.11	6.58×10^{-4}	Hamamo et. al, 1972
Soft contact lens	1.18	6.64×10^{-4}	Hamamo et. al, 1972
PMMA contact lens	1.04	4.4×10^{-4}	Hamamo et. al, 1972
All contact lens Polymers	1.21	4.01×10^{-4}	Martin and Fatt, 1986
Water	1.00	1.48×10^{-3}	Martin and Fatt, 1986
Human cornea	1.05	5.8×10^{-4}	Scott, 1988

Although this table presents some physical constants calculated *in vitro*, the research of contact lenses *in vivo* is limited. Hamano et al. reported that the thermal conductivity of the bovine cornea is similar to that of contemporary hydrogel-based soft contact lens (SCL) materials, being less than that of water. Rigid gas permeable contact lens (RGPCL) materials had a slightly lower thermal conductivity again from SCL (Hamano et al., 1972). Martin and Fatt used contact lenses which had embedded themistors as a direct method of recording the corneal temperature behind the lens (Martin and Fatt, 1986). Their findings indicated that contact lenses of higher water content (more than 50%) appeared to cause a smaller rise in measured ocular temperature than those of lower water content (less than 50%), presumably due to the increased

presence of water, which has a lower thermal conductivity. According to Purslow (2005), the thermal conductivity of contact lenses will always be less than the tear film and cornea due to differences in water content. Thus, when a contact lens with high thermal conductivity is worn, the measured temperature will be higher than when a material with low thermal conductivity is worn, as more heat can be transferred.

Since these earlier studies, silicone hydrogel lenses have become the new standard for soft contact lens materials, and newer RGPCL materials have also been introduced. The thermal conductivity of these lens materials is not known, nor has there been any reports into the effect of contact lens wear with these lens materials on the eye. It is hypothesised that the thermal conductivity of silicone-hydrogel contact lenses (SiHCL) may be lower than that of SCL, due to the higher concentration of polymer, since the thermal conductivity of a water polymer may affect its insulation rate (Makinae et al., 1992).

To further investigate the effect of contact lens wear on ocular temperature, it is important to first estimate the insulation effect of contact lenses made with these different material types.

In this chapter, a model eye set-up was developed that used a set of illuminating diodes as a heat source, encased in a plastic shell, to mimic the internal heat source for the ocular surface.

Using this simple model, the difference in insulation properties of several different types of

contact lenses of different water content and materials was investigated. The diode heat source represented heat derived from the core body temperature, delivered via the blood supply, to the plastic shell, representing the exposed ocular surface.

In a previous study, Purslow (2005) employed a similar experimental model eye set-up to examine the effect of ocular surface temperature on hydrogel contact lenses. With the contact lenses placed over the model ocular surface, the heat transferred through the lens was measured over time, by measuring the lens surface temperature using a thermal camera. A constant low voltage was applied to the lamps, representing the model eye, to produce visible light and thermal radiation similar to that of the human eye. However, without a means of removing excess heat created, as would happen in the eye through the blood supply, the stability of temperature in the model eye, under the lens, could not be confirmed, nor easily checked without an understanding of the local temperature beneath the lens, which may have caused excessive heat during the experiment. Also, moderation of the ocular surface temperature, which occurs naturally through the action of tear evaporation between natural blinks, was not controlled, leading to lens surface drying.

To control for these problems, an improved model eye was developed for use in this study, and both rigid gas permeable contact lenses and hydrogel contact lenses were examined to

investigate the effect of different thermal conductivities in contact lenses. To incorporate some aspects of the blinking process, an artificial tear-drop was regularly (2 μ l/min) applied onto the contact lens surface over the model eye during data collection.

To allow a comparison of results with differing experimental conditions, the study was undertaken in 3 parts:

- **Preliminary study:** examining the stability of the ocular surface heat generated by the model eye, without any contact lens in place.
- **Contact lens study:** several contact lenses were positioned, in turn, over the model eye surface, and the heating temperature effect observed on the contact lens surface.
- **Contact lens and eye drop study:** artificial tear drops were instilled over the contact lens surface, and the mitigating effect of these drops observed on the surface temperature of the contact lenses.

3.2. Preliminary study Aims

To compare the insulation effect of the contact lenses using the model eye, it is essential that the temperature produced is controlled and constant. Before examining the contact lenses, it was therefore necessary to confirm the stability of the model eye. In this section, the temperature distribution over the lens and the time to reach temperature equilibrium were investigated.

3.2.2. Methods

The experimental set-up was based upon the previous study (Purslow, 2005). The model eye used was a 20mm diameter hemisphere shaped plastic lamp (Giant Red Light, Maplin UK, Figure 3.1).

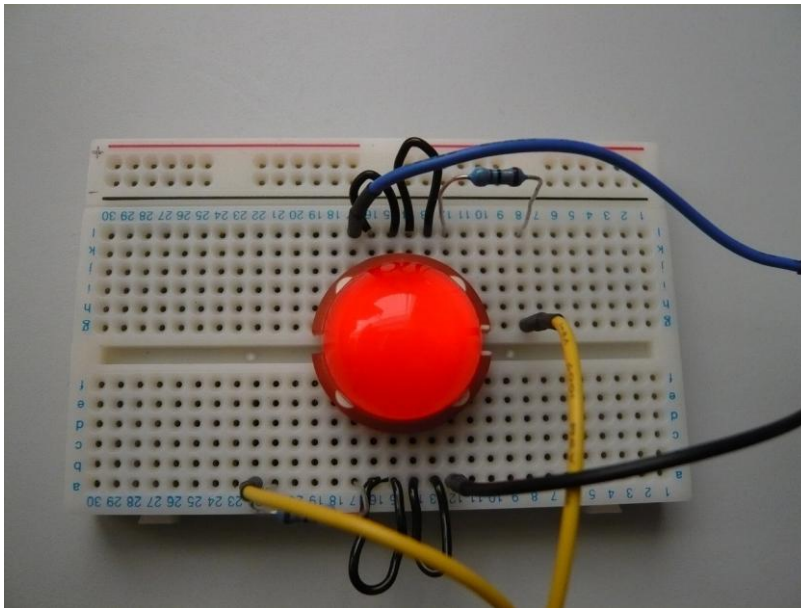


Figure 3.1: The model eye set on an electrical circuit board.

The lamp consisted of 6 light emitting diodes (LEDs) set inside a plastic shell with a radius of curvature of 7.80mm. The lamp was mounted on an electrical circuit board with resistors to control current flow, and placed in a simple protective chamber to prevent a heating effect from energy reflected from the surrounding environment or a cooling effect from any potential air movements. This set-up was connected to a power source, the voltage of which could be controlled from 3 to 12V.

To measure the surface temperature of the model eye, a thermal camera (ThermoVision A40M, FLIR Systems) was used. In addition to the basic configuration described in Chapter 2, a close-up lens (working distance, 80mm) was attached to the camera to allow measurement of the model eye surface at a short working distance. The camera was mounted vertically, on a tripod, above the model eye set-up. The thermal camera had a thermal sensitivity of 0.08°C and a wavelength detection range from 7.5 to 13µm.

The thermal camera was connected to a desktop computer (Figure 3.2) to record the temperature using analysis software (ThermaCAM™ Researcher, Professional edition. Version 2.9). The thermal image was continuously recorded with 12Hz frame rate for 90 minutes.

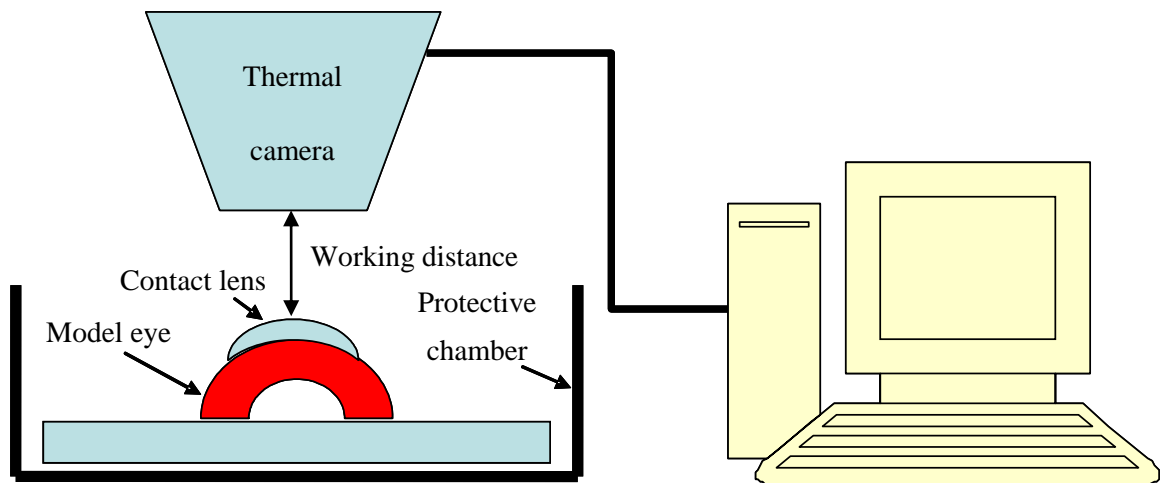


Figure 3.2: Schematic diagram illustrating the experimental set-up incorporating the model eye, thermal camera and desktop computer. A contact lens is shown in position on top of the model eye.

Room temperature and humidity in the laboratory were monitored throughout the study using an indoor/outdoor hygro-thermometer. The mean temperature during the study was $22.8 \pm 0.7^\circ\text{C}$ ($21.8\text{-}24.0^\circ\text{C}$); humidity was $30.9 \pm 12.7\%$ ($15.0\text{-}49.7\%$).

Since the aim of this study was to confirm the stability of the model eye, surface temperature was recorded over a period of 60 minutes, at one second intervals, while the electrical power was set at 7.5V . The measurement was repeated three times.

The surface temperature of the model eye was analysed, at five locations (X1: central, X2: superior, X3: inferior, X4: right, X5: left), and over the total surface area of the lamp (the average temperature across the whole surface within the area of the circle, Figure 3.3).

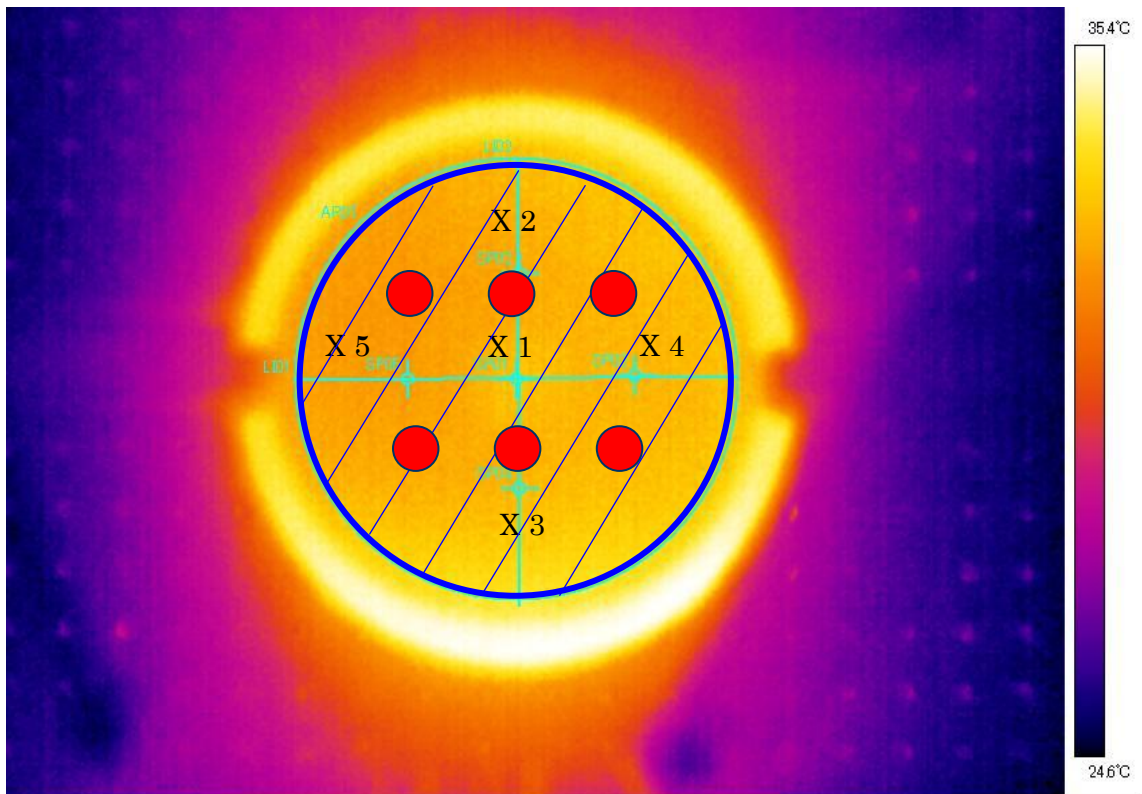


Figure 3.3: Thermal image of the model eye showing the location of the 6 LEDs (red dots), and the selected locations for temperature analysis (x1-5) and an area (striped area surrounded by blue circle).

3.2.3. Results

The temperature change that occurred during the initial heating phase is shown in Figure 3.4.

The temperature of all 6 locations and the overall surface area quickly rose to approximately 32°C and thereafter reached equilibrium. All of the test locations and the average area showed similar temperatures at each five minute interval until 20 minutes and 10 minutes thereafter (one-way repeated measures ANOVA, $p > 0.05$, Table 3.1). Statistically differences were found across 60 minutes at all 6 locations (one-way repeated measures ANOVA, $p < 0.05$, Table 3.1),

but Turkey's post-hoc testing revealed no statistical differences in temperatures measured after 20 minutes, meaning that the surface temperature of the model eye was constant. These results indicate that the surface of the model eye heated up equally and suggests that it can be thought of as a stable model, in terms of the thermal characteristics.

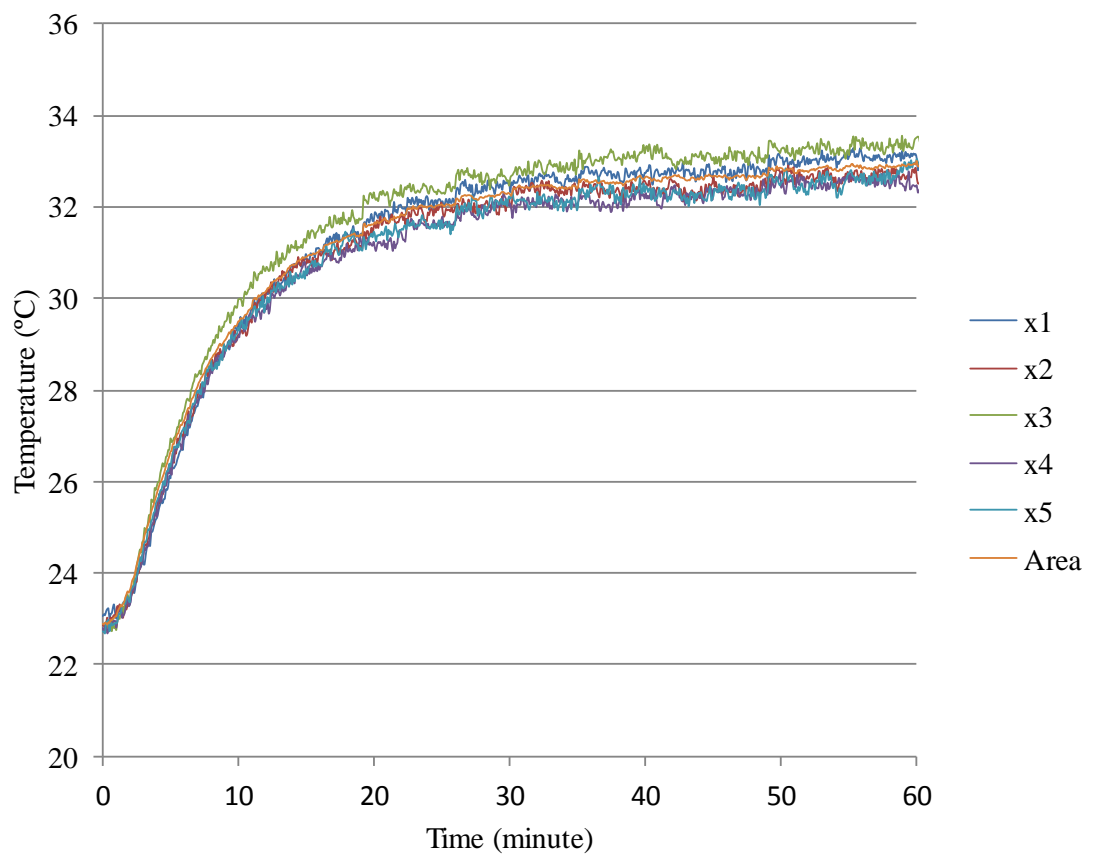


Figure 3.4: Temperature of the model eye without a contact lens.

Table 3.2: The temperature change on the model eye.

Time	Spot 1	Spot 2	Spot 3	Spot 4	Spot 5	Area	ANOVA
0	23.37±0.72	22.96±0.25	23.03±0.32	22.93±0.27	23.03±0.21	23.08±0.01	F=0.37 p=0.85
5	25.89±0.53	25.97±1.38	25.96±0.53	26.03±0.43	26.96±0.45	25.94±0.2	F=0.70 p=0.64
10	29.41±0.28	29.28±0.99	29.12±0.07	29.51±0.21	30.27±1.11	29.35±0.15	F=0.83 p=0.57
15	30.85±0.12	30.73±0.7	30.6±0.02	30.96±0.43	31.87±1.38	30.92±0.07	F=0.94 p=0.52
20	31.67±0.14	31.64±0.96	31.25±0.04	31.75±0.41	32.62±1.42	31.7±0.01	F=0.79 p=0.60
30	32.39±0.3	32.24±0.32	32.09±0.11	32.59±0.51	33.36±1.53	32.48±0.1	F=0.86 p=0.56
40	32.63±0.07	32.58±0.84	32.26±0.13	32.55±0.32	33.62±1.41	32.64±0.15	F=0.93 p=0.52
50	32.66±0.15	32.52±0.93	32.51±0.27	32.6±0.18	33.62±1.09	32.84±0.34	F=0.93 p=0.52
60	32.74±0.18	32.69±1.15	32.42±0.01	33.06±0.17	33.82±1.28	32.91±0.35	F=0.89 p=0.54
ANOVA	F=19.4 P<0.001	F=29.03 P<0.001	F=40.63 p<0.001	F=20.45 p<0.001	F=19.94 p<0.001	F=64.37 p<0.001	

3.3. Contact lens study

3.3.1. Aims

Knowing the thermal conductivities of each contact lens material will help to understand the temperature changes that occur in the eye with contact lens wear. Since the lens behaves as an insulator over the cornea, the normal heat transfer that occurs from the posterior cornea through the anterior cornea to the tear film will be altered. The actual effect on the rate of heat transfer will vary according to the lens material, the water content and so on. In this chapter, the model eye was used to investigate the dynamic temperature changes in different contact lens materials. The lenses were chosen from three categories: SCL, RGPCL and SiHCL. The findings from this study will be useful to expand the study in the *in vivo* phase.

3.3.2. Methods

Eight different contact lens types and materials were positioned onto the surface of the model eye, and the surface temperature of the combined lens/model eye investigated. The contact lenses used were: two SCLs, four SiHCLs, and two RGPCLs. The order of lens measurement was decided by use of a table of random numbers produced in Microsoft Excel.

Each individual lens package was opened 30 minutes prior to each experiment to allow the lens to stabilise with environmental conditions. When manipulating the lens, the edge of the lens was held by a soft plastic forceps, and any excess packing solution was removed by shaking. Each lens was then placed over the model eye.

Measurements were repeated five times for each lens type, with a new SCL used each time. For the RGPCL, each lens was re-used after cleaning with Menicare Plus (Menicon, Japan), on a further day. The specifications of the measured contact lenses are given in Table 3.3-

Table 3.5.

Table 3.3: Specifications of SCL.

Parameter (units)	1-day Acuvue	Dailies
USAN *	Etafilcon A	Nelfilcon A
Manufacturer	Vistakon	Ciba Vision
Water content (%)	58	69
Base curve (mm)	9.0	8.6
Diameter (mm)	13.8	13.8
Centre thickness (mm, -3.00D)	0.084	0.100

*USAN: United States Adopted Name

Table 3.4: Specifications of RGPCL.

Parameter (units)	Quasar	Menicon Z
USAN	Focon 5 (not USAN name)	Tisilfocon A
Manufacturer	No 7	Menicon
Water content (%)	<1	<1
Base curve (mm)	7.7	7.8
Diameter (mm)	9.6	9.2
Centre thickness (mm, -3.00D)	Not available	0.130

Table 3.5: Specifications of SiHCL.

Parameter (units)	AIR OPTIX	PureVision	PremiO	Biofinity
USAN	Lotrafilcon B	Balafilcon A	Asmofilcon A	Comfilcon A
Manufacturer	Ciba Vision	Bausch & Lomb	Menicon	CooperVision
Water content (%)	24	36	40	48
Base curve (mm)	8.6	8.6	8.6	8.6
Diameter (mm)	13.8	14.0	14.0	14.0
Centre thickness (mm, -3.00D)	0.080	0.090	0.080	0.080
Modulus (MPa)	1.40	1.10	0.91	0.75

The temperature measurements took place within a controlled environment (room temperature $23.0 \pm 0.4^\circ\text{C}$, humidity $24 \pm 8\%$). The temperature was recorded for 10 minutes at 12Hz frame rate, and measured only at the centre (apex) of the contact lens/model eye set-up. After each 10 minute measurement, the lens was removed and the model eye temperature was allowed to

stabilise for another 10 minutes before the next lens was assessed. The collected data was analysed for significant changes over time and between lenses using analysis of variance (ANOVA).

3.3.3. Results

The chronological temperature changes of each contact lens type on the model eye are shown in

Figure 3.5-Figure 3.7.

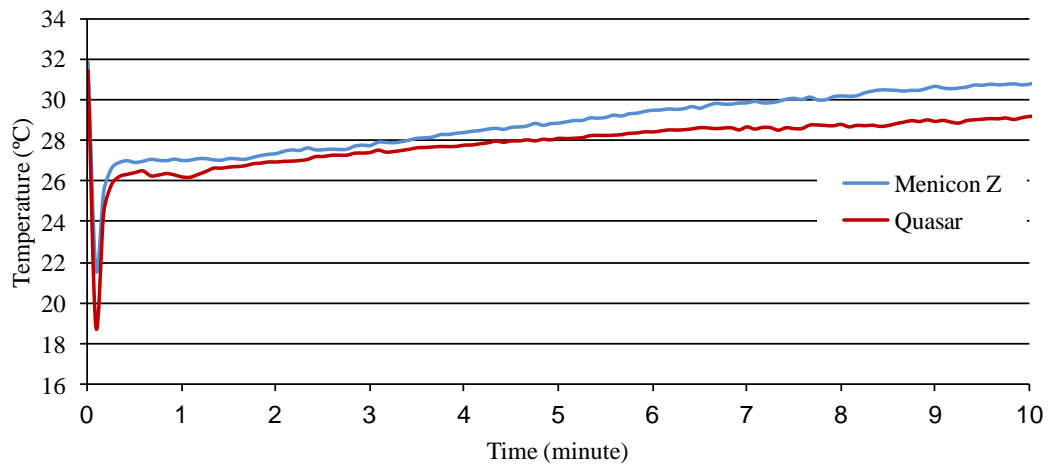


Figure 3.5: Surface temperature change produced with RGP.

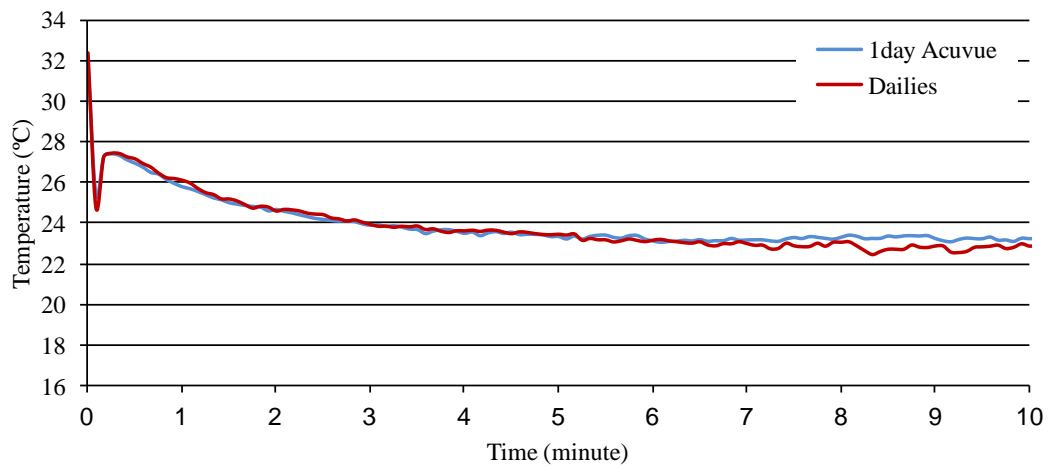


Figure 3.6: Surface temperature change produced with SCL.

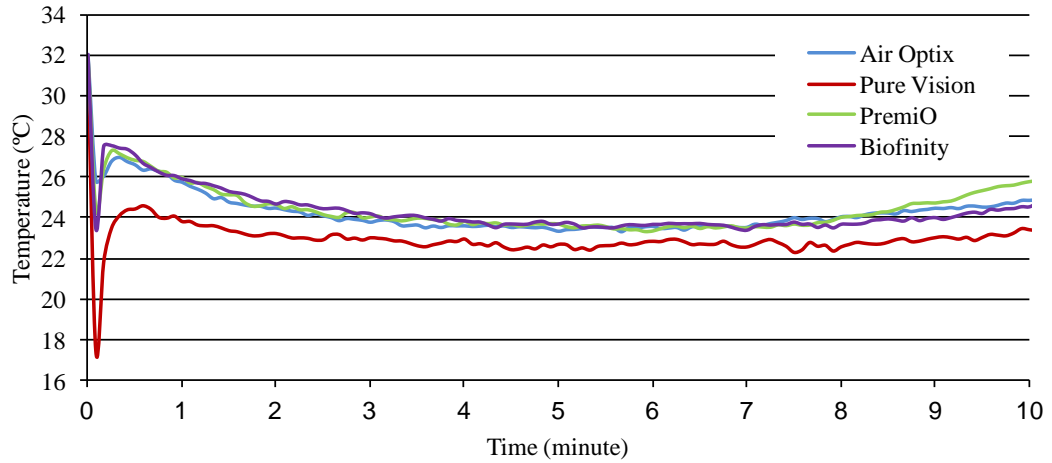


Figure 3.7: Surface temperature change produced with SiHCL.

An immediate decrease in surface temperature was observed when all lenses were applied. Thereafter, the rate of recovery in temperature varied between lens types. A linear increase was observed with RGPCL, but with all SCL a further decrease in temperature followed an initial recovery. A similar temperature pattern to SCL was observed for SiHCL, with the addition of a second recovery in temperature observed towards the end of the measurement period.

Taking a closer look at this temperature changes, the initial placing of a lens onto the model eye produces an immediate decrease in measured temperature change, since the thermal camera is now receiving infra-red radiation from the exposed contact lens surface, which had stabilised to the temperature of the room. To better analyse this initial change in detail, the initial temperature was defined as T_a , the negative deflection was defined as T_c and the recovered

stabilised temperature defined as T_b . Also, the temperature difference between T_a and T_c was calculated as Δt_1 and the difference between T_b and T_c was calculated as Δt_2 , as illustrated in Figure 3.8. The mean values for Δt_1 and Δt_2 are given in Table 3.6.

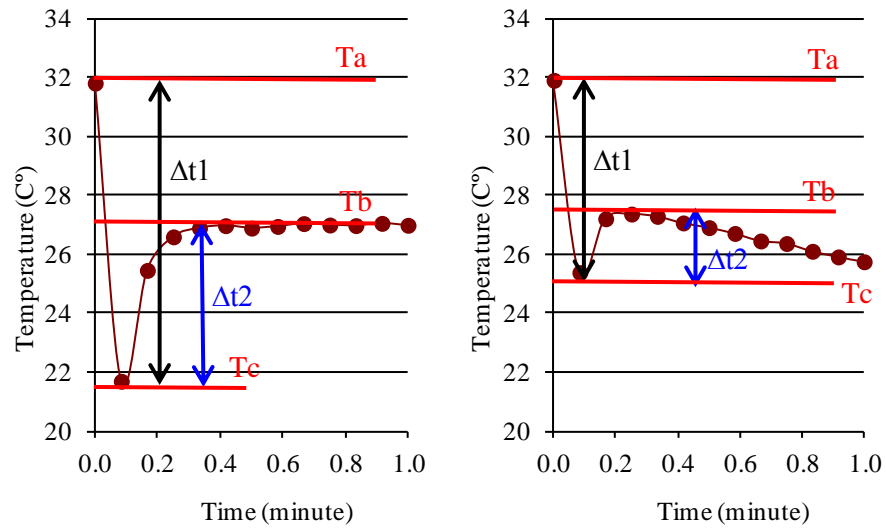


Figure 3.8: Example plot showing the initial temperature change of the model eye following positioning of a contact lens (Left: RGPCl, Right: SCL and SiHCL).

Category	Lens	Mean Δt_1 (°C±1sd)	Mean Δt_2 (°C±1sd)
RGPCl	Menicon Z	10.9±2.9	6.5±3.0
	Quasar	12.5±1.8	8.2±1.8
SCL	1-dayAcuvue	10.2±1.9	5.9±1.6
	Dailies	10.4±1.2	5.5±1.3
SiHCL	AIR OPTIX	7.4±2.3	2.9±1.8
	PureVision	14.2±1.7	7.5±1.5
	PremiO	8.3±1.0	3.8±0.9
	Biofinity	10.2±1.5	5.9±1.4

Table 3.6: Mean values for Δt_1 and Δt_2 .

Statistically significant changes were reported between the absolute values of T_a and T_c , and T_b and T_c , for all lenses (t-test, $p < 0.05$). In comparing the size of temperature change (Δt_1), no statistically differences were found between lens categories (ANOVA, Δt_1 : $F=1.479$, $p=0.251$). However, for Δt_2 a statistical difference was found between the different lens categories. These results suggest that while the initial temperature changes in the first few seconds have a similar environmental cause, the subsequent change depends on each lens material.

It is also important to analyse the time taken for temperature change to occur, as this may be related to the thermal conductivity of each lens material. The time from the initial to the negative deflection was defined as Δp_1 , and from the negative deflection to the recovered peak was defined as Δp_2 (Figure 3.9). Mean values of Δp_1 and Δp_2 can be seen in Table 3.7.

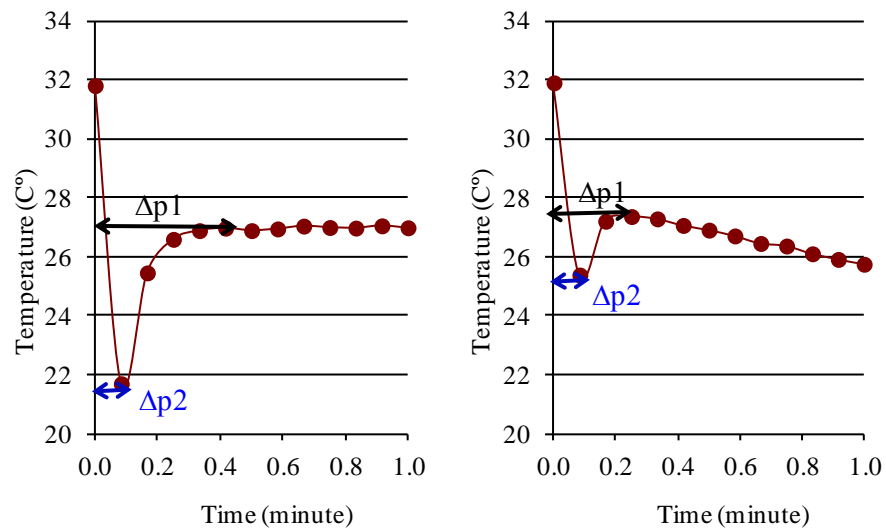


Figure 3.9: Time to reach (Δp_1) and (Δp_2), Left: RGPCL, Right: SCL and SiHCL.

Table 3.7: Mean values for Δp_1 and Δp_2 of SiHCL.

Category	Lens	Mean Δp_1 (second \pm 1sd)	Mean Δp_2 (second \pm 1sd)
RGPCL	Menicon Z	5.9 \pm 2.2	28.0 \pm 11.2
	Quasar	4.4 \pm 0.9	37.0 \pm 12.1
SCL	1-dayAcuvue	6.8 \pm 4.1	19.9 \pm 5.5
	Dailies	5.8 \pm 1.9	15.0 \pm 3.0
SiHCL	AIR OPTIX	5.4 \pm 3.0	15.6 \pm 7.8
	PureVision	2.4 \pm 1.2	19.2 \pm 1.2
	PremiO	3.0 \pm 0.6	13.2 \pm 3.6
	Biofinity	3.6 \pm 0.6	11.4 \pm 1.2

SiHCLs showed a statistically lower value of Δp_1 compared to SCLs (ANOVA, $F=17.123$, $p<0.001$). This means that SiHCLs react more rapidly than the other two materials. AIR OPTIX, which has the lowest water content, showed the highest value of Δp_1 compared to the other SiHCLs. The other three SiHCL materials responded in proportion to water content: PureVision (with the lowest water content) showed the fastest change, while Biofinity (with the highest water content) showed the slowest change.

As regards Δp_2 values, RGPCLs (Menicon Z and Quasar) showed statistically slower values compared to the other two categories (ANOVA, $F=4.644$, $p=0.016$). That is to say, RGPCLs take longer to adapt to the model eye conditions, presumably because the thermal conductivity of RGPCL is less than that of SCL or SiHCL, a factor related to the virtual lack of water content

inside of the RGP materials. The adaptation times for PureVision, PremiO and Biofinity were in proportion to their water content. PureVision showed the slowest adaptation and Biofinity showed the fastest. Similarly to Δp_1 , AIR OPTIX did not follow this tendency, moreover, in both Δp_1 and Δp_2 , AIR OPTIX had a relatively large standard deviation.

For all lenses, after an immediate temperature decrease, a temperature recovery started within one minute. To allow a comparison of the recovery rate between lenses, a normalised temperature change (calculated as the amount of decrease from the initial temperature) was calculated every one minute for ten minutes (Table 3.8).

Table 3.8: The temperature difference from the initial.

Lens / Time (min)	RGPCL		SCL		SiHCL			
	Menicon Z	Quasar	1-day Acuvue	Dailies	AIR OPTIX	PureVision	PremiO	Biofinity
1	-4.83±1.04	-5.22±1.34	-6.16±0.51	-6.25±0.39	-6.28±0.32	-7.25±0.29	-5.98±0.13	-6.12±0.17
2	-4.49±1.05	-4.48±0.62	-7.28±0.54	-7.64±0.53	-7.55±0.54	-7.84±0.29	-7.32±0.21	-7.36±0.29
3	-4.10±1.05	-4.01±0.70	-8.06±0.64	-8.31±0.74	-8.25±0.75	-8.05±0.29	-7.93±0.28	-7.84±0.36
4	-3.46±1.23	-3.65±0.77	-8.46±0.83	-8.58±0.63	-8.43±0.63	-8.11±0.33	-8.14±0.31	-8.19±0.33
5	-3.00±1.19	-3.32±1.07	-8.61±0.74	-8.79±0.59	-8.69±0.63	-8.37±0.12	-8.28±0.15	-8.34±0.24
6	-2.36±1.33	-3.00±1.17	-8.83±0.87	-9.00±0.72	-8.46±0.69	-8.22±0.38	-8.62±0.41	-8.36±0.24
7	-2.00±1.25	-2.76±1.52	-8.78±0.67	-9.19±0.76	-8.50±0.93	-8.50±0.55	-8.47±0.21	-8.65±0.26
8	-1.66±1.00	-2.63±1.35	-8.65±0.62	-9.13±0.67	-7.98±1.33	-8.50±0.69	-7.94±0.36	-8.36±0.32
9	-1.19±0.67	-2.49±1.48	-8.71±0.65	-9.27±0.66	-7.56±1.49	-8.04±0.16	-7.24±0.64	-8.03±0.46
10	-1.09±0.69	-2.24±1.45	-8.72±0.61	-9.24±0.77	-7.17±1.80	-7.66±0.40	-6.19±1.03	-7.50±0.60
Repeated ANOVA	F=37.73 P<0.001*	F=32.25 P<0.05*	F=54.37 P<0.001*	F=50.23 P<0.001*	F=6.30 P=0.051	F=3.643 P=0.084	F=16.07 P<0.05*	F=17.84 P<0.05*

Figure 3.10 shows the normalised temperature change of Menicon Z and Quasar at 1 minute intervals: the initial temperature was subtracted from the measured temperature at each time point. Although the graph shows the Menicon Z lens was more warmed up than the Quasar lens at 10 minutes, no statistically significant difference was found between the two RGPCLs (two-way repeated measures ANOVA, $p=0.4026$).

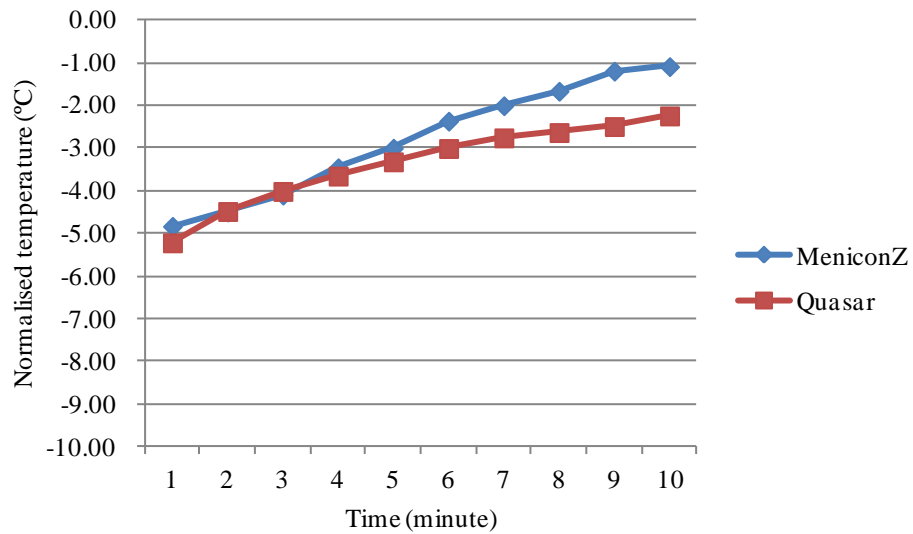


Figure 3.10: Normalised temperature change of RGPCLs

The normalised temperature change of SCLs were almost same (Figure 3.11), and, again, there was no significant difference between two the SCLs (two-way repeated measures ANOVA, $p=0.4966$)

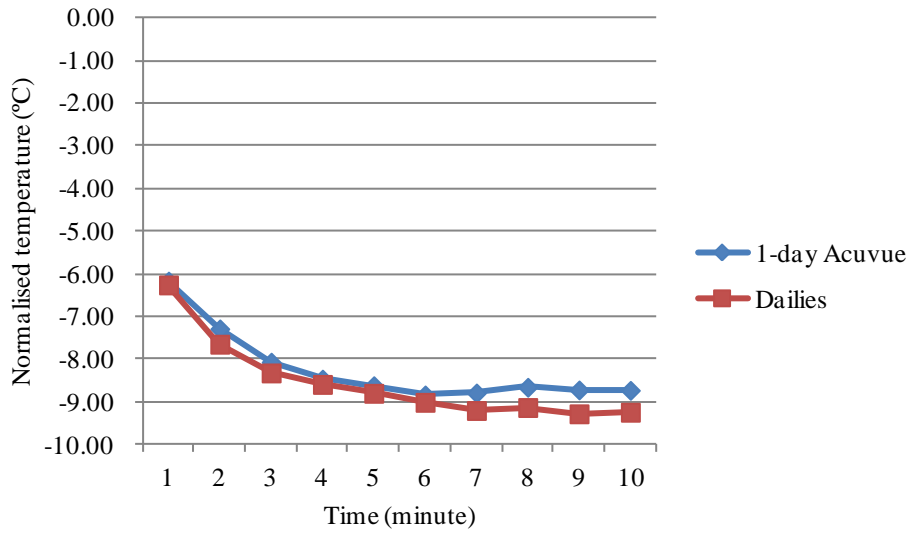


Figure 3.11: Normalised temperature change of SCLs

Lastly, for the SiHCLs, all lenses started to recover after 7 minutes (Figure 3.12). However, there was no statistically difference between them (two-way repeated measures ANOVA, $p=0.6202$).

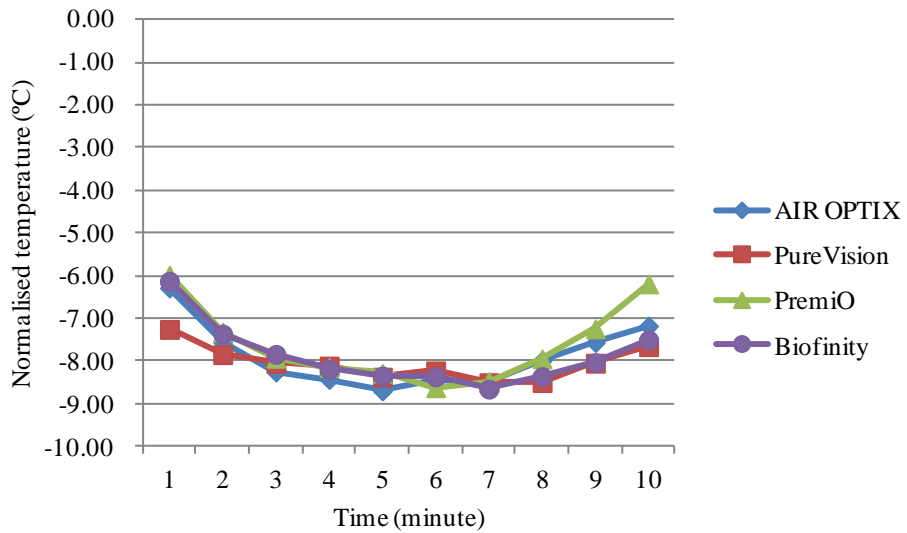


Figure 3.12: Normalised temperature change of SiHCLs

3.3.4. Discussion

This model eye experiment has been able to demonstrate the temperature changes that occur on the anterior lens surface following initial application of CLs on to the model eye. An initial significant temperature decrease was observed immediately after the lenses were applied in response to the very different environmental conditions the lenses were stored in. However, thereafter each type of lens showed a different characteristic thermal recovery pattern. The RGPCL showed a linear adaptation, with a progressive increase in the contact lens surface temperature towards the underlying model eye temperature. For the SCL and SiHCL, the adaptation was much reduced, and appeared to be affected by both the water content and lens polymer.

As Purslow suggested in her study, the initial temperature decrease can be attributed to the temperature of the storage solution in which the lens was soaked (Purslow, 2005). Purslow (2005) only analysed the temperature at initial, 3 seconds, 30 seconds, 1 minute and every 1 minute after that in her study, but as the data in this study was measured every five seconds, to give more detail about the temperature change.

The recovery rate analysis after the immediate decrease showed that: i) RGPCL materials insulate the cornea very effectively, presumably due to the minimal water content inside the

lens; ii) SCL had limited adaptation presumably because the higher water content allowed heat loss through evaporation; iii) SiHCL underwent greater adaptation after 5 minutes on the model eye, presumably due to the water reservoir within the lens being exhausted through evaporation, an effect which may occur on human eyes too. While the study did not continue beyond 10 minutes, this effect may have eventually occurred with SCL, and for the SiHCL it is possible to speculate that, with the water content removed after 10 minutes, the lenses might begin to behave like the RGP lenses, and experience a gradual increase in temperature. Confirmation of these hypotheses would require a longer testing time, along with a measurement of lens water content to confirm the evaporative loss of water from the lens.

This version of the model shows a partial effect of tear film evaporation on ocular surface temperature, but without the benefit of tear secretion and blinking, the effect cannot be sustained.

An improvement in the model would therefore be to continue to instil some artificial tear-drops at regular intervals to maintain the hydration of the lens surface to mimic a replenishment of the tears through blinking.

3.4. Contact lens and eye drop study

3.4.1. Aims

The Contact Lens Study found a limitation in the *in vitro* assessment of the insulation effects of the contact lenses from no consideration being given to the blinking process that would normally allow the tear film to lubricate the lenses *in vivo*. Consequently, the SiHCL lenses appeared to be particularly prone to drying during the experimental run. If a suitable fluid could be provided intermittently, the surface temperature of the model eye might more accurately reflect the *in vivo* situation.

The hypothesis is that hydrogel lenses, including silicon hydrogels, demonstrate increased thermal insulation effects when they dehydrate, so if dehydration can be reduced, the surface temperature of the model eye with the lens in place should show less adaptation to the underlying heat source than the results of the previous study.

3.4.2. Methods

The same experimental set-up as in Section 3.3 was used in this experiment. In addition to the model eye, a gutter made from waterproof modelling clay (Plasticine, Harbutt, UK) was added to surround the model eye in order to prevent the fluid reaching the circuit board.

Only SCL and SiHCL types were used in this study, and the characteristics of the contact lenses used are shown in Table 3.9. A 1-day Acuvue soft lens was chosen as a control lens. Four silicone hydrogel lens types were selected according to their water content ranging from 24% to 58%. Preparation of the lens and procedures of positioning it on the model eye were the same as Section 3.3.

Table 3.9: Contact lenses applied on the model eye.

	Hydrogel	Silicone Hydrogel			
Parameter	1-day Acuvue	AIR OPTIX	PureVision	PremiO	Biofinity
USAN*	Etafilcon A	Lotrafilcon B	Balafilcon A	Asmofilcon A	Comfilcon A
Manufacturer	Vistacon	Ciba Vision	Bausch & Lomb	Menicon	CooperVision
Water content (%)	58	24	36	40	48
Base curve (mm)	9.0	8.6	8.6	8.6	8.6
Diameter (mm)	14.2	13.8	14.0	14.0	14.0
Centre thickness (mm, -3.00D)	0.084	0.080	0.090	0.080	0.080
Modulus (MPa)	0.3	1.0	1.10	0.91	0.75

*USAN: United States Adopted Names

The lens surface temperature was recorded for 10 minutes, at 1 minute intervals. Each type of lens was measured randomly on the same day and repeated five times on five different days.

The average values were calculated and analysed. A 1-day ACUVUE lens was measured twice, with and without artificial tears, as a control. The experiments were conducted with a 10 minute

interval between measurements to allow the temperature of the model eye to recover and stabilise. The average room temperature was $25.5\pm 0.7^{\circ}\text{C}$, and the relative humidity was $35\pm 3\%$.

A saline solution (AVIZOR, UK) was used as the artificial tear in this study. Although the human tear film consists of three layers; lipid, aqueous and mucin, the aqueous layer performs the major role in preventing lens dehydration in this short time duration study. Before dropping the saline solution onto the contact lens positioned on the model eye, the saline was warmed in a water bath to match the temperature of human tears, which is almost equal to the body temperature: a range of $33.2\text{-}38.2^{\circ}\text{C}$ when it is measured orally (Sund-Levander et al., 2002).

Holly (1981a) referred to the tear volume in the open eye as consisting of about $1\mu\text{l}$ in the pre-ocular tear film and $3\mu\text{l}$ in the tear meniscus. However, the tear meniscus has the ability to keep $25\mu\text{l}$ without spilling (Ohashi, 1994). According to Korb et al. (2002), the rate of tear production from the lacrimal gland is estimated as $1\text{-}2\mu\text{l}$ per minute in normal subjects with a 16% turnover per minute. Therefore $2\mu\text{l}$ of artificial tears were dropped once a minute at the first trial. However, following initial trials, the drop was found to not spread equally over surface of the contact lens, and so the volume was changed to $10\mu\text{l}$ per minute. Each drop was instilled using a micro-pipette (BIOHIT PROLINE, $10\text{-}100\mu\text{l}$) to the apex of the lens from the vertical direction.

3.4.3. Result

After each lens was applied on the model eye, the measurement of lens surface temperature started. The dynamic changes in OST over nine minutes were analysed and compared using repeated ANOVA in each lens. The temperature changes from the initial application are plotted in Figure 3.13. 1-day Acuvue without artificial tear is written as “Acuvue without AT”, also with artificial tear is “Acuvue with AT”.

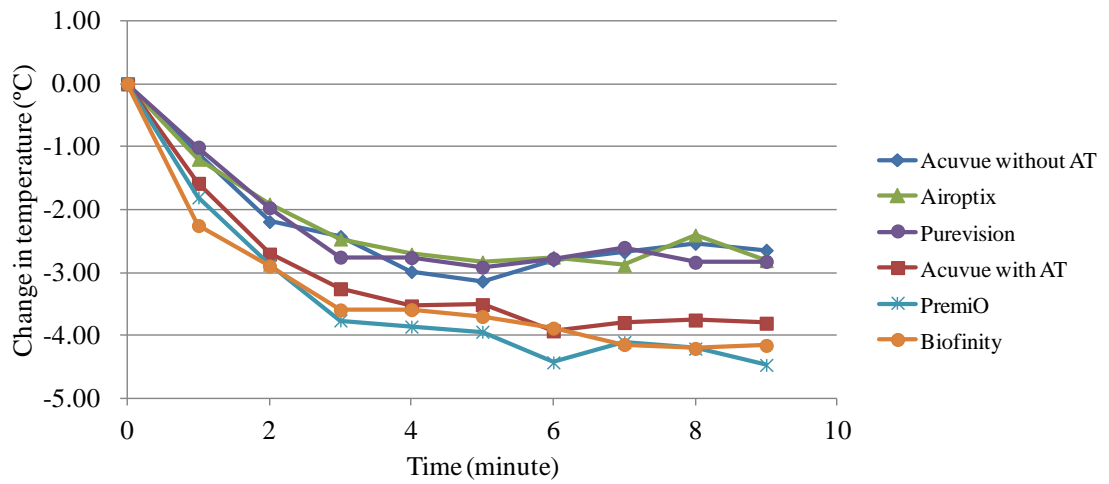


Figure 3.13: Surface temperature changes with artificial tears.

The results showed that the decrease in temperature for all lenses stabilised after 6 minutes, and thereafter reached stability. There were no statistical differences between the different lenses at each time point.

Two different response trends were noted: the silicone hydrogel lenses with lower water content (<40%) and the control lens (Acuvue) without artificial tears showed smaller temperature changes, compared with the silicone hydrogels with higher water content (>40%) and the Acuvue lens with tears.

A one-way ANOVA was conducted to explore the impact of time on the surface temperature of the different types of contact lenses on the model eye (Table 3.10: Decrease in temperature by time for contact lens groups.). Significant differences were observed across the lens types between the 2 and 9 minutes. Results of the post-hoc comparisons using the Tukey HSD are shown Table 3.11-Table 3.17.

Table 3.10: Decrease in temperature by time for contact lens groups.

Time (min)	1	2	3	4	5	6	7	8	9
Acuvue without AT	-1.11±0.45	-2.19±0.44	-2.43±0.40	-2.99±0.37	-3.14±0.36	-2.80±0.32	-2.67±0.38	-2.54±0.36	-2.65±0.31
Acuvue with AT	-1.58±0.73	-2.71±0.28	-3.26±0.44	-3.53±0.37	-3.51±0.31	-3.93±0.36	-3.80±0.38	-3.76±0.25	-3.81±0.44
AIR OPTIX	-1.20±0.84	-1.91±0.72	-2.47±1.00	-2.71±0.74	-2.83±0.46	-2.76±0.81	-2.88±0.93	-2.40±0.43	-2.81±1.22
PureVision	-1.01±0.65	-1.97±0.53	-2.76±0.88	-2.76±0.81	-2.91±0.92	-2.78±0.86	-2.60±0.97	-2.84±1.37	-2.82±1.32
PremiO	-1.81±0.63	-2.88±0.38	-3.76±0.35	-3.86±0.55	-3.94±0.45	-4.43±0.56	-4.11±0.37	-4.21±0.25	-4.47±0.28
Biofinity	-2.25±1.23	-2.90±0.54	-3.59±0.92	-3.59±0.27	-3.70±0.26	-3.88±0.22	-4.14±0.10	-4.21±0.22	-4.16±0.25
ANOVA	F=1.943 p=0.124	F=4.722 p=0.004	F=3.382 p=0.019	F=4.093 p=0.008	F=4.168 p=0.007	F=8.633 P<0.001	F=7.519 P<0.001	F=9.243 P<0.001	F=5.208 p=0.002

Table 3.11: Post-hoc test at 2 minutes.

	Control	1-day Acuvue	AIR OPTIX	PureVision	PremiO	Biofinity
Control						
1-day Acuvue	n.s.					
AIR OPTIX	n.s.	n.s.				
PureVision	n.s.	n.s.	n.s.			
PremiO	n.s.	n.s.	0.034	n.s.		
Biofinity	n.s.	n.s.	0.029	0.046	n.s.	

Table 3.12: Post-hoc test at 4 minutes.

	Control	1-day Acuvue	AIR OPTIX	PureVision	PremiO	Biofinity
Control						
1-day Acuvue	n.s.					
AIR OPTIX	n.s.	n.s.				
PureVision	n.s.	n.s.	n.s.			
PremiO	n.s.	n.s.	0.025	0.036		
Biofinity	n.s.	n.s.	n.s.	n.s.	n.s.	

Table 3.13: Post-hoc test at 5 minutes.

	Control	1-day Acuvue	AIR OPTIX	Pure Vision	PremiO	Biofinity
Control						
1-day Acuvue	n.s.					
AIR OPTIX	n.s.	n.s.				
PureVision	n.s.	n.s.	n.s.			
PremiO	n.s.	n.s.	0.017	0.031		
Biofinity	n.s.	n.s.	n.s.	n.s.	n.s.	

Table 3.14: Post-hoc test at 6 minutes.

	Control	1-day Acuvue	AIR OPTIX	Pure Vision	PremiO	Biofinity
Control						
1-day Acuvue	0.042					
AIR OPTIX	n.s.	0.032				
PureVision	n.s.	0.037	n.s.			
PremiO	0.002	n.s.	0.001	0.001		
Biofinity	n.s.	n.s.	0.041	0.048	n.s.	

Table 3.15: Post-hoc test at 7 minutes.

	Control	1-day Acuvue	AIR OPTIX	Pure Vision	PremiO	Biofinity
Control						
1-day Acuvue	n.s.					
AIR OPTIX	n.s.	n.s.				
PureVision	n.s.	0.040	n.s.			
PremiO	0.009	n.s.	0.034	0.006		
Biofinity	0.007	n.s.	n.s.	0.005	n.s.	

Table 3.16: Post-hoc test at 8 minutes.

	Control	1-day Acuvue	AIR OPTIX	Pure Vision	PremiO	Biofinity
Control						
1-day Acuvue	n.s.					
AIR OPTIX	0.044	n.s.				
PureVision	n.s.	0.020	n.s.			
PremiO	0.009	n.s.	0.001	0.018		
Biofinity	0.007	n.s.	0.001	0.018	n.s.	

Table 3.17: Post-hoc test at 9 minutes.

	Control	1-day Acuvue	AIR OPTIX	Pure Vision	PremiO	Biofinity
Control						
1-day Acuvue	n.s.					
AIR OPTIX	n.s.	n.s.				
PureVision	n.s.	n.s.	n.s.			
PremiO	0.012	n.s.	0.026	0.028		
Biofinity	0.050	n.s.	n.s.	n.s.	n.s.	

A mixed between analysis of variance was also conducted to assess the impact of different types of contact lenses on the surface temperature on the model eye. Both measurement periods and contact lens types showed significant differences.

3.4.4. Discussion

After conducting the study, it was seen that the contact lenses used could be divided into two groups: Group A with a lower water content: AIR OPTIX and PureVision, and the Acuvue control lens without drops; and Group B with a higher water content: 1-day Acuvue, PremiO and Biofinity.

The Group A lenses retained less water than the Group B lenses, and showed less conducting to the underlying heat source, since they were less able to lose heat by evaporation, leading to a more rapid adaptation in temperature. This suggests that contact lenses with higher water

content are better at insulating the lens surface from the underlying heat source, so long as that water content can be replenished through blinking.

In the human eye, the same phenomena is expected, therefore eyes wearing lenses with higher water content may lose more surface heat. However, water is not the sole ingredient of the tear film, there is also a lipid layer and a mucin layer. In particular, the lipid layer acts as a barrier to prevent the evaporation of tears and it makes the tear film stable (Korb et al., 2002, Bron et al., 2004, Rolando and Zierhut, 2001). However, the lipid layer is frequently not present over the anterior contact lens surface (Thai et al., 2004), and any beneficial effect from the lipid layer on reducing evaporation from the lens is limited. This suggests that the aqueous component of the tear film is the prime factor in the pre-lens tear film.

Measurement of this effect in the human eye may also be different since fresh, warm tears are spread over the surface of the lens during each blink. Since the thermal camera is predominantly measuring from the tear film, the changes in contact lens temperature may be partially hidden by this body-temperature 'wash'. Patients also blink more rapidly than every minute, so the post-lens tear film is not left to evaporate to the same extent as was permitted in this model study.

Finally, a difference in lens surface properties might also affect the wettability of the lens surface, and lead to differences in evaporation rates.

3.5. Conclusions

The surface temperature of RGPCL, SCL and SiHCL were successfully monitored on the model eye with and without adding the artificial tears. The use of infrared thermography revealed differences in thermal conductivity between the contact lens types used. It was shown that the water content of the lenses was a factor in producing different effects: contact lenses with high water were slower to adapt to the heat source. Therefore, the existence of the tear film, and also its stability and quality would be very important factor in human eye study. These findings will help to understand the human eye study.

Chapter 4. Investigating the relationship between tear film stability and ocular surface temperature

4.1. Introduction

Previous research has shown that the temperature of the eye is related to the quality and stability of the tear film; thus, OST is related to the thickness of the tear film (Hamano et al., 1969a). Although the tear film is spread over the ocular surface with each blink, its instability results in a gradual thinning of the pre-corneal tear film until a point is reached where a blink is triggered to re-form the tear film and re-start the process. Tear film thinning also causes temperature change over the ocular surface due to an associated evaporation of the tears from the eye. This produces cooling in the tear film, which can be observed with a thermal imaging camera. Since an increase in the thickness of the lipid layer results in an increase in the stability of the tear film, the same thickness increase may cause the tear film to cool less quickly, which can be detected by thermal imaging.

In order to further investigate this relationship, this study assessed the correlation between the non-invasive tear break-up time (NIBUT) and OST. NIBUT, which is an indicator of tear film stability, has been measured using a Tearscope (Keeler, Windsor, UK) in previous studies. This method works by projecting a grid pattern onto the tear film, and a distortion in the grid pattern is observed as the tear film thins and begins to break-up. The time that elapses from the previous blink to the first signs of distortion is a measure of tear film stability. However, detecting the point of distortion can be difficult in some patients, especially in those with thin tear films.

On the other hand, the DR-1 (Kowa, Nagoya, Japan, Figure 4.1) is a video interferometer that observes the interference patterns created in the tear film by differences in the lipid layer thickness. The DR-1 can show the image clearly as it eliminates the background iris colour and central image defect (Savini et al., 2008).



Figure 4.1: The DR-1 (Kowa, Nagoya, Japan).

The Tearscope and DR-1 are both non-invasive; however, the investigator must hold the Tearscope during the assessment because it is basically a handheld device, and this can interfere with the steady measurement of stability. Additionally, the subjects may not maintain a steady frontward gaze when the Tearscope is used, thus altering the natural extent of ocular surface exposure and affecting NIBUT. In contrast, the DR-1 is mounted on a table and the patient is positioned on a chin-rest. With these advantages, the Kowa DR-1 was used instead of the Tearscope in this study.

There were few previous publications on the relationship between NIBUT and OST. Giraldez et al. (2009) found no significant relationship between OST (measured as the average of the pre- and post-blink OST in the centre of the cornea) and NIBUT. However, Purslow (2005) reported negative correlations between NIBUT and the initial OST at five locations on the cornea (central, nasal, superior, inferior, and temporal) in normal subjects. In other words, the initial OST tends to be low if NIBUT is long. Purslow explained that this effect may be due to a stable tear-film having different emissivity properties due to lipid content, or that a longer break-up time may occur in a cooler eye where evaporation is less and therefore heat exchange occurs slowly. In assessing this hypothesis, she found that a subject with longer NIBUT exhibits smaller and slower temperature changes over time following a blink. Purslow measured NIBUT with the Tearscope which is considered to be influenced by both the stability of the lipid layer and the evaporation of the aqueous layer (Guillon, 1998), so if NIBUT is measured by the DR-1, it may be possible to see the sole effect from the stability of the lipid layer.

The purpose of this study was to investigate the effect of the quality of lipid layer of the tear film on OST by assessing the stability of the tear film using DR-1 and measuring OST using the thermal camera. The hypothesis tested in this study is that subjects with longer NIBUT will decrease their OST slowly due to the stable lipid layer preventing the evaporation. Although the subjects in this study were all Japanese, it has been reported that there is no difference in NIBUT between Asians and Caucasians (Cho and Douthwaite, 1995).

4.2. Methods

4.2.1. Subjects

The right eyes of 30 volunteers were assessed in this study. Subjects were recruited from amongst employees at Menicon Co., Ltd in Japan. The subject demographics are summarised in Table 4.1. All subjects in this study were Japanese.

Table 4.1: Number, gender and ages of subjects

Gender	Number of subjects	Age, Mean (SD) (yr)	Age, Range (yr)
Male	10	40.2 (7.9)	26–48
Female	20	35.3 (5.8)	28–49
Total	30	36.9 (6.9)	26–49

Inclusion criteria for this study were as follows:

- i) no history of eye disease
- ii) no contact lens wear for one night
- iii) good general health and well-being
- iv) no dry eye symptoms

Ethical approval was granted prior to commencement of the study from the Human Ethics Review Committee of Menicon in Japan, and informed consent was obtained from each subject.

If the subject wore contact lenses, he/she was asked to remove the lenses at least 1 day before the measurement to minimise the effect of contact lens wear on the tear film. The subjects were instructed to attend a single session, and measurements were made on the right eye only. The subjects were asked to remain in the laboratory during the entire session to avoid any

compromise of their OST due to changes in room temperature or humidity outside of the laboratory in Japan.

4.2.2. Tear film stability assessment

The quality of the tear film was examined non-invasively using the DR-1 (Kowa, Japan), which is a video interferometer that observes the interference patterns of the tear film on the cornea. This system uses a white light source, making it possible to observe specular reflected images from the tear surface. The subject was asked to sit in front of the DR-1 and to put his/her chin on the rest. After the focal length had been set, the subject was asked to blink naturally several times and to subsequently keep his/her eyes open for up to 10 secs to measure NIBUT (3 repeated measures).

In a previous report, NIBUT was measured for over 30 secs (Purslow, 2005). A disadvantage of this extended period is that, even if the tear film is not disrupted during such a long period of eye opening, reflex lacrimation is more likely to occur, which will interfere with NIBUT. Therefore, NIBUT will be measured only for up to 10 secs in this study. According to the definition and diagnosis of dry eye (Shimazaki, 2007), subjects whose NIBUT is less than 5 secs have a possible risk of dry eye; therefore by using a 10 secs cut-off, the effect of prolonged eye opening in dry eye subjects was limited, while still enabling a sufficient period to record a temperature change.

The DR-1 has two viewing modes (low and high magnification) that allow observation of 7 mm and 2mm circular areas in the central cornea, respectively. In this study, the low magnification

mode was selected to obtain the information about the behaviour of the lipid layer of the pre corneal tear film (Yokoi et al., 2008).

4.2.3. Ocular surface temperature measurement

To measure the OST, the subject was asked to move to another room and to sit in front of the thermal camera (A-315, FLIR SYSTEMS, Japan). The subject was allowed to adapt to room temperature before starting the assessment for 10 mins. The average environmental conditions during this study were: room temperature of $20.2 \pm 0.8^{\circ}\text{C}$ and humidity of $38.8 \pm 6.6\%$. The OST was recorded as a short video that consisted of a series of images of the magnified eye. The procedure was similar to that of the DR-1. After the adaptation time, the subject was asked to blink naturally several times and to subsequently keep his/her eyes open for up to 8 secs. The recorded images were analysed afterwards. The temperature of the centre of the cornea was calculated at each second after blinking. This was calculated both at the spot and in the circled area with a diameter of 8.5mm. The thermal image of the eye and tools for analysis were shown in Chapter 2 (2.2.3 Analytical localisation). Statistical analysis was used to compare the effect of the quality and stability of the tear film on OST.

4.2.4. Other assessments

Subjects were asked whether they had any subjective symptoms, and eight of the thirty subjects answered that they regularly felt itchiness because they suffered hay fever. An ophthalmologist checked the subject's anterior ocular surface by slit-lamp bio-microscopy to exclude subjects who failed the inclusion criteria. The CCLRU grading scales were used to grade limbal and conjunctival hyperaemia. Fluorescein was instilled to grade corneal and conjunctival staining.

Other aspects of anterior ocular health were also recorded, such as tarsal hyperaemia and papillary conjunctivitis. However, as the ocular conditions of all subjects were between normal and mild, the effects of each measures were not investigated in this study.

4.3. Results

4.3.1. Initial OST

The average NIBUT of all subjects was 5.41 ± 2.39 secs. The correlations between NIBUT and the initial central OST calculated on the spot and in the area are shown in Figure 4.2 and Figure 4.3, respectively. Although the initial OST tended to increase in line with increasing NIBUT, no significant correlations were observed (Spearman's rho: spot, $r = 0.343$ and $p = 0.064$; area, $r = 0.257$ and $p = 0.170$).

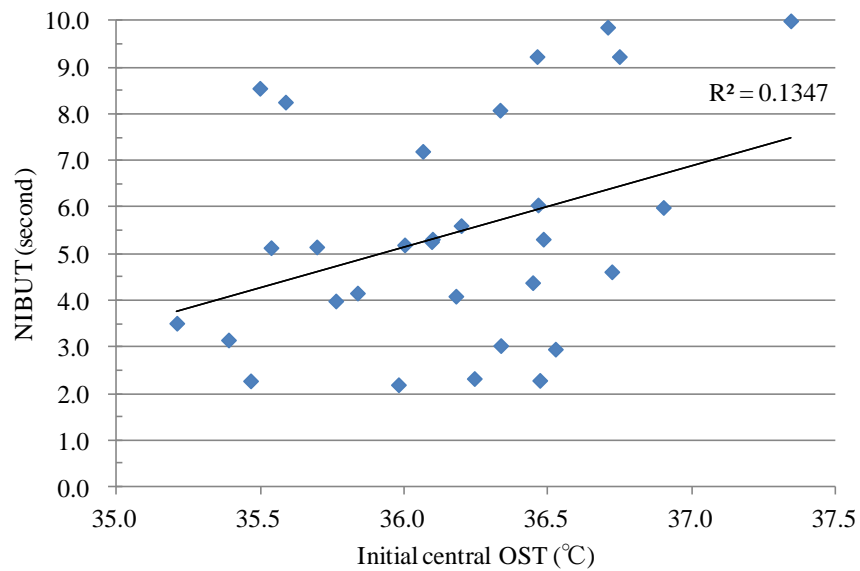


Figure 4.2: Correlation between the initial central OST at the central cornea and NIBUT.

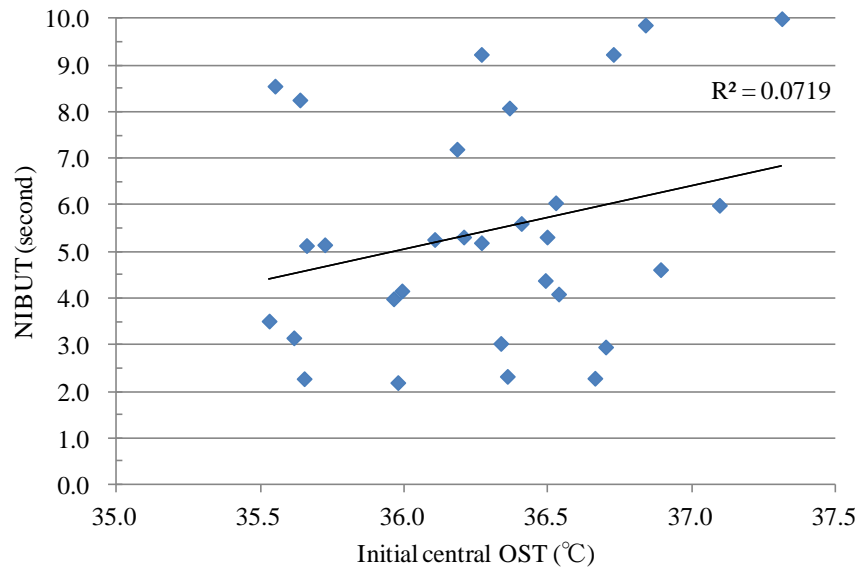


Figure 4.3: Correlation between the initial central OST over the test area and NIBUT.

4.3.2. Post-blink change in OST

The degree of change in the post-blink OST measured at the central cornea spot and in the area is plotted in Figure 4.4. The data after eye closure were not analysed because some subjects could not hold their eyes open for 8 secs. The amount of post blink change is summarised in Table 4.2.

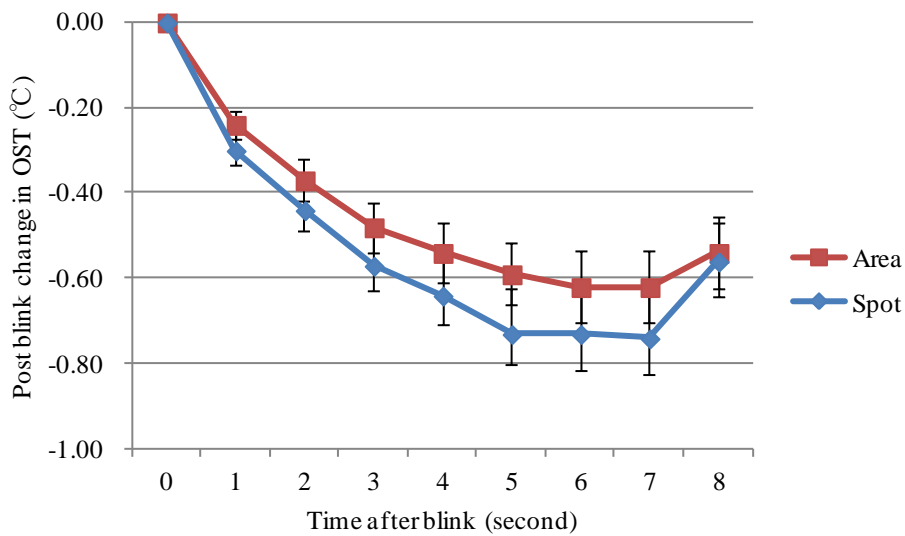


Figure 4.4: Post-blink change in OST (mean±1S.D.).

Table 4.2: Post-blink change in OST (mean±1S.D.).

	OST	Time (minute)								ANOVA (Time: 1-7)
		1	2	3	4	5	6	7	8	
Spot	Mean±SD (°C)	-0.30±0.24	-0.44±0.35	-0.57±0.42	-0.64±0.49	-0.75±0.54	-0.78±0.54	-0.78±0.54	-0.63±0.49	F=32.69
	Range (°C)	-0.03 - 0.95	-0.09 - 1.28	-0.08 - 1.59	0.03 - 1.78	0.00 - 2.15	0.04 - 1.75	0.07 - 1.85	0.06 - 1.55	P<0.0001
Area	Mean±SD (°C)	-0.24±0.18	-0.38±0.26	-0.50±0.31	-0.54±0.38	-0.59±0.40	-0.62±0.43	-0.62±0.42	-0.54±0.35	F=29.88
	Range (°C)	-0.03 - 0.75	0.02 - 1.01	0.04 - 1.13	0.02 - 1.34	0.04 - 1.46	0.01 - 1.53	0.06 - 1.52	0.04 - 1.12	P<0.0001
	N (eye)	30	30	30	30	30	26	25	18	

Post-blink change in OST decreased significantly (one-way repeated ANOVA). However, there was no statistical difference between spot and area (two-factor repeated ANOVA, $F=0.511$, $p=0.4781$). The post-blink OST decreased until 6 secs, whereupon it reached a plateau and subsequently decreased at 8 secs because of inappropriate data from subjects whose NIBUT was short. Therefore, the subjects were classified into 3 categories according to the NIBUT length: short (up to 5 secs), middle (from 5 to 8 secs), and long (from 8 to 10 secs). Table 4.3 shows the definition of each NIBUT group and measured NIBUT.

Table 4.3: NIBUT category.

Category	Short	Middle	Long
Range of NIBUT (sec)	0-5	5-8	8-10
NIBUT, Mean \pm SD (sec)	-3.53 \pm 1.23	-5.72 \pm 1.44	-8.94 \pm 1.09
N (eye)	12	12	6

Figure 4.5 shows the post-blink changes in OST at the central spot, and the mean results for each NIBUT category is summarised in Table 4.4.

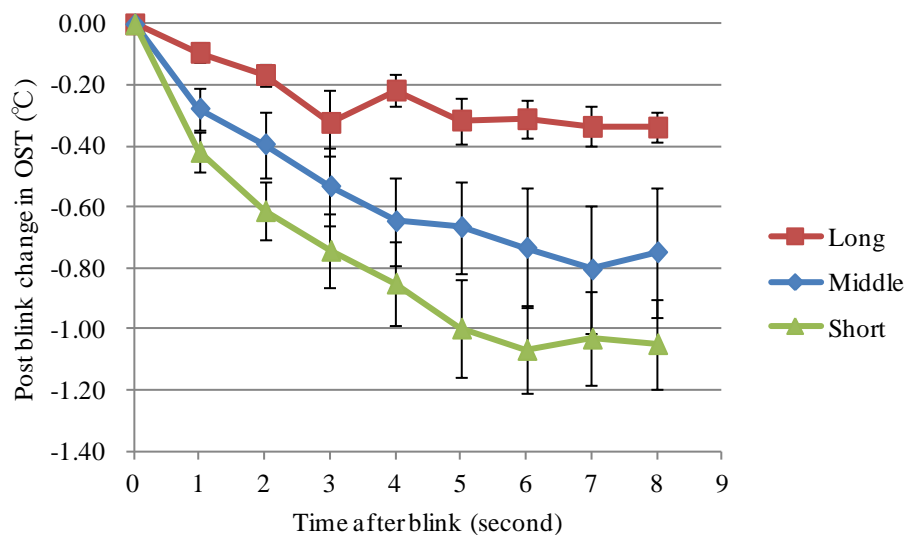


Figure 4.5: OST change on the spot (mean \pm 1S.D.).

Table 4.4: Post-blink change in OST on the spot (mean±1S.D.).

	Time (second)								
OST (°C)	1	2	3	4	5	6	7	8	ANOVA
Long	-0.09±0.08	-0.17±0.09	-0.32±0.26	-0.22±0.13	-0.32±0.18	-0.31±0.15	-0.34±0.16	-0.34±0.11	F=10.08 p<0.0001
N (eye)	6	6	6	6	6	6	6	6	N=6 (0-8 mins)
Middle	-0.28±0.24	-0.39±0.38	-0.53±0.44	-0.65±0.50	-0.67±0.52	-0.73±0.62	-0.80±0.67	-0.75±0.60	F=10.81 p<0.0001
N (eye)	12	12	12	12	12	10	10	8	N=10 (0-7 mins)
Short	-0.42±0.24	-0.61±0.33	-0.74±0.42	-0.85±0.48	-1.00±0.56	-1.07±0.46	-1.03±0.43	-1.05±0.21	F=31.39 p<0.0001
N (eye)	12	12	12	12	12	10	8	2	N=8 (0-7 mins)
Total (eye)	30	30	30	30	30	26	24	15	

Post-blink change in OST in each category decreased. However, some subjects in the short and middle NIBUT categories could not hold their eyes open for eight secs after a blink. Therefore, the number of eyes used for the statistical analysis were smaller than the original cohort number, and the range of time was limited to allow enough eyes to be included. The amount of OST decrease became larger in long, middle and short in this order. As can be seen in Table 4.4, they were all statistically significant changes.

Figure 4.6 shows the post-blink changes in OST in the circular area, and the mean results for each NIBUT category is summarised in Table 4.5.

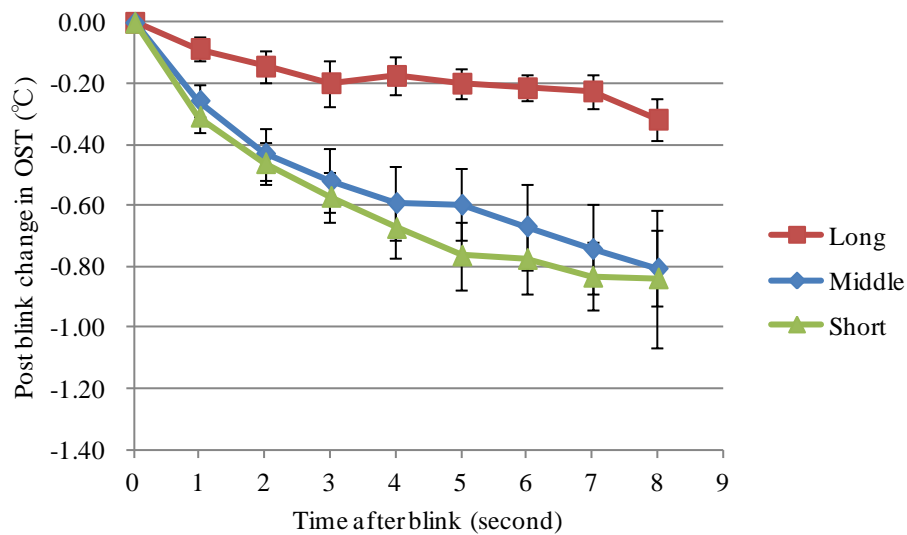


Figure 4.6: OST change in the area (mean±1S.D.).

Table 4.5: OST change in the area (mean±1S.D.).

	Time (second)								
OST (°C)	1	2	3	4	5	6	7	8	ANOVA
Long	-0.09±0.09	-0.14±0.13	-0.20±0.18	-0.17±0.15	-0.20±0.12	-0.21±0.11	-0.23±0.14	-0.32±0.17	F=5.866 p<0.0001
N (eye)	6	6	6	6	6	6	6	6	N=6 (0-8 mins)
Middle	-0.26±0.18	-0.43±0.27	-0.52±0.35	-0.59±0.40	-0.60±0.39	-0.67±0.45	-0.74±0.46	-0.81±0.33	F=17.14 p<0.0001
N (eye)	12	12	12	12	12	10	10	8	N=10 (0-7 mins)
Short	-0.31±0.19	-0.46±0.23	-0.57±0.29	-0.67±0.34	-0.76±0.38	-0.77±0.37	-0.83±0.30	-0.84±0.32	F=27.15 p<0.0001
N (eye)	12	12	12	12	12	10	8	2	N=10 (0-6 mins)
Total (eye)	30	30	30	30	30	26	24	15	

Post-blink change in OST in each category decreased in the same pattern as the results measured at the central spot. As can be seen in Table 4.5, post-blink change in OST decreased in all categories and were statistically significant changes. The size of decrease in the short and middle NIBUT groups was similar and also greater than the long NIBUT group, and there was no statistically difference between them (two-way repeated ANOVA, $F=0.73$, $p=0.6053$). This suggests that more post-blink OST changes may have occurred at peripheral areas in subjects in the middle NIBUT group.

4.4. Discussion

In this chapter, the relationship between NIBUT of the lipid layer and the OST were investigated. NIBUT obtained from this study tended to be shorter, since NIBUT from normal eyes is typically within the range of 40-60 seconds (Tonge et al., 1991). This variation may be due to the differences in the instruments and examiners (Tomlinson et al., 2011).

In this study, the OST was measured at both a central spot and over a circular area, for up to eight seconds after a blink. In previous research, Purslow measured the initial OST at five different regions of the ocular surface: central, nasal, superior, inferior and temporal (Purslow, 2005), but found no statistically significant difference in the initial OST across the five areas. A decrease in OST was observed after a blink, with the level of post-blink OST decrease significantly different between corneal location. The central area especially showed the greatest decrease after eight secs. This suggested that the geometrical centre loses more heat energy after blinking because it has the highest exposure to the environment. Therefore, the OST measured on the spot would reveal a clear difference amongst subjects with different NIBUT lengths.

In this study, a weak positive correlation was found between the NIBUT and the initial OST. Purslow (2005) reported an opposite trend, with a significant negative correlation. It was proposed that, a lower initial OST tended to retain a similar temperature after a blink because there was less evaporation and heat exchange. As the stability of the lipid layer was measured by DR-1 in this study, a small change in OST would suggest a thick and stable tear film, which prevents evaporation.

Although the correlation between NIBUT and the initial OST was opposite in this study compared to Purslow, the same tendency was found in the post-blink change: eyes with a longer NIBUT exhibited smaller and slower temperature changes over eight secs following a blink. This is consistent with a stable tear film that can maintain heat energy for a longer period with less heat loss.

The OST decrease after a blink has been reported by many researchers and widely-accepted (Efron et al., 1989, Purslow, 2005, Morgan et al., 1995). It has also been reported that dry eye is a factor that leads to lower tear film stability and rapid cooling after a blink (Morgan et al., 1996, Craig et al., 2000). Also, correlations have been found between the quality of the tear film and post-blink cooling, with lipid-deficient dry eyes having an increase in evaporation, showed as faster cooling (Morgan et al., 1996).

In this study, the result obtained from the central spot revealed the most dynamic change in the OST, and that the circular area followed the effect of the OST in the periperal cornea. The magnitude of the OST decrease at the central cornea was different depending on the quality of the tear film lipid layer. When measuring the OST across the overall cornea, the incomplete lipid layer was associated with greater heat loss, while the stable lipid layer was not affected (Figure 4.6).

Similarly, existing contact lens wearers with dry eye symptoms and subjects who stop using contact lenses may have a rapid OST decrease because of the unstable tear film on the contact lens. Therefore, it would be useful to measure the OST to determine its rate of change in contact

lens wear. While this step is not being performed in this study, the outcome of this study will provide findings regarding OST changes in normal subjects and whether OST is correlated with the NIBUT measured by using a different instrument, the DR-1, allowing future research to investigate the effect of contact lens wear.

4.5. Conclusions

The results from this study provide additional information about the source of the OST measured by infrared thermography and further support the idea that the OST measured by infrared thermography is principally that of the tear film and will therefore be related to tear film stability.

Chapter 5. An investigation of ocular surface temperature change with contact lens wear

5.1. Introduction

The previous *in vitro* studies in this thesis have demonstrated that contact lenses can be affected by the thermal environment in which they are placed, and that their response to this environment depends on the lens material, the lens water content, and the tear replenishment over the lens surface. The findings can be summarised as:

- Contact lenses will absorb thermal energy from an underlying heat source and re-emit this energy as infrared radiation, detectable by a thermal camera.
- Contact lenses with higher water content will adapt more slowly in temperature to the underlying heat source than other contact lenses (Chapter 3).
- The presence of surface moisture replenished over the lens surface is an important factor in moderating temperature change in a contact lens (Chapter 3).
- The speed of temperature change differs according to NIBUT (Chapter 4)

Having established that contact lenses are affected by an underlying heat source, the next step is to investigate the effect of the human eye and tear film on the contact lens, in order to investigate the primary hypothesis of this thesis of whether changes in the ocular surface temperature are produced by contact lens wear, and whether those changes are altered by lens material, lens water content and tear replenishment over the lens surface during blinking.

Although tear exchange under the lens is an important factor in maintaining good corneal health (Kam et al., 1999), the non-invasive assessment of tear exchange with contact lenses is technically

challenging. It is hypothesised that measuring the temperature difference between the lens periphery surface and the nearby ocular surface will give some indication that tear exchange is occurring. To investigate this further, OST was compared between the lens periphery and conjunctiva in this study.

In establishing the study design, it is useful to review the work by Purslow (2005), previously reported in Chapter 1:

- Contact lens wear increases OST compared to a non-lens wearing eye.
- There is no statistical difference in OST change produced between daily wear and continuous lens wear.
- OST during lens wear is lower with traditional hydrogel lenses than with silicone hydrogel lenses.
- Silicone hydrogels with higher water content are likely to decrease OST in the short term.

From this it can be concluded that contact lens wear alters the OST, that the thermal properties of a soft lens affects the type and extent of OST change, and that wearing time (at least between daily and continuous wear) has no differential effect on OST (Purslow et al., 2005).

Although helpful in understanding the effect of contact lenses on OST, the report by Purslow et al. had an experimental design that limited the conclusions that could be made. In the study Purslow measured OST at 23 points across the ocular surface and found significance in the rate of OST change in the temporal and superior corneal areas with lenses in situ. However, the location of these test points (Figure 5.1) was not specified in relation to the contact lens position on the eye, and so it is possible that the test points recording temperature on the lens edge may instead have been measuring from the conjunctiva.

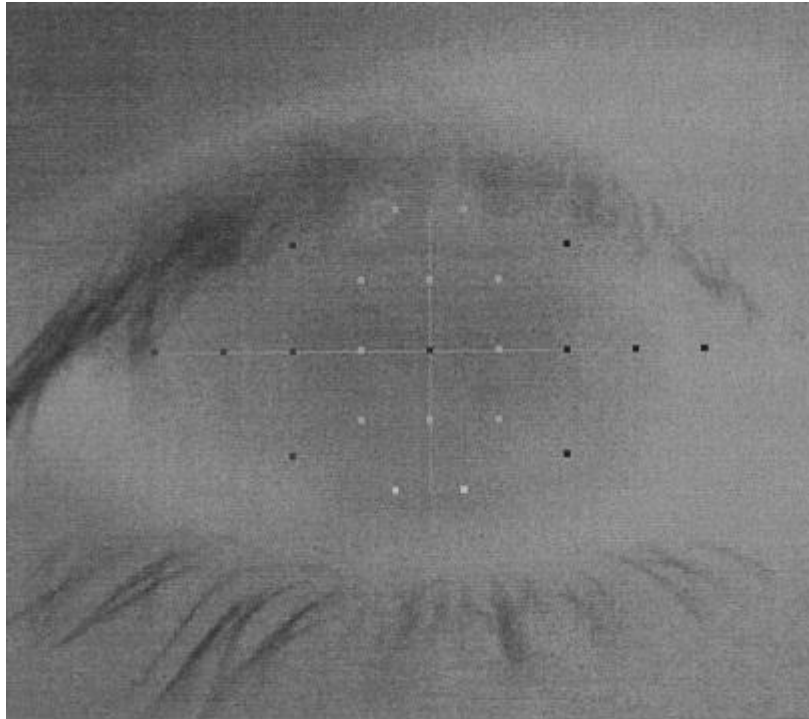


Figure 5.1: Position of the OST recording points across the anterior eye as used by Purslow et al. (taken from the doctoral thesis of Purslow (2005)).

Furthermore, Purslow and other researchers did not investigate the effect of different lens materials including rigid gas permeable contact lenses (RGPCl) on OST in the same subjects. Reviewing the literature, there have been few reports which investigated the effect of silicone hydrogel contact lenses or rigid gas permeable contact lenses on OST (Hamano et al., 1969b, Fatt and Chaston, 1980, Purslow et al., 2005), and no studies were found that reported on the effect of tear exchange rate for soft and rigid lenses. Since Purslow's studies were completed, silicone hydrogel lens materials have changed, with some of the latest silicone hydrogels having a water content of more than 50%, which may change the previously seen effects from lens wear in OST.

The aims and hypothesis of this study were divided into two parts.

Part A: To investigate the thermal effect on OST of different contact lens materials.

For studies in the first part of this chapter, the OST was measured at the centre of the cornea only.

i. To test the hypothesis that the post-blink OST of RGPCL will decrease faster than that of SCL/SiHCL

During soft contact lens (SCL) wear the lens temperature may increase due to heat retention in the lens, whereas with gas permeable (GP) lens wear increased tear evaporation from an unstable pre-lens tear film may promote general cooling. In other words, since the pre-lens tear film on a RGPCL is likely to disrupt more quickly than that on a SCL, the OST over a RGPCL should decrease faster. It is also possible that tear exchange may interact with this effect.

ii. To test the hypothesis that the thermal conductivity of SiHCL and SCL are the same in lenses with the same water content.

The studies in Chapter 3 showed that the water content of a lens will affect the thermal properties of a contact lens, but the contribution of the lens polymer is not known. It is thought that the silicone hydrogel lens material has a lower thermal conductivity than the traditional hydrogel (Table 5.1), and so it should retain heat energy less efficiently than SCLs.

Table 5.1: Typical values of thermal conductivity

Material	Thermal conductivity [W/m.K]
Cornea (bovine)*	0.28
Soft contact lens material*	0.28
Hard contact lens material*	0.19
Silicone rubber	0.16
Water	0.60
Air	0.0241

*Adapted from an original table by Hamano et al. (1972). Unit was converted from [cal/cm.sec.°C] to [W/m.K]. Other values were taken from Chronological scientific tables (National Astronomical Observatory of Japan, 2011).

iii. To compare the effect of water content of SiHCL (low vs. high)

The *in vitro* study (Chapter 3) compared four SiHCLs in the same FDA group (Group I : low water content, non-ionic material). Lenses with higher water content (>40%) showed a smaller decrease in the surface temperature on the model eye with the artificial tear, compared to the other lenses. This indicates the importance of the tear film in replenishing water evaporated from the lens surface during wear.

In this study, lenses from different groups, I and II : low and high water content with non-ionic material, respectively, were compared. It is hypothesised that the OST change with Group II lenses will increase more slowly and have less post-blink temperature decrease.

Part B: To investigate the effect of tear exchange.

For the studies in the second part of this chapter, the OST was measured at both the peripheral cornea (OSTP; OST on the lens edge) and on the adjacent conjunctiva (OSTC).

This study investigated the thermal characteristics of the lens by providing a direct comparison of OST between the peripheral lens surface and the conjunctiva, and whether local tear exchange in the lens periphery influenced this comparison.

5.2. Methods

5.2.1. Subjects

The right eyes of fifteen healthy volunteers were assessed in this study (Table 5.2). Subjects were recruited from amongst colleagues in Cardiff University. All of the subjects had no history of eye disease, had good general health and had no history of dry eye symptoms.

Six subjects had worn soft contact lenses (SCL), six had worn rigid gas permeable contact lenses (RGPCL), and three subjects did not wear contact lenses. Subjects who were lens wearers were asked to not wear their contact lenses on the day of the study. The contact lens wearers were all known to have good lens fits, and had no history of ocular inflammation.

Table 5.2: Details of subjects used in this study

Gender	Number of subjects	Mean age \pm 1SD (yr), range (yr)	Mean corneal radius \pm 1SD (mm), range (mm)
Male	5	32.2 \pm 6.7 25-43	7.88 \pm 0.13 766-806
Female	10	27.2 \pm 6.6 22-44	7.55 \pm 0.25 710-797
Total	15	28.9 \pm 6.9 22-44	7.67 \pm 0.27 710-806

Ethical approval for the study was granted from the Cardiff University School of Optometry and Vision Sciences Human Ethics Review Committee prior to commencement of the study, and informed consent was obtained from each subject.

5.2.2. Contact lens types

To compare the effect of material, four different contact lenses were examined in this study: one gas permeable lens, one silicone hydrogel lens with low water content, one silicone hydrogel lens with medium water content, and one hydrogel lens with medium water content. The lens specifications are shown in Table 5.3.

Table 5.3: Specifications of lenses

Lens name	Menicon Z- α	AIR Optix	Clariti	1-day Acuvue
Type of contact lens	Rigid gas permeable (RGPCL)	Silicone hydrogel (SiHCL)	Silicone hydrogel (SiHCL)	Hydrogel (SCL)
USAN	Tisilfocon A	Lotrafilcon B	Filcon II 3	Etafilcon A
Manufacturer	Menicon	Ciba Vision	Sauflon	Vistacon
FDA Group	III (Contains silicone and fluorine)	I (Non-ionic, low water content)	II (Non-ionic, high water content)	VI (Ionic, high water content)
Water content (%)	<1	33	56	58

Lens packages were opened before each experiment and allowed to equilibrate to room temperature for 30 minutes. For the Menicon Z- α RGPCL, each lens was re-used, after cleaning with Menicare Plus (Menicon, Japan), on a further day. For the silicone hydrogel and hydrogel lenses, each lens was disposed of after use.

5.2.3. Study design and procedure

Subjects were asked to attend for four single sessions and to wear a different contact lens type at each visit. Measurements were made on the right eye only. During each session, subjects were asked to stay in the laboratory to avoid any compromise of their OST due to changes in room temperature or humidity outside of the laboratory. If the subject was an existing contact lens wearer, they were requested to remove their lenses at least one day before the measurement.

Before starting the experiment, subjects were adapted to room temperature for 10-15 minutes. Prior to lens insertion by the researcher, a preliminary measurement of OST for each subject was made at each session as a baseline data. Subjects were then randomly assigned to a lens wear sequence, so that they had worn all four lenses and all three lens types by the end of the fourth session. Radiated temperature from the anterior eye was recorded, as described in Chapter 2.

Measurements were taken at three locations: the centre of the cornea, lens periphery, and conjunctiva. To measure the temperature at these locations, seven spots were chosen: one spot on the centre of the cornea, three each on the peripheral cornea and the conjunctiva. To ensure consistency of location choice, a transparent template, on which was marked the position of the seven test spots, was placed over the OST output display computer screen. The examiner used this template to make the correct test location spots on the thermal image output on the screen. The central OST location was chosen since previous studies had shown the most dynamic temperature changes at this spot. The lens periphery and conjunctiva locations were chosen to assess the effect of the tear exchange by allowing a comparison of temperature inside and outside of the lens edge. The spots on the conjunctiva positioned beyond the contact lens edge were labeled OSTC, while the spots on the lens periphery

were labeled OSTP. Figure 5.2 and Figure 5.3 show examples of the thermal image when wearing a RGPCL and SCL, respectively, along with the marked locations of the test spots. The circle tool (diameter, 10mm) is marked on the image to demonstrate the relative positioning of the spots for each lens type. The 10mm diameter is almost same as the diameter of the RGPCL (9.6mm) used in this study, and so the inner three OSTP spots for the RGPCL were placed inside the circle, whereas for the SCL, which has a larger diameter, the inner OSTP spots were placed further out, but still inside the SCL.

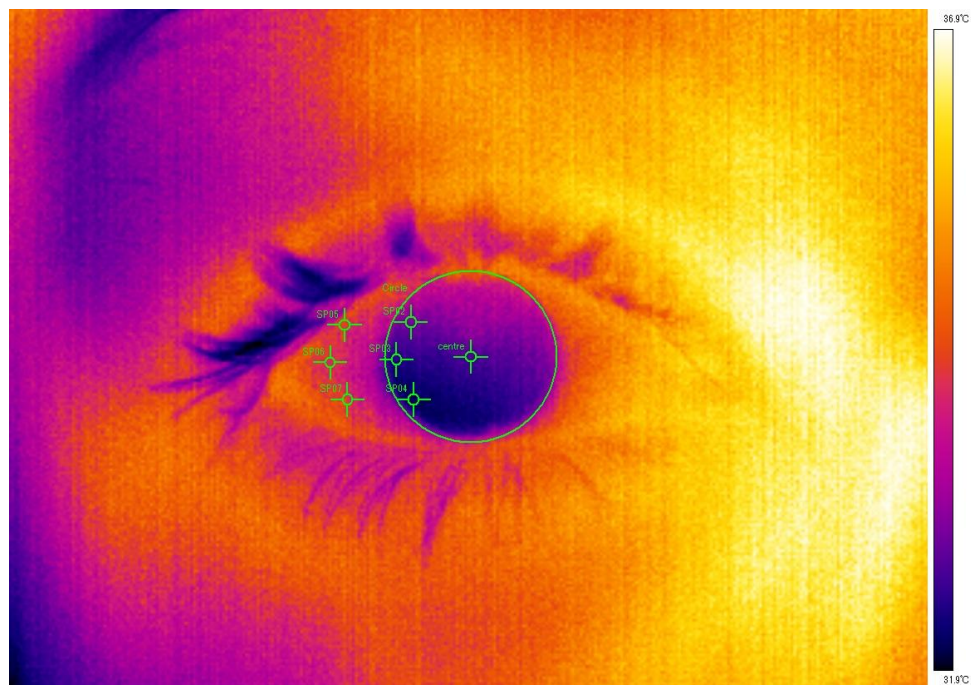


Figure 5.2: The thermal image of the eye with RGP lens wear marked up with the software analysis tools.

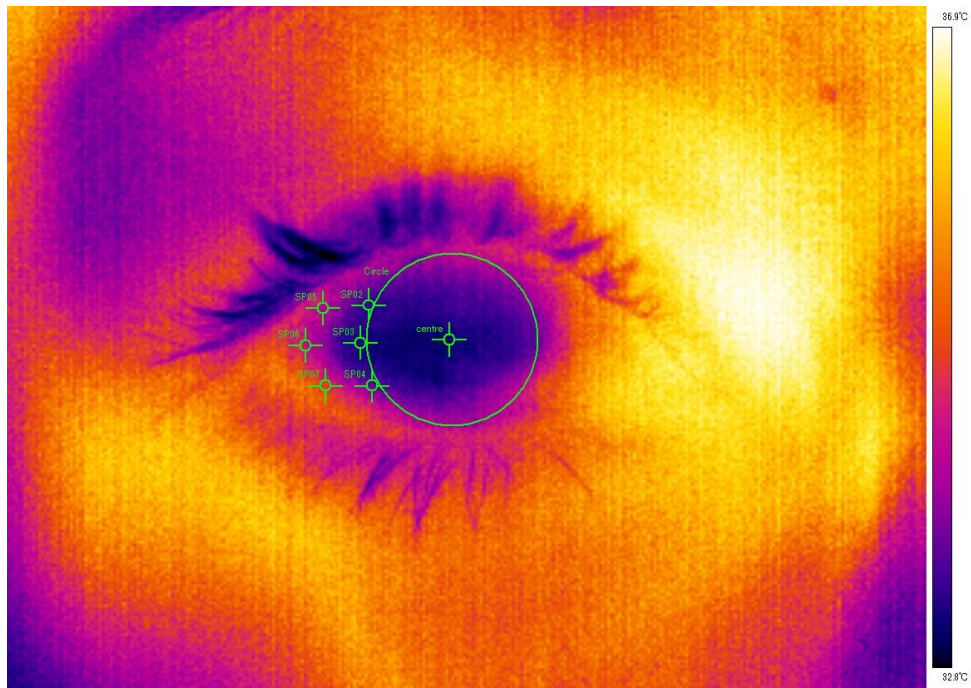


Figure 5.3: The thermal image of the eye with SCL wear marked up with the software analysis tools.

Measurements were repeated at 2, 5, 10, 20, 30 and 60 minutes after lens insertion. After 60 minutes, the contact lens was removed and OST was taken at 2, 5 and 10 minutes. Initial OST after a blink was calculated after 0.2 seconds at each time point, and again 8 seconds after the blink. Results for each subject were normalised to their pre-lens wear baseline (the preliminary OST without a lens wear), and the temperature difference between 0.2 and 8 seconds was calculated as the post-blink OST change. These values can be graphically seen in Figure 5.4 as A and B-A, respectively.

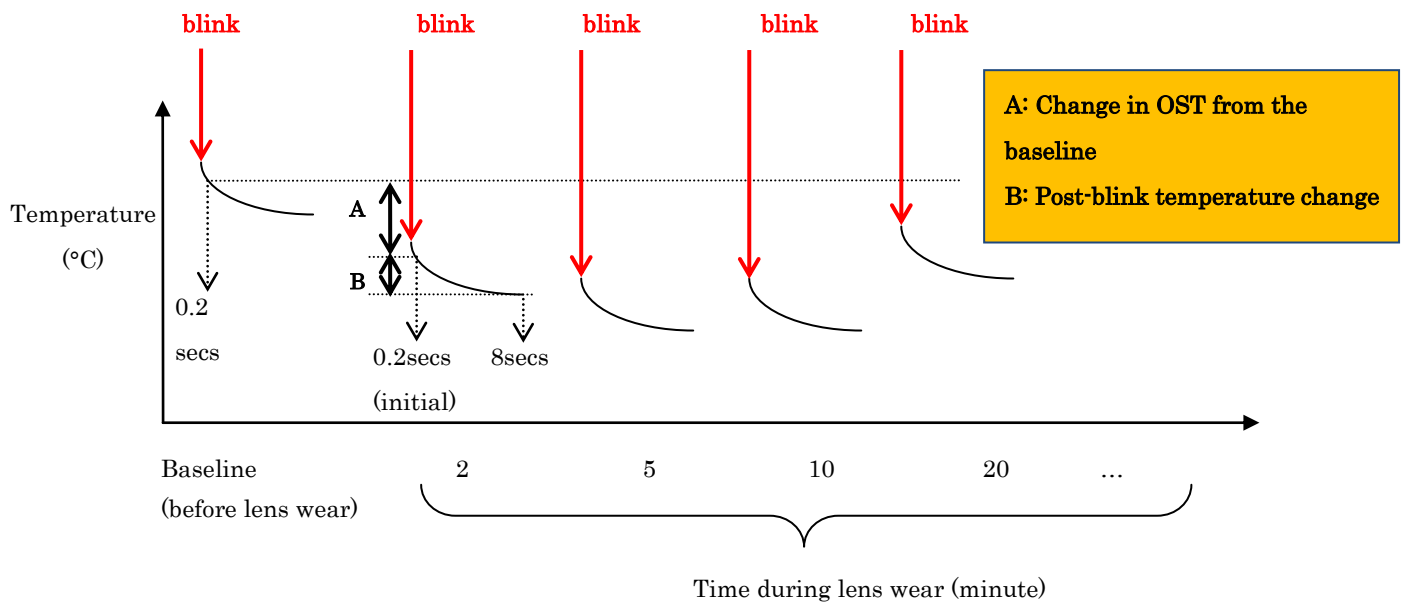


Figure 5.4: Diagram illustrating time points for temperature measurement and analysis.

Since some of the data sets obtained from this chapter were not normally distributed (Kolmogorov-Smirnov test, $p < 0.05$), non-parametric tests were used to compare the within-group differences (time) and between-group differences (lens type) using Friedman and Kruskal-Wallis tests, respectively. The analysis was conducted separately during lens wear and after removal. Also, when the different types of lenses were compared at the same time point, Menicon Z- α was excluded, as its physical properties were different from other lenses: SCL and SiHCLs.

The temperature measurements took place within a controlled environment (room temperature $24.9 \pm 1.2^\circ\text{C}$, humidity $23 \pm 11\%$).

5.2.4. Other assessment

Each subject's anterior ocular surface was checked by slit-lamp bio-microscopy to exclude subjects who failed the inclusion criteria. The CCLRU grading scales were used to grade limbal and conjunctival hyperaemia.

5.3. Results

Changes in OST from the baseline and post-blink changes in OST are presented separately. The former is the OST measured at 0.2 seconds after a blink, normalised against the pre-lens wear baseline at the same location (centre, periphery and conjunctiva) at each time point through the session in each lens type. The latter is the difference in temperature between the 0.2 secs OST and the temperature after 8 seconds at each time point.

5.3.1. Change in OST from the baseline

5.3.1.1. Central OST

To investigate the effect of lens wear over time on the OST during lens wear and after removal, the initial OST over a lens measured at 0.2 seconds was normalised against the baseline pre-lens wear OST. The median change in OST for each test lens are plotted in Figure 5.5 and summarised in Table 5.4.

There was a significant decrease in OST from the baseline during a lens wear for Menicon Z- α , AIR Optix and Clariti (Friedman test, $p < 0.05$). Menicon Z- α , especially, showed a decrease between 2 mins and 20 and 30 mins, and a greater decrease, compared against the other lens types, at the 20, 30 and 60 mins time points during lens wear. The other lenses showed no significant difference in OST across all time points when compared against each other, except for at 60 mins, and significant differences were found at 60 minutes for AIR Optix and Clariti.

After lens removal, the OST stabilised and remained close to the baseline. Although Menicon Z- α continued with a lower OST than the other lens types, this was not significant. Only AIR Optix

showed a significant decrease at 10 minutes. However, further post-hoc analysis did not confirm this significance.

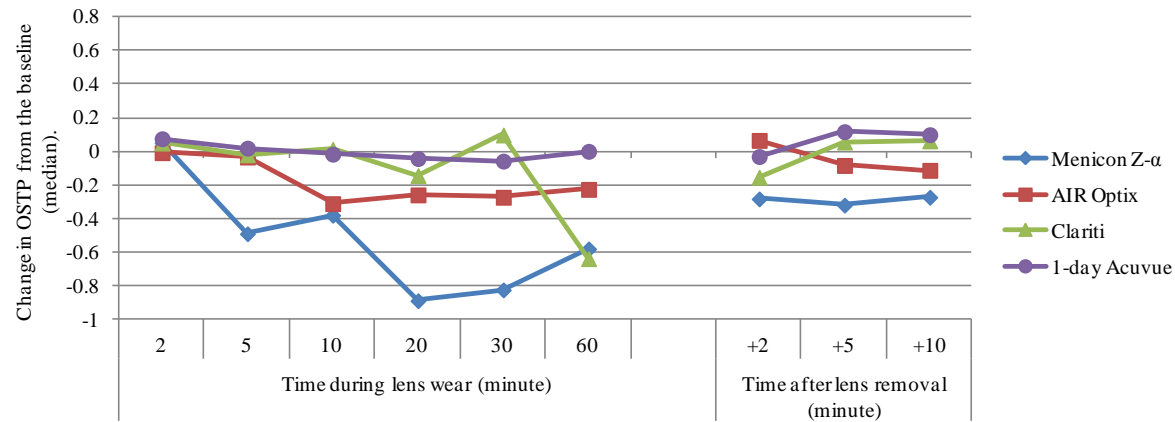


Figure 5.5: Median change at 0.2 secs in the central OST, from the pre-lens baseline, during and after lens wear.

Table 5.4: Median change in the central OST, from the pre-lens baseline, during and after lens wear, with statistical analysis.

	Time during lens wear (minutes)						Friedman Test	Post-hoc test ^{*1}	Time after lens removal (minutes)			Friedman test	Post-hoc test ^{*2}
	2	5	10	20	30	60			+2	+5	+10		
a) Menicon Z- α	0.051	-0.489	-0.379	-0.887	-0.823	-0.579	p<0.05	20, 30	-0.282	-0.319	-0.272	p=0.1677	-
b) AIR Optix	-0.007	-0.033	-0.310	-0.258	-0.272	-0.225	p<0.05	60	0.066	-0.083	-0.112	p<0.05	ns
c) Clariti	0.050	-0.020	0.013	-0.143	0.098	-0.637	p<0.05	60	-0.153	0.056	0.063	p=0.2466	-
d) 1-day Acuvue	0.076	0.020	-0.016	-0.042	-0.057	0.001	p=0.1114	-	-0.030	0.118	0.100	p=0.3442	-
Kruskal-Wallis test ^{*3}	p=0.483	p=0.401	p=0.095	p=0.646	p=0.318	p<0.05			p=0.389	p=0.741	p=0.775		
Post-hoc test ^{*4}	-	-	-	-	-	ns			-	-	-		
Kruskal-Wallis test ^{*5}	p=0.783	p=0.267	p=0.150	p<0.05	p<0.05	p<0.05			p=0.323	p=0.101	p=0.246		
Post-hoc test ^{*4}	-	-	-	ns	ns	a) and d)			-	-	-		

*1: Dunnett test, compared to 2 minutes, *2: Dunnett test, compared to +2 minutes, *3: Menicon Z- α was excluded, *4: Mann-Whitney test, *5: all lenses were compared, ns: not significant

5.3.1.2. Comparison of OSTP and OSTC

To give further information about the effect of tear exchange, the OST were also measured at the lens periphery and the conjunctiva, as OSTP and OSTC, respectively. Once again, the 0.2 secs OSTs were normalised against the pre-lens wear baseline temperature at each time point.

Considering first the Menicon Z- α lens, the medians are plotted in Figure 5.6 and the values are summarised in Table 5.5. Both OSTP and OSTC when wearing the Menicon Z- α significantly decreased during lens wear (Friedman test, $p < 0.05$), with significant changes occurring between 2 mins and 20, 30 and 60 mins. After lens removal, the magnitude of cooling became smaller. OSTP remained close to the baseline, while OSTC showed a significant decrease (Friedman test, $p < 0.05$). No significant differences were found between OSTP and OSTC when compared at the same time points through the session.

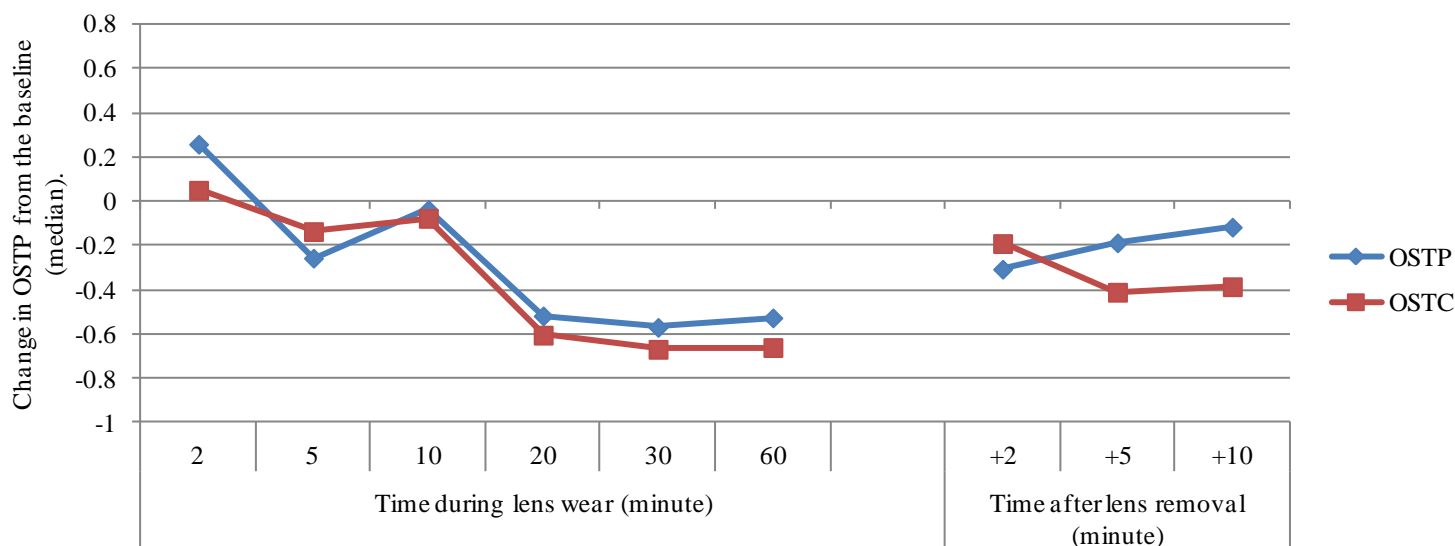


Figure 5.6: Comparison of the change in OSTP and OSTC from the baseline (median, Menicon Z- α).

Table 5.5: Comparison of the change in OSTP and OSTC from the baseline (median), with statistical analysis.

	Time during lens wear (minutes)						Friedman test	Post-hoc test ^{*1}	Time after lens removal (minutes)			Friedman test	Post-hoc test ^{*2}
	2	5	10	20	30	60			+2	+5	+10		
OSTP	0.260	-0.255	-0.036	-0.516	-0.568	-0.525	p<0.05	20, 30, 60	-0.305	-0.186	-0.115	p=0.5258	-
OSTC	0.052	-0.135	-0.075	-0.603	-0.667	-0.659	p<0.05	10, 20, 30, 60	-0.189	-0.409	-0.384	p<0.05	+5, +10
t-test	p=0.791	p=0.924	p=0.956	p=0.979	p=0.761	p=0.546			p=0.776	p=0.657	p=0.575		

*1: Dunnett test, compared to 2 minutes, *2: Dunnett test, compared to +2 minutes

The same analyses were conducted for the other lens types and the results are presented in Figure 5.7-5.9 and Table 5.6-5.8.

For AIR Optix, both OSTP and OSTC decreased during lens wear, but only OSTC was significantly changed (Friedman test, $p < 0.05$), and post-hoc testing revealed a significant change at each time point compared to 2 mins. There was no difference between OSTP and OSTC at each time point during lens wear, except for at 2 mins. After lens removal, the magnitude of cooling became smaller and remained close to the baseline, except for OSTP at 10 mins (Friedman test, $p < 0.05$). OSTC also showed a significant increase at 5 mins, but this was small in size and not significant clinically.

For Clariti, the effect of lens wear was significant for both OSTP and OSTC, although there was no obvious pattern of effect. OSTP and OSTC differed significantly at 10 and 60 mins, and OSTC varied from baseline at 10, 20 and 30 mins of wear. After lens removal, OSTP increased and was significantly higher than baseline after 10 mins. There was no variation in OSTC after lens removal.

For 1-day Acuvue, both OSTP and OSTC were relatively stable and, while they tended to be slightly higher than the baseline, no significant differences were found for both locations during lens wear and after removal. Also, there was no significant difference between OSTP and OSTC at each time point.

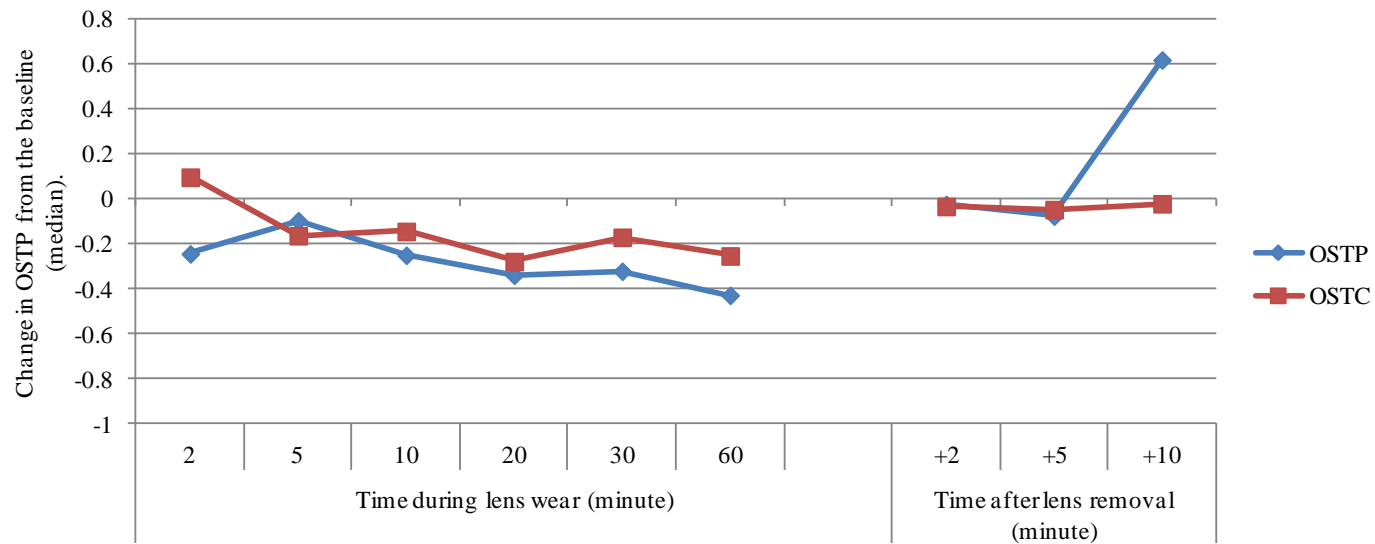


Figure 5.7: Comparison of the change in OSTP and OSTC from the baseline (median, AIR Optix).

Table 5.6: Comparison of the change in OSTP and OSTC from the baseline (median, AIR Optix), with statistical analysis.

	Time during lens wear (minutes)						Friedman test	Post-hoc test*1	Time after lens removal (minutes)			Friedman test	Post-hoc test*2
	2	5	10	20	30	60			+2	+5	+10		
OSTP	-0.242	-0.094	-0.248	-0.337	-0.319	-0.426	p=0.0725	-	-0.022	-0.074	0.620	p<0.05	+10
OSTC	0.099	-0.161	-0.142	-0.276	-0.168	-0.251	p<0.05	5, 10, 20, 30, 60	-0.031	-0.045	-0.019	p<0.05	+5
t-test	p<0.05	p=0.519	p=0.661	p=0.915	p=0.561	p=0.186			p=0.694	p=0.528	p=0.211		

*1: Dunnett test, compared to 2 minutes, *2: Dunnett test, compared to +2 minutes

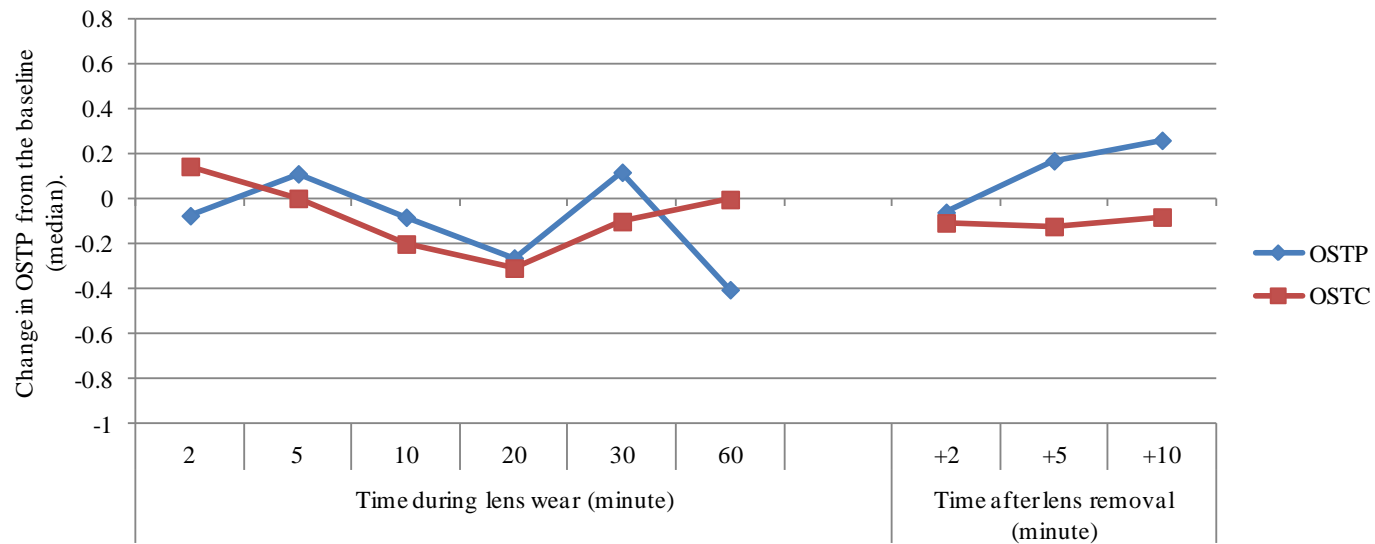


Figure 5.8: Comparison of the change in OSTP and OSTC from the baseline (median, Clariti).

Table 5.7: Comparison of the change in OSTP and OSTC from the baseline (median, Clariti), with statistical analysis.

	Time during lens wear (minutes)						Friedman test	Post-hoc test ^{*1}	Time after lens removal (minutes)			Friedman test	Post-hoc test ^{*2}
	2	5	10	20	30	60			+2	+5	+10		
OSTP	-0.072	0.114	-0.079	-0.260	0.121	-0.401	p<0.05	60	-0.057	0.172	0.263	p<0.05	+10
OSTC	0.147	0.005	-0.198	-0.305	-0.098	0.000	p<0.05	10, 20, 30	-0.104	-0.120	-0.078	p=0.6271	-
t-test	p=0.763	p=0.645	p<0.05	p=0.582	p=0.788	p<0.05			p=0.975	p=0.248	p=0.153		

*1: Dunnett test, compared to 2 minutes, *2: Dunnett test, compared to +2 minutes

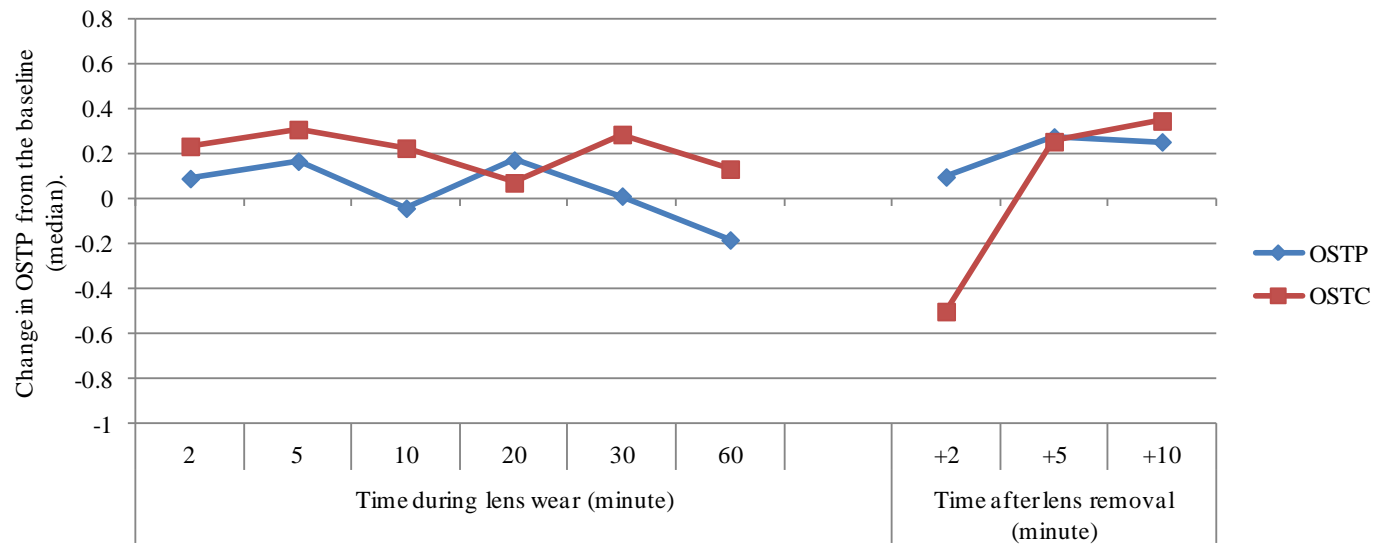


Figure 5.9: Comparison of the change in OSTP and OSTC from the baseline (median, 1-day Acuvue).

Table 5.8: Comparison of the change in OSTP and OSTC from the baseline (median, 1-day Acuvue), with statistical analysis.

	Time during lens wear (minutes)						Friedman test	Post-hoc test ^{*1}	Time after lens removal (minutes)			Friedman test	Post-hoc test ^{*2}
	2	5	10	20	30	60			+2	+5	+10		
OSTP	0.093	0.170	-0.039	0.175	0.015	-0.180	p=0.4324	-	0.100	0.278	0.256	p=0.2818	-
OSTC	0.236	0.311	0.228	0.074	0.289	0.135	p=0.0877	-	-0.498	0.257	0.349	p=0.0743	-
t-test	p=0.31	p=0.494	p=0.168	p=0.666	p=0.576	p=0.656			p=0.172	p=0.738	p=0.924		

*1: Dunnett test, compared to 2 minutes, *2: Dunnett test, compared to +2 minutes

5.3.2. Post-blink changes in OST with contact lens wear

5.3.2.1. Post-blink change in the central OST

Post-blink change in OST describes the temperature difference between the initial (0.2 secs) and 8 secs following a blink. The hypotheses from *Part A– i*, that “*the post-blink OST of RGPCL will decrease faster than that of SCL/SiHCL*” was examined in this analysis. The median of post-blink change in OST over 8 seconds was measured at the centre for each time point, and the data plotted in Figure 5.10 and summarised in Table 5.9.

After 2 mins and 60 mins of lens wear, Menicon Z- α was significantly different in OST compared to other lens types, but similar at all other time points. The time point differences for Menicon Z- α alone during lens wear were statistically significant, and post-hoc testing showed significances between 2 mins and 5, 10, 20, and 30 mins. The Friedman test also found a significant change for Clariti during lens wear, but subsequent post-hoc testing found no specific time points compared to the 2 mins time point. No significance differences were found between SCL and SiHCLs when compared at each time point.

After lens wear, there was a significant difference between Clariti and 1-day Acuvue at 2 mins after removal, but all other comparisons were not significant.

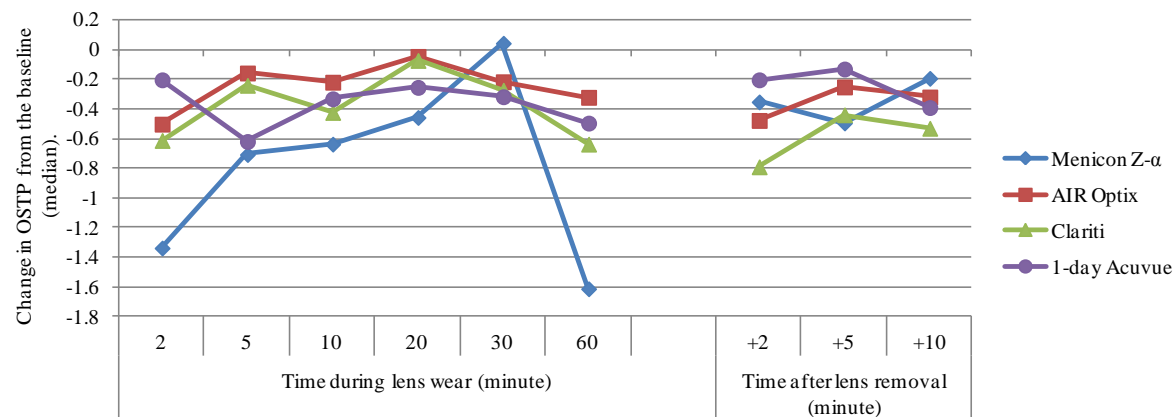


Figure 5.10: Post-blink change in the central OST (median).

Table 5.9: Post-blink change in the central OST (median), with statistical analysis.

	Time during lens wear (minutes)						Friedman test	Post-hoc test ^{*1}	Time after lens removal (minutes)			Friedman test	Post-hoc test ^{*2}
	2	5	10	20	30	60			+2	+5	+10		
a) Menicon Z- α	-1.440	-0.691	-0.723	-0.176	-0.088	-1.712	p<0.05	5, 10, 20, 30	-0.400	-0.800	-0.333	p=0.0498	-
b) AIR Optix	-0.598	-0.125	-0.212	-0.051	-0.272	-0.607	p=0.0698	-	-0.690	-0.324	-0.170	p=0.1653	-
c) Clariti	-0.588	-0.480	-0.485	-0.239	-0.260	-0.491	p<0.05	ns	-0.750	-0.396	-0.496	p=0.0774	-
d) 1-day Acuvue	-0.165	-0.479	-0.296	-0.051	-0.294	-0.610	p=0.5091	-	-0.135	-0.253	-0.256	p=0.4831	-
Kruskal-Wallis test ^{*3}	p=0.128	p=0.056	p=0.308	p=0.940	p=0.914	p=0.349			p<0.05	p=0.402	p=0.130		
Post-hoc test ^{*4}	-	-	-	-	-	-			c) and d)	-	-		
Kruskal-Wallis test ^{*5}	p<0.05	p=0.125	p=0.307	p=0.949	p=0.778	p<0.05			p<0.05	p=0.117	p=0.254		
Post-hoc test ^{*4}	a) and d)	-	-	-	-	a) and b), c) and d)			ns	-	-		

*1: Dunnett test, compared to 2 minutes, *2: Dunnett test, compared to +2 minutes, *3: Menicon Z- α was excluded, *4: Mann-Whitney test, *5: all lenses were compared, ns: not significant

5.3.2.2. Post-blink changes in OSTP and OSTC

To further investigate the potential effect of tear exchange around the lens edge, the post-blink changes were also measured at the lens periphery and the conjunctiva, and the temperature difference compared between the initial (0.2 secs) and 8 secs.

For Menicon Z- α , the median OSTP and OSTC for each time point are plotted in Figure 5.11 and summarised in Table 5.10. The post-blink change in OSTP were statistically greater than for OSTC at 2 and 60 mins of lens wear (t-test, $p < 0.05$). For OSTP, significant changes from 2 mins occurred at 5 and 30 mins of lens wear. On the other hand, the magnitude of post-blink change in OSTC was relatively small and stable through the session. After lens removal, both OSTP and OSTC showed small changes, with OSTP being significantly different from 2 mins after 10 mins (Friedman test, $p < 0.05$). At both 2 and 5 mins after removal, OSTP was statistically lower than OSTC (t-test, $p < 0.05$).

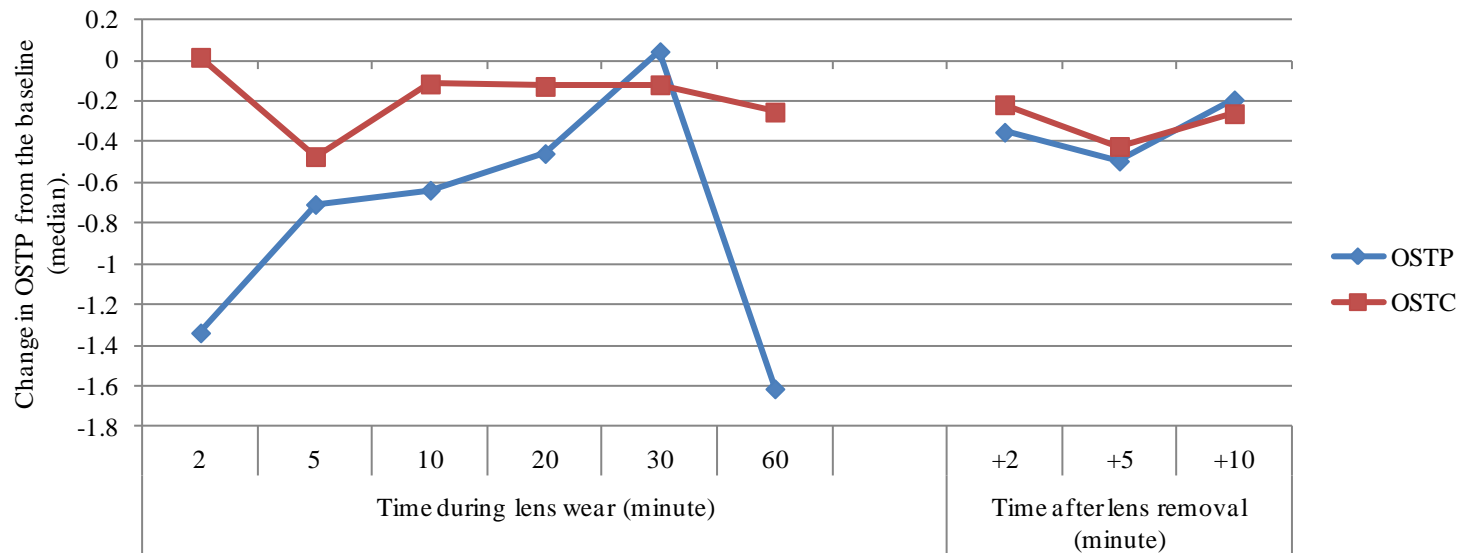


Figure 5.11: Comparison of post-blink change in OSTP and OSTC (median, Menicon Z- α).

Table 5.10: Comparison of post-blink change in OSTP and OSTC (median, Menicon Z- α), with statistical analysis.

	Time during lens wear (minutes)						Friedman test	Post-hoc test ^{*1}	Time after lens removal (minutes)			Friedman test	Post-hoc test ^{*2}
	2	5	10	20	30	60			+2	+5	+10		
OSTP	-1.337	-0.706	-0.636	-0.456	0.045	-1.612	p<0.05	5, 30	-0.351	-0.493	-0.192	p<0.05	10
OSTC	0.017	-0.471	-0.114	-0.126	-0.118	-0.252	p=0.3451	-	-0.216	-0.421	-0.260	p=0.1462	-
t-test	p<0.05	p=0.361	p<0.05	p=0.201	p=0.672	p<0.05			p<0.05	p<0.05	p=0.741		

*1: Dunnett test, compared to 2 minutes, *2: Dunnett test, compared to +2 minutes

The same analysis was conducted with the other lens types and the results are presented in Figure 5.12-5.14 and Table 5.11-5.13.

The magnitude of post-blink changes in OSTP with SCL and SiHCLs were smaller than that of Menicon Z- α . This may reflect a more stable tear film over a SCL compared with that over a RGPCL. For AIR Optix, OSTP and OSTC were statistically different at 2 and 60 mins (t-test, $p < 0.05$). OSTP was significantly different from 2 mins at 5 and 20 mins (Friedman test, $p < 0.05$), whereas OSTC showed no significant change during the lens wear period. After lens wear, no significant change was found for both OSTP and OSTC.

For Clariti, post-blink change in OSTP was significantly lower than OSTC at 2 and 60 mins during lens wear (t-test, $p < 0.05$). OSTP was significant different at 20 mins (Friedman test, $p < 0.05$), while OSTC had no significant change during lens wear. After lens wear, OSTP was significantly different from OSTC at 2 and 5 mins.

For 1-day Acuvue, there were no significant post-blink changes in both OSTP and OSTC during lens wear. After lens removal, only OSTC showed a significant change (Friedman test, $p < 0.05$), but post-hoc testing did not confirm this significance. OSTP and OSTC were not statistically different through the session.

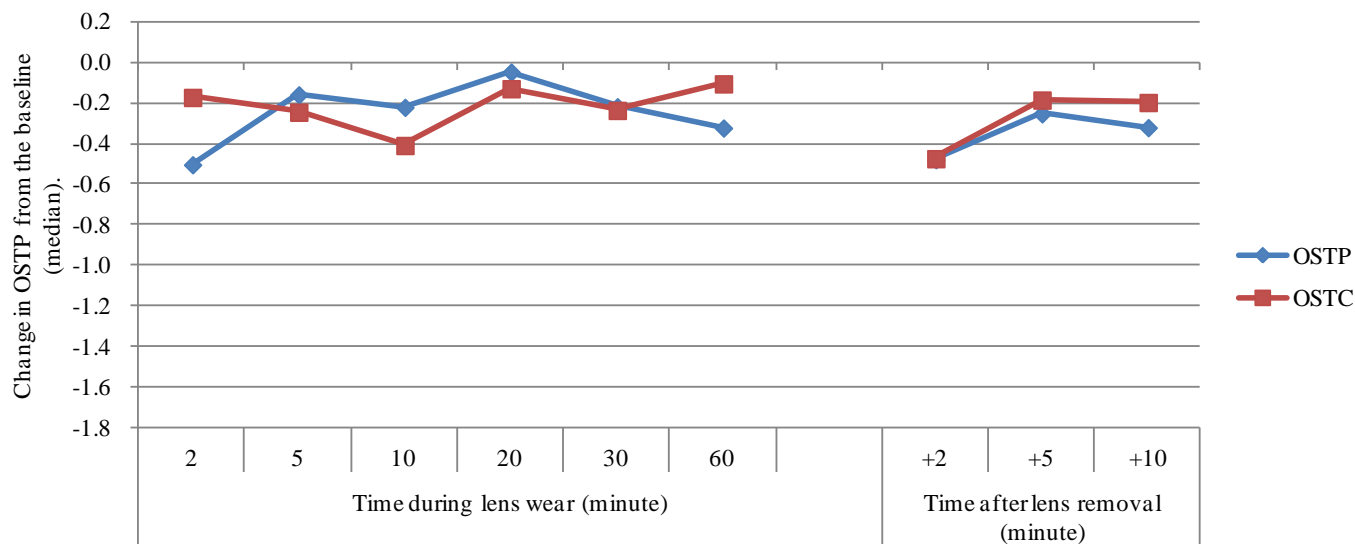


Figure 5.12: Comparison of post-blink change in OSTP and OSTC (median, Air Optix).

Table 5.11: Comparison of post-blink change in OSTP and OSTC (median, Air Optix), with statistical analysis.

	Time during lens wear (minutes)						Friedman test	Post-hoc test ^{*1}	Time after lens removal (minutes)			Friedman test	Post-hoc test ^{*2}
	2	5	10	20	30	60			+2	+5	+10		
OSTP	-0.501	-0.156	-0.218	-0.044	-0.215	-0.320	p<0.05	5, 20	-0.476	-0.250	-0.318	p=0.2818	-
OSTC	-0.169	-0.242	-0.406	-0.126	-0.233	-0.102	p=0.7972	-	-0.471	-0.182	-0.194	p=0.8187	-
t-test	p<0.05	p=0.755	p=0.414	p=0.909	p=0.308	p<0.05			p=0.215	p=0.073	p=0.993		

*1: Dunnett test, compared to 2 minutes, *2: Dunnett test, compared to +2 minutes

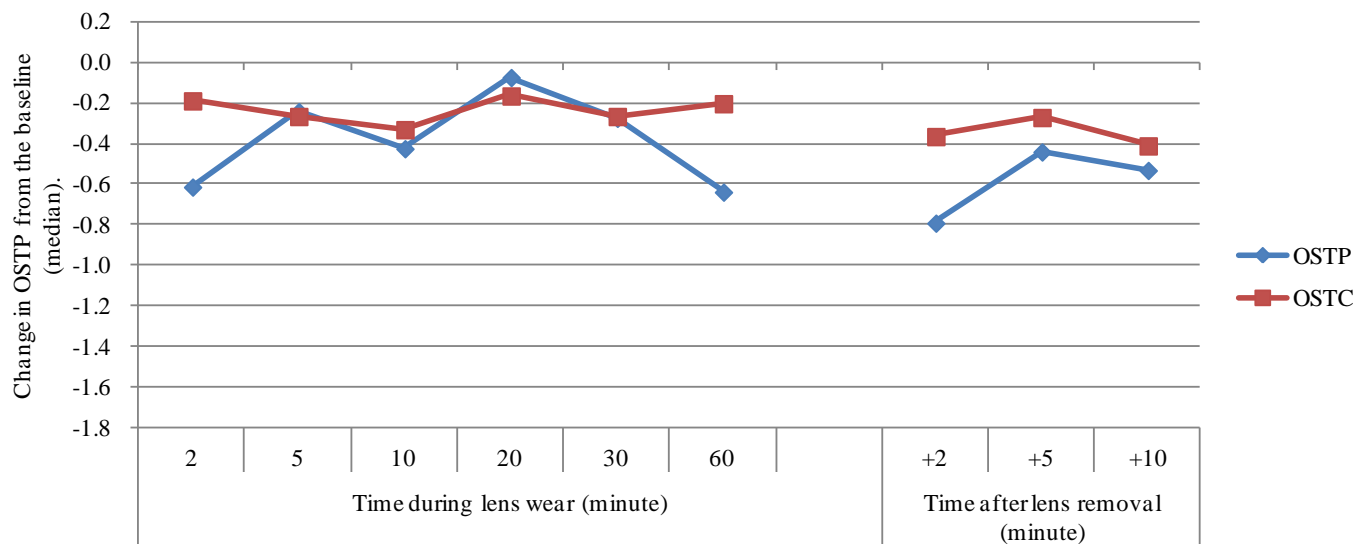


Figure 5.13: Comparison of post-blink change in OSTP and OSTC (median, Clariti).

Table 5.12: Comparison of post-blink change in OSTP and OSTC (median, Clariti), with statistical analysis.

	Time during lens wear (minutes)						Friedman test	Post-hoc test ^{*1}	Time after lens removal (minutes)			Friedman test	Post-hoc test ^{*2}
	2	5	10	20	30	60			+2	+5	+10		
OSTP	-0.611	-0.239	-0.422	-0.071	-0.272	-0.636	p<0.05	20	-0.789	-0.438	-0.529	p=0.2466	-
OSTC	-0.186	-0.263	-0.328	-0.162	-0.263	-0.200	p=0.8772	-	-0.362	-0.268	-0.408	p=0.2818	-
t-test	p<0.05	p=0.634	p=0.878	p=0.851	p=0.365	p<0.05			p<0.05	p<0.05	p=0.812		

*1: Dunnett test, compared to 2 minutes, *2: Dunnett test, compared to +2 minutes

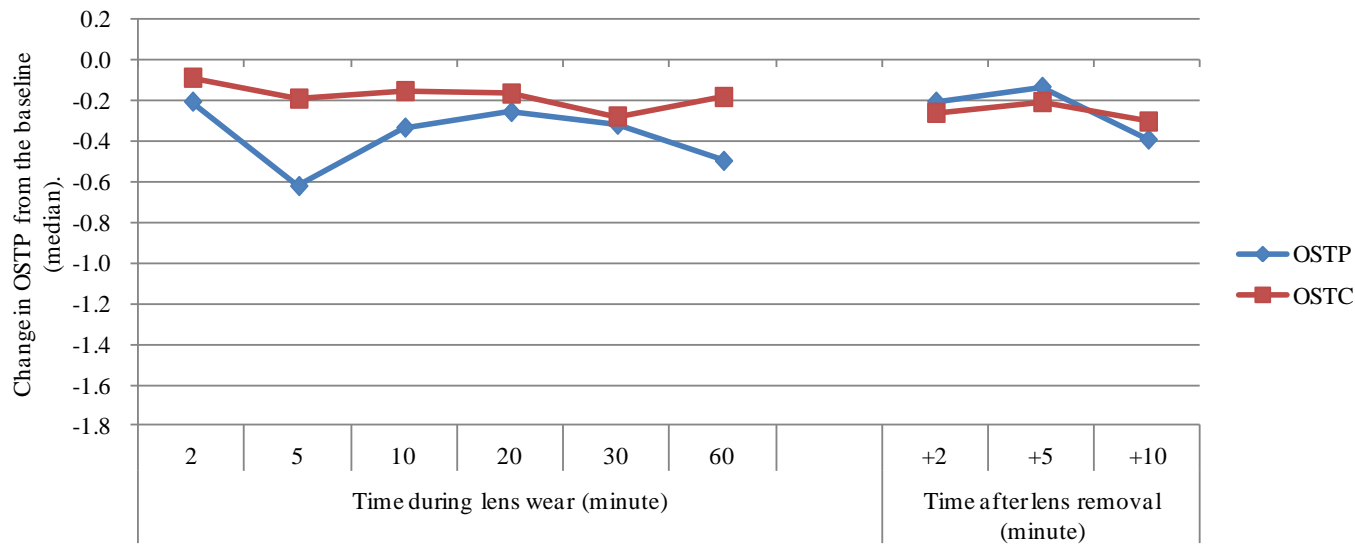


Figure 5.14: Comparison of post-blink change in OSTP and OSTC (median, 1-day Acuvue).

Table 5.13: Comparison of post-blink change in OSTP and OSTC (median, 1-day Acuvue), with statistical analysis.

	Time during lens wear (minutes)						Friedman test	Post-hoc test ^{*1}	Time after lens removal (minutes)			Friedman test	Post-hoc test ^{*2}
	2	5	10	20	30	60			+2	+5	+10		
OSTP	-0.202	-0.618	-0.330	-0.253	-0.316	-0.494	p=0.2545	-	-0.202	-0.129	-0.389	p=0.6951	-
OSTC	-0.084	-0.187	-0.150	-0.162	-0.275	-0.179	p=0.4725	-	-0.257	-0.204	-0.300	p<0.05	ns
t-test	p=0.384	p=0.125	p=0.447	p=0.567	p=0.455	p=0.055			p=0.164	p=0.648	p=0.104		

*1: Dunnett test, compared to 2 minutes, *2: Dunnett test, compared to +2 minutes

5.4. Discussion

To investigate the effect of contact lens wear, specifically the lens material, water content and tear replenishment over the lens surface during blinking, the OST was successfully recorded as a short video both during lens wear and after removal and its change was analysed over time.

Through the experiments and analyses of the OST measured at different locations with different lens types, the main findings in this chapter can be summarised as:

- The temperature change with lens wear was successfully measured.
- The type of lens appeared to affect the temperature change.
- The pre-lens tear film, especially on the RGPCL, had an effect.
- After removing the lens, the OST returned to the baseline very quickly.
- There was no obvious effect from tear exchange under the lens.

The first aim was to test the hypothesis that the post-blink OST of an RGPCL will decrease faster than that of an SCL or SIHCL. This was assessed in two ways: as an initial temperature change at 0.2 secs post-blink, and after 8 secs. For the initial temperature change, the RGPCL was shown to have a lower temperature, with significant differences in surface temperature to the other lenses at 20, 30 and 60 mins (Figure 5.5), whereas the soft lenses retained a consistent temperature, with non-significant differences between them over the initial 0.2 secs. By contrast, at the 8 secs time point post-blink, there were only a significant difference between the RGPCL and the soft lenses at 2 mins, and nothing thereafter, excluding the apparent outlier result for the RGPCL at 60 mins, which might be due to reflex tearing effects.

To help explain these results, it is useful to consider the effect of the pre-lens wear temperature of each contact lens, the effect of the warmer tear film, the effect of tear film thickness, and the effect of tear film evaporation from the lens surface during the 8 secs time period of the study. It was reported that the tear film is affected by contact lens wear even in the short term (Glasson et al., 2006, Holly, 1981b) and the type of lenses or the water content would also be associated with the dehydration rate of the pre-lens tear film.

Since each lens was allowed a period of time to become equilibrated with room temperature, lenses were therefore inserted with a core temperature of around 25°C, substantially cooler than pre-lens wear OST. However, once inserted into the eye, the lens was bathed in the warm tear film, and would begin a process of gradually warming to the ocular temperature. At the same time, between blinks the tear film over the anterior surface of the contact lens will rapidly become unstable, particularly so for the RGPCL, and this will encourage a reduction in temperature. Immediately post-blink, the tear film will also be at its thickest, and so the relative contribution of the tear film compared with the underlying cornea or contact lens will be at its highest. Of the two study post-blink time points, the 0.2 secs time is not affected by any pre-lens inter-blink tear film evaporation, but will have the thickest pre-lens wear tear film (used as the baseline), whereas at the 8 secs time point evaporation will have an effect and the tear film will be thinnest, or even non-existent. At both time points, the other two effects will be similar.

Considering the results, and these effects, it can be observed that the RGPCL shows a gradual reduction in temperature over the 60 mins of the study, with the most obvious relative temperature change occurring at the 0.2 secs time period. Two principle effects appear to

explain this effect: firstly, the baseline for OST measurements was taken from pre-lens wear temperature, when the tear film is thick and at its warmest, meaning that subsequent temperature comparisons are accentuated; and secondly, while on immediately post-blink a tear film will be able to form over the RGPCL, this will rapidly evaporate from the lens surface, thereby cooling the lens, producing the gradual reduction in temperature observed. At 8 secs, the cooling effect is no longer seen, but this primarily reflects the different baseline starting point for the analysis – after 8 secs, the pre-lens wear tear film has cooled, and is now thinner. While some further cooling of the RGPCL will occur in the inter-blink period between 0.2 and 8 secs, the effect is not so obviously seen.

In contrast, the soft lenses retain a similar OST throughout their lens wear. They achieved an equilibrium between surface cooling from evaporation and warming from fresh tear film after each blink. This finding addressed the second aim of the study, which was to test the hypothesis that the thermal conductivity of SiHCL and SCL are the same in lenses with the same water content, and the third aim, which was to compare the effect of water content in low and high water content SiHCL. It appears that even though SiHCL materials have different thermal conductivity characteristics, the ongoing replenishment of the in-lens hydration from the tear film ensures that no significant tear evaporation and subsequent dehydration of the lenses occurred, regardless of whether they were of low or high water content.

A further aim of the study was to investigate whether there was any local effect from tear exchange at the lens periphery. No observable effect was seen, which might be expected in the SCL and SiHCL since the level of tear exchange under these lenses is negligible. For the

RGPCl, tear exchange under the lens occurs with each blink and its amount is obviously different from SCL (Kok et al., 1992, McNamara et al., 1999, Lin et al., 2002). However any localised effect from tear exchange under RGPCl, which might promote warming of the lens, would be small in comparison to the more significant tear evaporation cooling effect.

The final aim of the study was to investigate whether there was any prolonged effect from wearing a lens on the underlying ocular surface. No pattern of effect or statistically significant change was observed. This is in contrast to the results from Purslow (2005), which found an increase in OST following SiHCL lens wear. However, the Purslow study extended for 120 mins, compared to the 60 mins of this study, which suggests that a longer period of wear might reveal a difference. However, the lack of difference, is most likely due to the predominance of the infrared radiation being detected by the thermal camera arising from the tear film in the OST assessment (Lerman, 1980), compared to the underlying ocular surface. So even if there was some localised heating effect from the presence of the contact lens, perhaps arising from an insulating effect from the contact lens preventing ocular surface cooling due to heat transfer during tear film evaporation reaching the ocular surface, the size of that change was insufficient to be detected.

The strength of this study is that all test lenses were worn by same subjects and that the measurement points were well-controlled by using the overlay on the screen. These would have improved the accuracy of the measurement. Whereas the weakness can be considered as that the wearing background of subjects were not controlled and this might have caused the reflex tearing when RGPCl was worn. Also, the number of subjects can be improved in the future

study to investigate the effect of the tear film quality according to their NIBUT or other assessment of the tear film.

5.5. Conclusion

The results from this study show that RGPCL has a larger effect on the OST than SCL and SiHCL at each test location: central, peripheral and conjunctiva. The post-blink OST decrease was influenced by the tear film stability over the contact lens and, in line with the quicker pre-lens BUT, RGPCL showed a greater decrease over the other lens types. However, the effect of tear film exchange under the lens was not observed. This study was the first to compare the OST with different types of contact lenses including RGPCL within the same subjects.

Chapter 6. Summary and future work

The contact lens is a common way to correct refractive error. As lens materials and designs have developed through the past few decades, the safety of wear and the quality of vision have become much improved. However, despite these improvements, the number of serious eye complications reported has remained high (Stapleton et al., 2008). Also it was shown that a severe microbial keratitis related to contact lens wear is more likely to be seen in warmer, humid regions (Stapleton et al., 2007). The study of this thesis was drawn from these findings, with the hypothesis that ocular surface temperature and the influence of a contact lens on that temperature, could be factors in successful contact lens wear.

Before conducting the study *in vivo*, the insulation effect of the contact lens material was examined using the *in vitro* model eye in Chapter 3. The model eye was heated to simulate the human eye. Several contact lenses were applied with and without the artificial tears, and the thermal change in the contact lens examined both as an initial change, and during the measurement period. As a result, it was found that a contact lens with a high water content was better able to adapt to the heat source, and changed in surface temperature more slowly.

As the preliminary study for later *in vivo* studies, the stability of the tear film lipid layer and its effect on the OST were investigated in Chapter 4. To measure NIBUT, the DR-1 instrument (Kowa, Japan) was used. This instrument is able to measure the sole effect of the stability of the lipid layer. The advantage of this equipment was that the subject was positioned on a chin-rest

so that they could keep their faces frontward. This experiment showed the positive relationship between the NIBUT and the stability of the tear film lipid layer.

Finally, the thermal differences of contact lenses in the eye were investigated in Chapter 5. The effect of difference of material and the effect of the tear exchange were examined. The RGPCL showed the greatest effect on the post-blink OST change, which was related to pre-lens tear film stability, as previously suggested. The effect of the tear exchange beneath the lens was not observed through OST measurement. However, most subjects in this study were not habitual RGPCL wearers, and this may have caused reflex tearing. To improve the study design, it would be better to use subjects who were adapted to RGPCL.

In this thesis, the use of the infrared camera was confirmed as a useful instrument for measuring ocular surface temperature (OST) with and without contact lens wear. To identify the location to measure OST, the overlay was set over the screen which displays the image obtained from the thermo-camera in real time. This increased the accuracy of the analysis by ensuring the same ocular surface location was identified for each repeated measurement, and between subjects. This offered an improvement in technique over previous studies. Further improvements in experimental technique were obtained by being more selective of test location, which when combined with the overlay allowed closer alignment of test locations with areas of interest on the ocular surface.

Some ideas can be proposed for future study. Since the stability of the tear film over the contact lens has been shown to be an important factor, the volume of the tear film over the lens surface

might also affect the OST. It is reported that the volume and the thickness of the tear film are correlated (Wang et al., 2006). Therefore, if the original tear film is abundant and it forms thicker tear film, the OST would be stable and able to retain thermal energy for longer. Moreover, if the thickness of each layer of the tear film can be measured, it would give more detail about how each components of the tear film affect the OST.

Also, the long-term effect of lens wear on OST was not investigated in this thesis. It was reported that there was no significant difference in OST between daily wear and continuous wear in a previous long-term study (Purslow, 2005). Further study could repeat this study, and also examine the relationship between subjective comfort and OST during lens wear. Previously, the relationship between subjective sensitivity and OST was investigated (Hill and Leighton, 1965c). However, the terms and measured temperature were in the inverse order: “burning” having the lowest, “cool” the highest and “warm” in between. This may be due to the inaccuracy of the direct method, and if the infrared camera was used, the result might be different.

For further application of thermography, it would be interesting to investigate the effect of lens care solution. It would be interesting to see the effect of lens care solutions to the tear film and the eye, particularly how tear stability over the lens might be affected. As previously reported, some combination of lens and care solution can cause serious corneal staining (Andrasko and Ryen, 2008). Recent care solutions have been developed to enhance wearing comfort and the wettability of the lens. However, it is difficult to see these effects and to quantify the difference of subjective comfort. The infrared camera would be useful to estimate the effect on tear

film stability. If this technique is employed, contact lens wearers might obtain useful information that can assist in selecting the most comfortable lens and care solution combination.

In conclusion, the use of infrared thermography has shown further potential to give information about evaluating the contact lens through measuring OST over time. Despite insignificant results on the observation of tear film exchange, this study was successful in comparing the different types of contact lenses with the same subjects.

References

- ALIO, J. & PADRON, M. 1982. Influence of age on the temperature of the anterior segment of the eye. Measurements by infrared thermometry. *Ophthalmic Res*, 14, 153-9.
- AMERICAN ACADEMY OF OPHTHALMOLOGY. 2012. *Contact Lens-Related Infections* [Online]. American Academy of Ophthalmology. Available: <http://www.geteyesmart.org/eyesmart/diseases/contact-lens-related-infections.cfm> [Accessed 11 July 2012 2012].
- ANDRASKO, G. & RYEN, K. 2008. Corneal staining and comfort observed with traditional and silicone hydrogel lenses and multipurpose solution combinations. *Optometry*, 79, 444-54.
- BAILEY, S. 1999. Contact lens complications. *Optometry Today*, 26-33.
- BARR, J. T. 2005. 2004 Annual Report. *Contact Lens Spectrum*.
- BENNETT, E. S. & WEISSMAN, B. A. 2005. *Clinical Contact Lens Practice*, Lippincott Williams & Wilkins.
- BRACCO, G. & HOLST, B. 2013. *Surface Science Techniques*, Berlin, Springer-Verlag Berlin Heidelberg.
- BREITHAUPT, J. 2003. *Physics*, Palgrave Macmillan.
- BRENNAN, N. A. 2001. A model of oxygen flux through contact lenses. *Cornea*, 20, 104-8.
- BRENNAN, N. A. 2005. Corneal oxygenation during contact lens wear: comparison of diffusion and EOP-based flux models. *Clinical and Experimental Optometry*, 88, 103-108.
- BRON, A. J., TIFFANY, J. M., GOUVEIA, S. M., YOKOI, N. & VOON, L. W. 2004. Functional aspects of the tear film lipid layer. *Exp Eye Res*, 78, 347-360.
- CEDARSTAFF, T. H. & TOMLINSON, A. 1983. A comparative study of tear evaporation rates and water content of soft contact lenses. *Am J Optom Physiol Opt*, 60, 167-74.
- CHENG, L., MULLER, S. J. & RADKE, C. J. 2004. Wettability of silicone-hydrogel contact lenses in the presence of tear-film components. *Curr Eye Res*, 28, 93-108.
- CHO, P. & DOUTHWAITE, W. 1995. The relation between invasive and noninvasive tear break-up time. *Optom Vis Sci*, 72, 17-22.
- COLLEGE OF OPTOMETRISTS. 2013. Clinical Management Guidelines: CL-associated Papillary Conjunctivitis (CLPC), Giant Papillary Conjunctivitis (GPC). Available: <http://www.college-optometrists.org/en/utilities/document-summary.cfm/docid/7ADE8F8C-6ADC-419A-B24823461E936873>.
- COOPERVISION. 2014. *Common questions about contact lenses* [Online]. Available: <http://www.thejourneyoflife.co.uk/did-you-know> [Accessed 5th, June 2014].
- CRAIG, J. P., SINGH, I., TOMLINSON, A., MORGAN, P. B. & EFRON, N. 2000. The role of tear physiology in ocular surface temperature. *Eye*, 14 (Pt 4), 635-41.
- DAVIS, R. L. & BECHERER, P. D. 2005. Techniques for Improved Soft Lens Fitting. Available: <http://www.clspectrum.com/articleviewer.aspx?articleid=12852> [Accessed 11/8/2014].
- DIAKIDES, N. A. 1998. From the Guest Editor - Infrared Imaging: An Emerging Technology in Medicine. *Engineering in Medicine and Biology Magazine, IEEE*, 17, 17-18.

- DIXON, J. M. & BLACKWOOD, L. 1991. Thermal variations of the human eye. *Trans Am Ophthalmol Soc*, 89, 183-90; discussion 190-3.
- DUMBLETON, K. 2003. Noninflammatory Silicone Hydrogel Contact Lens Complications. [Miscellaneous Article]. *Eye and contact lens*, 29, SS186-189.
- EFRON, N. & MORGAN, P. B. 2009. Are hypoxia or modulus causes of contact lens-associated keratitis? *Clin Exp Optom*, 92, 329-30.
- EFRON, N., YOUNG, G. & BRENNAN, N. A. 1989. Ocular surface temperature. *Curr Eye Res*, 8, 901-6.
- FATT, I. & CHASTON, J. 1980. Temperature of a Contact Lens on the Eye. *International Contact Lens Clinic*, 195-198.
- FINK, B. A., HILL, R. M. & CARNEY, L. G. 1992. Influence of rigid contact lens base curve radius on tear pump efficiency. *Optometry & Vision Science*, 69, 60-65.
- FLIR SYSTEMS. 2009. 7 Things to know when selecting an IR Camera for R&D.
- FLIR SYSTEMS 2010. The Ultimate Infrared Handbook for R&D Professionals.
- FORISTER, J. F. Y., FORISTER, E. F., YEUNG, K. K., YE, P., CHUNG, M. Y., TSUI, A. & WEISSMAN, B. A. 2009. Prevalence of Contact Lens-Related Complications: UCLA Contact Lens Study. *Eye & Contact Lens*, 35, 176-180
10.1097/ICL.0b013e3181a7bda1.
- FREEMAN, R. D. & FATT, I. 1973. Environmental influences on ocular temperature. *Invest Ophthalmol*, 12, 596-602.
- FUJISHIMA, H., TODA, I., YAMADA, M., SATO, N. & TSUBOTA, K. 1996. Corneal temperature in patients with dry eye evaluated by infrared radiation thermometry. *Br J Ophthalmol*, 80, 29-32.
- GIRALDEZ, M. J., NAROO, S. A. & RESUA, C. G. 2009. A preliminary investigation into the relationship between ocular surface temperature and lipid layer thickness. *Contact Lens and Anterior Eye*, 32, 177-180.
- GLASSON, M. J., STAPLETON, F., KEAY, L. & WILLCOX, M. D. 2006. The effect of short term contact lens wear on the tear film and ocular surface characteristics of tolerant and intolerant wearers. *Cont Lens Anterior Eye*, 29, 41-7; quiz 49.
- GUILLOIN, J.-P. 1998. Non-invasive tearscope plus routine for contact lens fitting. *Contact Lens and Anterior Eye*, 21, S31-S40.
- HAMANO, H., KOMATSU, S. & MINAMI, S. 1969a. Observation of the distribution of the ocular surface temperature by Thermography -Change of the temperature distribution depended with contact lens wear-. *Journal of Japan Contact Lens Society*, 11, 67-70.
- HAMANO, H., MINAMI, S. & SUGIMORI, T. 1969b. Experiments in Thermometry of the Anterior Portion of the Eye Wearing a Contact Lens by Means of Infrared Thermometer.
- HAMANO, H., MIYABE, K. & MITSUNAGA, S. 1972. Measurement of Thermal Constants of Cornea and Hard and Soft Contact Lens Material (Thermal Diffusivity and Conductivity). *Contacto*, 16, 5-8.
- HATA, S., URAYAMA, K., FUJISHIMA, H. & TSUBOTA, K. 1994. Corneal Temperature and Inter Blinking Time. *Investigative Ophthalmology & Visual Science*, 35, S999.
- HEITING, G. 2010. *When contact lenses were invented* [Online]. Available: <http://www.allaboutvision.com/contacts/faq/when-invented.htm> [Accessed 1st Oct 2012].

- HILDEBRANDT, C., RASCHNER, C. & AMMER, K. 2010. An Overview of Recent Application of Medical Infrared Thermography in Sports Medicine in Austria. *Sensors*, 10, 4700-4715.
- HILL, R. M. & LEIGHTON, A. J. 1965a. Temperature changes of human cornea and tears under a contact lens. 1. The relaxed open eye, and the natural and forced closed eye conditions. *Am J Optom Arch Am Acad Optom*, 42, 9-16.
- HILL, R. M. & LEIGHTON, A. J. 1965b. Temperature changes of human cornea and tears under a contact lens. 2. Effects of intermediate lid apertures gaze. *Am J Optom Arch Am Acad Optom*, 42, 71-77.
- HILL, R. M. & LEIGHTON, A. J. 1965c. Temperature changes of human cornea and tears under contact lenses. 3. Ocular sensation. *Am J Optom Arch Am Acad Optom*, 42, 584-8.
- HOLDEN, B. A. & MERTZ, G. W. 1984. Critical oxygen levels to avoid corneal edema for daily and extended wear contact lenses. *Invest Ophthalmol Vis Sci*, 25, 1161-7.
- HOLLY, F. J. 1981a. Tear Film Physiology and Contact Lens Wear. I. Pertinent Aspects of Tear Film Physiology. *Am J Optom Physiol Opt*, 58, 324-330 <2>.
- HOLLY, F. J. 1981b. Tear Film Physiology and Contact Lens Wear. II. Contact Lens-Tear Film Interaction. *Am J Optom Physiol Opt*, 58, 331-341.
- ITOI, M., INABA, M., UEDA, K., OHASHI, Y., KAJIDA, M., KANAI, J., KAMEI, Y., KINOSITA, S., KODAMA, Y., SAKIMOTO, Y., SANO, K., SAWA, M., SHIOYA, H., TAKAMURA, E., MAEDA, N., MIZUTANI, Y. & WATANABE, K. 2005. CL complications. *Nihon Ganka Gakkai Zasshi*, 109, 654-656.
- JONES, L., BRENNAN, N. A., GONZALEZ-MEIJOME, J., LALLY, J., MALDONADO-CODINA, C., SCHMIDT, T. A., SUBBARAMAN, L., YOUNG, G. & NICHOLS, J. J. 2013. The TFOS International Workshop on Contact Lens Discomfort: Report of the Contact Lens Materials, Design, and Care Subcommittee. *Invest Ophthalmol Vis Sci*, 54, TFOS37-TFOS70.
- KAM, H. C., SIU, L. L., HANS, W. H., BEEKHUIS, W. H., PAUL, G. H. M., ANNETTE, J. M. G. & AIZE, K. 1999. Incidence of contact-lens-associated microbial keratitis and its related morbidity. *Lancet*, 354, 181-185.
- KESSEL, L., JOHNSON, L., ARVIDSSON, H. & LARSEN, M. 2010. The relationship between body and ambient temperature and corneal temperature. *Invest Ophthalmol Vis Sci*, 51, 6593-7.
- KING-SMITH, P. E., FINK, B. A., FOGT, N., NICHOLS, K. K., HILL, R. M. & WILSON, G. S. 2000. The Thickness of the Human Precorneal Tear Film: Evidence from Reflection Spectra. *Invest Ophthalmol Vis Sci*, 41, 3348-3359.
- KOJIMA, T., MATSUMOTO, Y., IBRAHIM, O. M. A., WAKAMATSU, T. H., UCHINO, M., FUKAGAWA, K., OGAWA, J., DOGRU, M., NEGISHI, K. & TSUBOTA, K. 2011. Effect of Controlled Adverse Chamber Environment Exposure on Tear Functions in Silicon Hydrogel and Hydrogel Soft Contact Lens Wearers. *Investigative Ophthalmology & Visual Science*, 52, 8811-8817.
- KOK, J. H., BOETS, E. P., VAN BEST, J. A. & KIJLSTRA, A. 1992. Fluorophotometric assessment of tear turnover under rigid contact lenses. *Cornea*, 11, 515-7.
- KORB, D., CRAIG, J., DOUGHTY, M. J., GUILLON, J.-P., TOMLINSON, A. & SMITH, G. 2002. *The tear film structure, function and clinical examination*, Oxford, Butterworth-Heinemann.
- KORB, D. R. 1994. Tear film-contact lens interactions. *Adv Exp Med Biol*, 350, 403-10.

- KORB, D. R. & BRITISH CONTACT LENS, A. 2002. *The tear film structure, function and clinical examination*, Oxford, Butterworth-Heinemann.
- KWAN, M., NIINIKOSKI, J. & HUNT, T. K. 1972. In Vivo Measurements of Oxygen Tension in the Cornea, Aqueous Humor, and Anterior Lens of the Open Eye. *Invest Ophthalmol Vis Sci*, 11, 108-114.
- LERMAN, S. 1980. *Radiant energy and the eye* New York, Macmillan.
- LERNER, L. S. 1996. *Modern physics for scientists and engineers*, Boston, Jones and Bartlett Publishers.
- LIN, M. C., CHEN, Y. Q. & POLSE, K. A. 2003. The effects of ocular and lens parameters on the postlens tear thickness. *Eye Contact Lens*, 29, S33-6; discussion S57-9, S192-4.
- LIN, M. C., GRAHAM, A. D., FUSARO, R. E. & POLSE, K. A. 2002. Impact of rigid gas-permeable contact lens extended wear on corneal epithelial barrier function. *Invest Ophthalmol Vis Sci*, 43, 1019-24.
- LIN, M. C. & SVITOVA, T. F. 2010. Contact lenses wettability in vitro: effect of surface-active ingredients. *Optom Vis Sci*, 87, 440-7.
- MAH-SADORRA, J. H., YAVUZ, S. G. A., NAJJAR, D. M., LAIBSON, P. R., RAPUANO, C. J. & COHEN, E. J. 2005. Trends in Contact Lens-Related Corneal Ulcers. *Cornea*, 24, 51-58.
- MAKINAE, Y., TANNO, S., MIURA, T., DAIKOKU, M. & AOKI, H. 1992. Measurement of Thermophysical Properties of Water-absorbent Polymer. *The Thirteenth Japan Symposium on Thermophysical Properties*.
- MAPSTONE, R. 1968a. Determinants of corneal temperature. *Br J Ophthalmol*, 52, 729-41.
- MAPSTONE, R. 1968b. Measurement of corneal temperature. *Exp Eye Res*, 7, 237-43.
- MAPSTONE, R. 1968c. Normal thermal patterns in cornea and periorbital skin. *Br J Ophthalmol*, 52, 818-27.
- MARTIN, D. K. & FATT, I. 1986. The presence of a contact lens induces a very small increase in the anterior corneal surface temperature. *Acta Ophthalmol (Copenh)*, 64, 512-8.
- MARUYAMA, K., YOKOI, N., TAKAMATA, A. & KINOSHITA, S. 2004. Effect of environmental conditions on tear dynamics in soft contact lens wearers. *Invest Ophthalmol Vis Sci*, 45, 2563-8.
- MCNAMARA, N. A., POLSE, K. A., BRAND, R. J., GRAHAM, A. D., CHAN, J. S. & MCKENNEY, C. D. 1999. Tear mixing under a soft contact lens: effects of lens diameter. *Am J Ophthalmol*, 127, 659-65.
- MONTES-MICO, R. 2007. Role of the tear film in the optical quality of the human eye. *J Cataract Refract Surg*, 33, 1631-5.
- MORGAN, P. B., SOH, M. P., EFRON, N. & TULLO, A. B. 1993. Potential applications of ocular thermography. *Optom Vis Sci*, 70, 568-76.
- MORGAN, P. B., TULLO, A. B. & EFRON, N. 1995. Infrared thermography of the tear film in dry eye. *Eye*, 9, 615-8.
- MORGAN, P. B., TULLO, A. B. & EFRON, N. 1996. Ocular surface cooling in dry eye -- a pilot study. *Journal of The British Contact Lens Association*, 19, 7-10.
- MORGAN, P. B., WOODS, C. A., KNAJIAN, R., JONES, D., EFRON, N., TAN, K.-O., PESINOVA, A., GREIN, H.-J., MARX, S., SANTODOMINGO, J., RUNBERG, S.-E., TRANOUDIS, I. G., CHANDRINOS, A., ITOI, M., BENDORIENE, J., WERP, E. V. D., HELLAND, M., PHILLIPS, G., GONZ LEZ-M IJOME, J. M., BELOUSOV, V. &

- MACK, C. J. 2007. International Contact Lens Prescribing in 2007. Available: <http://www.clspectrum.com/articleviewer.aspx?articleid=101241>.
- MORGAN, P. B., WOODS, C. A., TRANOUDIS, I. G., EFRON, N., KNAJIAN, R., GRUPCHEVA, C. N., JONES, D., TAN, K.-O., PESINOVA, A., RAVN, O., SANTODOMINGO, J., VODNYANSZKY, E., MONTANI, G., ITOI, M., BENDORIENE, J., WORP, E. V. D., HELLAND, M., PHILLIPS, G., GONZ LEZ-M IJOME, J. M., RADU, S., BELOUSOV, V., SILIH, M. S., HSIAO, J. C. & NICHOLS, J. J. 2008. International Contact Lens Prescribing in 2008. Available: <http://www.clspectrum.com/article.aspx?article=102545>.
- MORGAN, P. B., WOODS, C. A., TRANOUDIS, I. G., HELLAND, M., EFRON, N., GRUPCHEVA, C. N., JONES, D., TAN, K.-O., PESINOVA, A., RAVN, O., SANTODOMINGO, J., MALET, F., RAGUŽ, H., ERDINEST, N., HREINSSON, H. I., ITOI, M., CHU, B. S., BENDORIENE, J., WORP, E. V. D., AWASTHI, S., LAM, W., GONZ LEZ-M IJOME, J. M., RADU, S., BELOUSOV, V., GUSTAFSSON, J., SILIH, M. S., HSIAO, J. & NICHOLS, J. J. 2010. International Contact Lens Prescribing in 2010. Available: <http://www.clspectrum.com/articleviewer.aspx?articleid=105084>.
- MORGAN, P. B., WOODS, C. A., TRANOUDIS, I. G., HELLAND, M., EFRON, N., GRUPCHEVA, C. N., JONES, D., TAN, K.-O., PESINOVA, A., SANTODOMINGO, J., MALET, F., ERDINEST, N., HREINSSON, H. I., CHANDE, P., MONTANI, G., ITOI, M., CHU, B. S., BENDORIENE, J., WORP, E. V. D., AWASTHI, S., LAM, W., GONZ LEZ-M IJOME, J. M., DAVILA-GARCIA, E., RADU, S., BELOUSOV, V., JOHANSSON, O., SILIH, M. S., HSIAO, J. & NICHOLS, J. J. 2011. International Contact Lens Prescribing in 2011. Available: <http://www.clspectrum.com/articleviewer.aspx?articleid=106551>.
- MORGAN, P. B., WOODS, C. A., TRANOUDIS, I. G., HELLAND, M., EFRON, N., KNAJIAN, R., GRUPCHEVA, C. N., JONES, D., TAN, K.-O., PESINOVA, A., SANTODOMINGO, J., VODNYANSZKY, E., ERDINEST, N., HREINSSON, H. I., MONTANI, G., ITOI, M., BENDORIENE, J., WORP, E. V. D., HSIAO, J., PHILLIPS, G., GONZ LEZ-M IJOME, J. M., RADU, S., BELOUSOV, V. & NICHOLS, J. J. 2009. International Contact Lens Prescribing in 2009. Available: <http://www.clspectrum.com/articleviewer.aspx?articleid=103881>.
- MORGAN, P. B., WOODS, C. A., TRANOUDIS, I. G., HELLAND, M., EFRON, N., ORIHUELA, G. C., GRUPCHEVA, C. N., JONES, D., TAN, K.-O., PESINOVA, A., RAVN, O., SANTODOMINGO, J., MALET, F., CHENG, L. S. A. P., V GH, M., ERDINEST, N., RAGNARSD TTIR, J. B., MONTANI, G., DAVILA-GARCIA, E., ITOI, M., CHU, B. S., BENDORIENE, J., WORP, E. V. D., AWASTHI, S., LAM, W., CASABLANCA, J., GONZ LEZ-M IJOME, J. M., JOHANSSON, O., SILIH, M. S., HSIAO, J. & NICHOLS, J. J. 2012. International Contact Lens Prescribing in 2012. Available: <http://www.clspectrum.com/articleviewer.aspx?articleID=107854>.
- MORGAN, P. B., WOODS, C. A., TRANOUDIS, I. G., HELLAND, M., EFRON, N., TEUFL, M., GRUPCHEVA, C. N., JONES, D., TAN, K.-O., PESINOVA, A., PULT, H., RAVN, O., GIEROW, P., SANTODOMINGO, J., MALET, F., PLAKITSI, A., V GH, M., ERDINEST, N., CHANDE, P. K., RAGNARSD TTIR, J. B., ITOI, M., CHU, B. S., BENDORIENE, J., WORP, E. V. D., AWASTHI, S., LAM, W., LESZCZYŃSKA, W., GONZ LEZ-M IJOME, J. M., BELOUSOV, V., SILIH, M. S., HSIAO, J. & NICHOLS, J. J. 2013. International Contact Lens Prescribing in 2013. Available:

<http://www.clspectrum.com/articleviewer.aspx?articleID=109321> [Accessed 30 June 2014].

- NATIONAL ASTRONOMICAL OBSERVATORY OF JAPAN 2011. Chronological scientific tables. Maruzen.
- NICHOLS, J. J. 2009. Contact Lenses 2008. *Contact Lens Spectrum*, 24, 24-32.
- NICHOLS, J. J. 2010. Contact Lenses 2009. *Contact Lens Spectrum*, 25, 20-27.
- NICHOLS, J. J. 2011. Contact Lenses 2010. *Contact Lens Spectrum*, 26, 20-27.
- NICHOLS, J. J. 2012. Contact Lenses 2011. *Contact Lens Spectrum*, 27, 20-25.
- NICHOLS, J. J. 2013. Contact Lenses 2012. *Contact Lens Spectrum*, 28, 31-38, 44.
- NICHOLS, J. J. 2014. Contact Lenses 2013. *Contact Lens Spectrum*, 29, 22-28.
- NICHOLS, J. J. & KING-SMITH, P. E. 2003. Thickness of the pre- and post-contact lens tear film measured in vivo by interferometry. *Invest Ophthalmol Vis Sci*, 44, 68-77.
- OHASHI, Y. 1994. *Eye drops* Medical view.
- PAUGH, J. R., STAPLETON, F., KEAY, L. & HO, A. 2001. Tear Exchange under Hydrogel Contact Lenses: Methodological Considerations. *Invest Ophthalmol Vis Sci*, 42, 2813-2820.
- PFLUGFELDER, S., BEUERMAN, R. & STERN, M. E. 2004. *Dry Eye and Ocular Surface Disorders*, New York, Marcel Dekker.
- PHILLIPS, A. J. & SPEEDWELL, L. 2007. *Contact Lenses*, Butterworth-Heinemann.
- POLSE, K. A. 1979. Tear flow under hydrogel contact lenses. *Invest Ophthalmol Vis Sci*, 18, 409-13.
- PURSLOW, C. 2005. *Dynamic Ocular Thermography*. Doctor of Philosophy, Aston University.
- PURSLOW, C., WOLFFSOHN, J. S. & SANTODOMINGO-RUBIDO, J. 2005. The effect of contact lens wear on dynamic ocular surface temperature. *Cont Lens Anterior Eye*, 28, 29-36.
- RABINOVITCH, J., COHEN, E. J., GENVERT, G. I., DONNENFELD, E. D., ARENTSEN, J. J. & LAIBSON, P. R. 1987. Seasonal variation in contact lens-associated corneal ulcers. *Can J Ophthalmol*, 22, 155-6.
- READ, M. L., MORGAN, P. B. & MALDONADO-CODINA, C. 2009. Measurement errors related to contact angle analysis of hydrogel and silicone hydrogel contact lenses. *J Biomed Mater Res B Appl Biomater*, 91, 662-8.
- RING, E. F. & AMMER, K. 2012. Infrared thermal imaging in medicine. *Physiol Meas*, 33, R33-46.
- RING, E. F. J. 1998. Progress in the measurement of human body temperature. *Engineering in Medicine and Biology Magazine, IEEE*, 17, 19-24.
- ROLANDO, M. & ZIERHUT, M. 2001. The Ocular Surface and Tear Film and Their Dysfunction in Dry Eye Disease. *Surv Ophthalmol*, 45, Supplement 2, S203-S210.
- RYSA, P. & SARVARANTA, J. 1974. Corneal temperature in man and rabbit. Observations made using an infra-red camera and a cold chamber. *Acta Ophthalmol (Copenh)*, 52, 810-6.
- SABINS, F. F. 1987. Remote Sensing. Principles and Interpretation, 2nd ed. *Geological Magazine*, 124, 296-297.
- SAVINI, G., PRABHAWASAT, P., KOJIMA, T., GRUETERICH, M., ESPANA, E. & GOTO, E. 2008. The challenge of dry eye diagnosis. *Clin Ophthalmol*, 2, 31-55.
- SCHEIN, O. D., MCNALLY, J. J., KATZ, J., CHALMERS, R. L., TIELSCH, J. M., ALFONSO, E., BULLIMORE, M., O'DAY, D. & SHOVLIN, J. 2005. The incidence of

- microbial keratitis among wearers of a 30-day silicone hydrogel extended-wear contact lens. *Ophthalmology*, 112, 2172-9.
- SCHWARTZ, B., PACKER, S. & HIMMERLSTEIN, S. C. 1968. Ocular thermoradiometry. *The Sectional Meetings of the Association for Research in Ophthalmology*. Wasington, D. C.
- SEED. 2011. Contact lens market in Japan. Available: <http://www.seed.co.jp/company/ir/document/html/10.html> [Accessed June 2014].
- SHIMAZAKI, J. 2007. Definition and diagnosis of dry eye 2006. *Atarashiiganka*, 24, 181-184.
- STAPLETON, F., DART, J. K. & MINASSIAN, D. 1993. Risk factors with contact lens related suppurative keratitis. *CLAO J*, 19, 204-10.
- STAPLETON, F., KEAY, L., EDWARDS, K., NADUVILATH, T., DART, J. K., BRIAN, G. & HOLDEN, B. A. 2008. The incidence of contact lens-related microbial keratitis in Australia. *Ophthalmology*, 115, 1655-62.
- STAPLETON, F., KEAY, L. J., SANFILIPPO, P. G., KATIYAR, S., EDWARDS, K. P. & NADUVILATH, T. 2007. Relationship between climate, disease severity, and causative organism for contact lens-associated microbial keratitis in Australia. *Am J Ophthalmol*, 144, 690-698.
- STONE, J. & PHILLIPS, A. J. 1986. *Contact lenses*, London, Butterworths.
- SUND-LEVANDER, M., FORSBERG, C. & WAHREN, L. K. 2002. Normal oral, rectal, tympanic and axillary body temperature in adult men and women: a systematic literature review. *Scand J Caring Sci*, 16, 122-128.
- SWEENEY, D. 2004. *Silicone Hydrogels: Continuous Wear Contact Lenses*, Sydney, Butterworth-Heinemann.
- THAI, L. E. E. C. B. M., TOMLINSON, A. D. F. F. & DOANE, M. G. P. 2004. Effect of Contact Lens Materials on Tear Physiology. *Optom Vis Sci*, 81, 194-204.
- TOMLINSON, A., BRON, A. J., KORB, D. R., AMANO, S., PAUGH, J. R., PEARCE, E. I., YEE, R., YOKOI, N., ARITA, R. & DOGRU, M. 2011. The International Workshop on Meibomian Gland Dysfunction: Report of the Diagnosis Subcommittee. *Invest Ophthalmol Vis Sci*, 52, 2006-2049.
- TONGE, S. R., HUNSAKER, J. & HOLLY, F. J. 1991. Non-invasive assessment of tear film break-up time in a group of normal subjects - implications for contact lens wear. *Journal of The British Contact Lens Association*, 14, 201-205.
- TSUBOTA, K. & NAKAMORI, K. 1995. Effects of ocular surface area and blink rate on tear dynamics. *Arch Ophthalmol*, 113, 155-158.
- WANG, J., AQUAVELLA, J., PALAKURU, J., CHUNG, S. & FENG, C. 2006. Relationships between Central Tear Film Thickness and Tear Menisci of the Upper and Lower Eyelids. *Invest Ophthalmol Vis Sci*, 47, 4349-4355.
- WANG, J., FONN, D., SIMPSON, T. L. & JONES, L. 2003. Precorneal and pre- and postlens tear film thickness measured indirectly with optical coherence tomography. *Invest Ophthalmol Vis Sci*, 44, 2524-8.
- WILSON, W. S., DUNCAN, A. J. & JAY, J. L. 1975. Effect of benzalkonium chloride on the stability of the precorneal tear film in rabbit and man. *Br J Ophthalmol*, 59, 667-9.
- YOKOI, N., YAMADA, H., MIZUKUSA, Y., BRON, A. J., TIFFANY, J. M., KATO, T. & KINOSHITA, S. 2008. Rheology of Tear Film Lipid Layer Spread in Normal and Aqueous Tear-Deficient Dry Eyes. *Invest Ophthalmol Vis Sci*, 49, 5319-5324.